THERMAL PERFORMANCE OF A BURIED NUCLEAR WASTE STORAGE CONTAINER STORING A HYBRID MIX OF PWR AND BWR SPENT FUEL RODS

G. L. Johnson
Thermo-Fluids Group
Nuclear Test Engineering Division

September 1988

Lawrence Livermore National Laboratory

DISCLAIMER

Price Code	Page Range
A01	Microfiche
Papercopy Prices	
A02	001 - 050
A03	051 - 100
A04	101 - 200
A05	201 - 300
A06	301 - 400
A07	401 - 500
A08	501 - 600
A09	601

The following number is for Office of Civilian Radioactive
Waste Management Records Management purposes only and
should not be used when ordering this document:

Accession Number: <u>NNA.881221.0098</u>

THERMAL PERFORMANCE OF A
BURIED NUCLEAR WASTE CONTAINER
STORING A HYBRID MIX OF PWR AND BWR SPENT FUEL RODS

Gary L. Johnson
Thermo-Fluids Group
Nuclear Test Engineering Division

September 1988

Abstract

Lawrence Livermore National Laboratory will design, model, and test nuclear waste packages for use at the Nevada Nuclear Waste Storage Repository at Yucca Mountain, Nevada. One such package would store tightly packed spent fuel rods from both pressurized and boiling water reactors. The storage container provides the primary containment of the nuclear waste and the spent fuel rod cladding provides secondary containment. A series of transient conduction and radiation heat transfer analyses was run to determine for the first 1000 yr of storage if the temperature of the tuff at the borehole wall ever falls below 97 $^{\circ}$C and whether the cladding of the stored spent fuel ever exceeds 350 $^{\circ}$C. Limiting the borehole to temperatures of 97 $^{\circ}$C or greater helps minimize corrosion by assuring that no condensed water collects on the container. The 350 $^{\circ}$C cladding limit minimizes the possibility of creep-related failure in the spent fuel rod cladding. For a series of packages stored in a 8 X 30 m borehole grid where each package contains 10-yr-old spent fuel rods generating 4.74 kW or more, the borehole wall stays above 97 $^{\circ}$C for the full 1000-yr analysis period. For the 4.74-kW load, the peak cladding temperature rises to just below the 350 $^{\circ}$C limit about 4 years after emplacement. If the packages are stored using the spacing specified in the Site Characterization Plan (15 ft X 126 ft), a maximum of 4.1 kW per container may be stored. If the 0.05-m-thick void between the container and the borehole wall is filled with loosely packed bentonite, the peak cladding temperature rises more than 40 $^{\circ}$C above the allowed cladding limit. In all cases the dominant heat transfer mode between container components is thermal radiation.

TABLE OF CONTENTS

LIST OF FIGURES

LIST OF TABLES

SUMMARY

Researchers in the Yucca Mountain Project (YMP) are designing containers for the long-term disposal of spent nuclear fuel and high-level radioactive waste. The proposed site of this repository is above the water table in the volcanic tuff under Yucca Mountain, Nevada. Lawrence Livermore National Laboratory (LLNL) is responsible for designing, modeling, and testing the waste forms and containment barriers. Data from these efforts will be incorporated in the final waste package designs and specifications. One such preliminary design involves the tightly packed storage in metal containers of a combination of spent fuel rods from both boiling water reactors (BWR) and pressurized water reactors (PWR). Consolidating the waste in fewer containers can minimize the number of packages in the repository. However, groups of consolidated waste containers, with their higher thermal loads, would be exposed to higher temperatures than those containing unconsolidated waste. Thus, it is imperative to determine the limit on the thermal performance under these increased-load operating conditions.

This report documents the results of a series of transient conduction and radiation heat-transfer analyses to predict the thermal response of both the container design and also the nearby tuff around the borehole where the container is emplaced. Specifically, these thermal analyses predict if the temperature of the tuff at the borehole wall will fall below 97 $^{\circ}$C and if the peak temperature of the spent fuel cladding will exceed 350 $^{\circ}$C. The 97 $^{\circ}$C borehole limit is set to minimize corrosion of the container shell by assuring that no condensed water collects on its outer surface. The container provides the primary containment for the radioactive material. Limiting the spent fuel rod cladding to 350 $^{\circ}$C or less will minimize creep-related failure, thus improving secondary containment of the radioactive fuel.

The heat transfer analyses involve two geometric models, i.e., a three-dimensional (3-D) model predicting the thermal response of the tuff surrounding the borehole subjected to the total thermal load from

the waste storage container and a two-dimensional (2-D) model predicting the thermal response of a mean cross section of the container with its individual heat-generating fuel storage canisters. The borehole wall temperatures predicted by the 3-D analyses define the thermal sink conditions for the 2-D analyses. These analyses quantify the relative effects on thermal performance of (a) the thermal loads from the decay heat of the container contents, (b) the container structural materials, (c) filling the annulus between container and borehole wall with loosely or firmly packed bentonite, and (d) the model for heat transfer inside the container. The analytic effort culminates in a best model thermal analysis to define the response of the container under a probable design-limiting thermal load.

For this work the geometric model assumes that a large number of 0.711-m-diam containers are buried 350 m below the surface of the earth in 0.812-m-diam X 4.5-m-long vertical boreholes arranged in rows down the center of drift tunnels. Boreholes in the simulated region of the repository are spaced on 8-m centers along the drift and on 30-m centers between drifts. This spacing is larger than that defined by the repository's Site Characterization Plan[1] (SCP) since fewer boreholes would be needed.

If the container being analyzed is surrounded by equivalently loaded containers emplaced at about the same time, each container in the array deposits its heat into a section of tuff 8 X 30 X 700 m. No heat is removed by ventilation in the drift tunnels or by evaporation of the moisture in the tuff. Previous studies have shown that, for the 1000-yr analysis period, the tuff below the assumed 700-m maximum interaction depth is relatively unaffected by the container thermal load. The thermal behavior at 700 m predicted by this study also verifies this assumption.

The thermal output of the contents of the container represents a hybrid load containing 4 canisters of spent BWR fuel and 3 canisters of spent PWR fuel. At the reactor facility, each fuel canister is

packed with two assemblies of BWR or PWR spent fuel rods (called 2:1 at-reactor-consolidation). Also both the BWR and PWR spent fuel rods contain normally enriched fuel and were used in the reactor for the normal 7.5-yr power generation period (called normal burnup fuel). For most analyses, both fuels are assumed to have been stored outside of the reactor for 10 yr at the time of emplacement in the borehole. At the time of emplacement, the total power output of the container with 10-yr-old fuel is 4740 W. The local power density (LPD) at emplacement, based on the local borehole spacing, is 80 kW/acre. Because these highly loaded packages will really only be used at a few selected locations in the repository, an areal power density (APD) for the whole repository based on this power output has little meaning.

For the emplacement of this hybrid-filled container surrounded by an infinite array of equivalently loaded containers on 8 X 30 m spacings, the following conclusions result from a review of the analyses documented herein. For a 4.74-kW load or greater, the borehole wall stays above 97 $^{\circ}$C for the full 1000-yr analysis period. The tuff 1 m in from the borehole wall never exceeds 200 $^{\circ}$C, even if the 10-yr-old fuel is replaced with an equivalent weight of 5-yr-old fuel. Because the borehole wall surface temperature nears 200 $^{\circ}$C, it is possible that the floor of the drift tunnel near these containers might surpass the 50 $^{\circ}$C maximum temperature allowable under general repository manned-use design criteria. Previous studies, modeling the effect of drift tunnel, have shown 5 to 10 $^{\circ}$C decreases in borehole wall temperature due to ventilation.

For all but two cases, the peak cladding temperature remains below, <u>but near</u>, the 350 $^{\circ}$C limit. The best model analysis gives a peak cladding temperature of 336 $^{\circ}$C. The two cases that do not satisfy the maximum cladding temperature limit requirement (i.e., (1) replacing the 10-yr-old fuel with an equivalent weight of 5-yr-old fuel and (2) backfilling the 0.05-m-thick annulus between the container and the borehole wall with loosely packed bentonite) results in peak cladding temperatures about 40 to 60 $^{\circ}$C hotter than the maximum allowable. Packing the bentonite firmly in the annulus, with

its resultant increase in thermal conductivity over the loose pack, gives a peak cladding temperature of 341 $^{\circ}$C. The highly sensitive nature of these results to the assumed thermal properties of the backfill makes use of accurately measured values of these properties crucial to further analyses guiding backfill design decisions.

Some general comments can be added to these specific conclusions. For boreholes with no backfill, heat balance calculations on heat transferred from the container to the borehole wall show that thermal radiation causes most of the heat flow. That radiative heat transfer is also the dominant mode inside the container is demonstrated by three results of the analyses: (1) The small effect on predicted peak cladding temperatures of the conductivity of the container assembly structural material. (2) The minor decrease in peak cladding temperature resulting from modeled heat transfer by conduction through the gas fill. (3) The obvious sensitivity of the predicted temperatures to the value of the surface emissivity for the surfaces inside the container. Including the effect of heat transfer from natural convection in the cavities between the fuel canisters and the inner surface of the container shell would make the gas-fill model contribution more significant. The assumed value of the "effective" thermal conductivity for the "homogenized" fuel rods/fuel canister assembly is the other main parameter that strongly affects predictions of peak cladding temperatures. This thermal property should also be accurately determined for all load conditions to assure realistic predictions of the cladding temperatures.

On the basis of these conclusions and an overall view of the repository layout and expected container emplacement history, I make the following recommendations for additional thermal performance evaluations.

a. Establish accurate values for the effective thermal conductivity of the homogenized fuel canisters for all possible fuel packing configurations. Determine the relationship between the actual peak cladding temperature and that predicted by the homogenized model.

b. Add natural convection in the gas fill to the internal-heat-transfer model of the vertical container.

c. Determine the surface emissivity of the tuff and the materials to be used in the waste package designs for various expected surface conditions.

d. Establish more accurate values for the thermal conductivity of potential container backfills at various densities.

e. Using a best model, complete a 3-D analysis of the vertical container including axial variations in power output, material geometries, and thermal properties.

f. Do transient, 3-D thermal analysis of various combinations of emplaced packages and emplacement histories for whole sections of the repository using the planned waste delivery scenario (e.g., Ref. 2).

g. Model the effect of the drift tunnels in detail, including the drift tunnel geometry and its associated humidity and heat removal by ventilation

I.   Introduction

      The Yucca Mountain Project (YMP) is part of the U.S. Department
of Energy's Civilian Radioactive Waste Management Program. The Waste
Package task of the YMP will design containers for the disposal of
spent fuel and high-level waste in a repository. The proposed site
for the repository is in the unsaturated zone of the volcanic tuff
under Yucca Mountain, which is located at the DOE Nevada Test Site.
Lawrence Livermore National Laboratory (LLNL) is responsible for
designing, modeling, and testing the waste forms and barriers. These
designs will be incorporated in the final waste package designs and
specifications.   The   final barrier system design will be some
combination of a waste form, container, borehole liner, borehole and
drift backfill, and the near-field host rock.   Engineering this
barrier system will require analyses to predict the thermal
performance of the design.

      Information produced by the thermal analyses of the container
and the near-field host rock may be used to:

      1.   Demonstrate that the waste form or the near-field host rock
           will not exceed the maximum allowable temperatures set by
           phenomena affecting containment: i.e., thermal strain in the
           host rock, container corrosion, spent fuel cladding creep.

      2.   Calculate the approximate time periods of steam/water
           contact with the waste package.

      3.   Provide temperature-time histories for material selections,
           corrosion testing, and release rate testing.

      4.   Provide component temperatures for transportation, handling,
           storage, and retrieval while in the repository.

      Previous thermal studies by LLNL have reviewed the thermal
performance of various conceptual container designs, their waste

loads, and storage conditions.[3-7] (See Appendix A for a list of additional LLNL-internal documentation.) One proposed design involves the tightly packed storage of a combination of spent fuel rods from both boiling water reactors (BWR) and pressurized water reactors (PWR) in a vertically stored container. The thermal performance of a container with this type of load was expected to operate near the upper temperature limits allowed for long-term storage of this fuel form.

This report documents the results of a series of transient conduction and radiation heat-transfer analyses on a vertically stored nuclear waste storage container containing a hybrid mix of PWR and BWR spent fuel rods. The container will be buried in a borehole deep in the earth in volcanic tuff. The heat transfer analyses are separated into two parts: 3-D analyses modeling the thermal response of the tuff, and 2-D analyses modeling the thermal response of a cross section of the container. The 3-D analyses of the tuff use the total thermal contents of the container to determine the temperature-time history of the borehole wall. This history is then used as a temperature boundary condition for the 2-D analyses of the container. The temperature-time histories are determined up to 1000 yr after emplacement in the storage borehole.

These analyses quantify the relative effects on thermal performance of (a) the thermal loads from the decay heat of the container contents, (b) the container structural materials, (c) the annulus between container and borehole wall filled with loosely or firmly packed bentonite, and (d) the model for heat transfer inside the container. The analytic effort culminates in a best model thermal analysis to define the response of the container with a design-limiting thermal load. The effect of container orientation is left to a later study. As with most analytic efforts, model improvements in terms of material property choices and important modes of heat transfer became more apparent as the effort progressed. Documentation of the effects of each change is referenced to an early model. Thus, for all but the best model analysis, the temperatures are used more

for relative comparisons with the appropriate reference cases (Case 1a/3-D:coarse mesh or Case 3/2-D:IN825) rather than as absolute magnitudes.

As performance evaluations, these thermal analyses determine if the predicted temperature of the tuff at the borehole wall ever falls below 97 $^{\circ}$C or if the predicted peak temperature of the PWR or BWR fuel cladding ever exceeds 350 $^{\circ}$C. The borehole wall temperature limit is set to minimize corrosion of the primary containment barrier by assuring that no condensed water collects on the container. At the altitude associated with the 350 m burial depth below Yucca Mountain, water condenses at 97 $^{\circ}$C. The 350 $^{\circ}$C spent fuel rod cladding limit is set to minimize creep in the fuel rod's cladding which provides secondary containment of the radioactive material.[1] An additional check determines if the tuff temperature 1 m in from the borehole wall exceeds 200 $^{\circ}$C. This helps avoid stresses in the tuff from the mineral crystobalite dispersed in the tuff which changes phase and expands by 5% between 200 $^{\circ}$C and 250 $^{\circ}$C.[8]

The remainder of this document will discuss the models of the host rock and the container in terms of the geometry, thermal loads, material properties, and initial and boundary conditions. The results are compared with the appropriate reference case and the NNWSI program-defined performance limits. The report concludes with a summary of the results and conclusions and a list of suggestions for further analytic efforts to support definition of repository and container design criteria.

II.   Thermal Models

Geometry

The heat-transfer analyses are separated into two parts: 3-D
analyses modeling the thermal response of the tuff subjected to the
total thermal load from the waste storage container and 2-D analyses
modeling the thermal response of a mean cross section of the
container. The geometry of the borehole is documented in
Figure 1a.[9-11] The 0.711-m-diam X 3.66-m-long container is buried
350 m below the surface of the earth in a 0.812-m-diam X 4.50-m-long
vertical borehole. Boreholes in the simulated region of the
repository are spaced on 8-m centers along the drift and on 30-m
centers between drifts. This spacing is larger than the 15 X 126 ft
spacing (4.6 X 38.4 m) defined in the SCP because fewer boreholes
would be needed for storage of hybrid-loaded containers storing 1.4
times the 3300-W SCP reference thermal load. These hybrid-loaded
waste storage packages contain seven spent fuel canisters located in
compartments separated by structural supports. One final analysis
will determine the hybrid-mix thermal load stored on SCP borehole
spacings which gives a thermal response equivalent to 4740-W loaded
containers stored on 8 X 30 m spacings.

The thermal analyses assume that the container being modeled is
surrounded by an infinite array of similarly loaded and spaced
containers emplaced on the same date. No heat is removed by
ventilation in the drift tunnels or by evaporation of the moisture in
the tuff. Heat from the container load flows primarily upwards toward
the ambient-cooled earth's surface as well as downward toward the
center of the earth. I chose to model only the first 350 m of the
downward heat flow because previous analyses have indicated that the
heat wave from the source barely reaches 350 m from the source after
the first 1000 yr. Thus, each container dumps its heat into a
section of tuff 8 X 30 X 700 m. For the 3-D analyses this results in
adiabatic heat transfer conditions on planes midway between boreholes
(i.e., at 4 and 15 m from the container centerline). These adiabatic

planes are normal to the respective 8- and 30-m dimensions. Earlier studies determined that the heat flow in the tuff near the borehole is approximately symmetric about the container's horizontal midplane. Thus, for all but one 3-D case, I only modeled the 350 m of the tuff between the container midplane and the earth's surface. The primary 3-D finite element (f.e.) model used in these analyses is one-eighth of the container and its associated tuff. The one-eighth section is bounded by the earth's surface, the container midplane, the adiabatic planes between adjacent boreholes, and the vertical planes through the container axis, which are parallel to these adiabatic planes. Figure 2a shows one f.e. mesh for this 3-D model.

Another 3-D model quantifies the effect of modeling both the 350 m above the container midplane and the 350 m below. One additional 3-D model investigates the effect of a refined mesh zoning and decreased calculative time step size. This model uses twice the reference model's number of divisions along the 350 m dimension and half the calculative time step size. A follow-on study using even finer finite-element model zoning will define the mesh that gives a zoning-independent temperature distribution.

The 2-D f.e. model uses the geometry of an average cross section of the container centered in the borehole. The geometry of the container is documented in Figure 1b. Perturbations in response due to non-concentric emplacement are to be considered in later studies. The small distortions of the corners of the central BWR fuel canister outline were made for ease of heat-transfer modeling. For minimized computer costs and ease of modeling, the reference 2-D f.e. model has no elements to represent heat transfer in the container's gas fill. Figure 2b shows the f.e. mesh for this model. Three additional 2-D cases were run to model heat conduction through the gas fill between the fuel cans, the support structure, and the container shell (Figure 2c). Natural convection in the gas fill was not modeled because no good heat transfer correlation was found for the cavity geometry being modeled. Cases involving backfill outside the

container have additional elements to model heat conduction through this backfill.

Analyzing a 2-D planar cross section of the container is acceptable for these parametric studies because of the relatively uniform distribution of the thermal load and the large length-to-diameter ratio. Eventually, because of the axial vs radial variations in the heat transfer of an actual container, a 3-D analysis of the container and tuff will be necessary.

Thermal Load

The power density distribution along the container's centerline varies from a volumetric-average value. However, this variation is sufficiently small that, for easier analysis, the present work uses the average condition in a 2-D model.

The thermal output of the contents of the container represent a hybrid load containing 4 canisters of normal burnup, 2:1 at-reactor-consolidation, spent BWR fuel and 3 canisters of normal burnup, 2:1 at-reactor-consolidation, spent PWR fuel. For all but one analysis, I assumed that both fuels were 10 yr out of the reactor at the time of emplacement in the borehole. The remaining analysis assumes that the same number of spent fuel rods contain fuel 5 yr out of the reactor at the time of emplacement. For the case with the 5 yr old fuel the thermal load at emplacement is 56% greater than the 10 yr old fuel reference case thermal load. All fuel canisters are double-packed (200% of reactor density), except for the SCP layout case which contains rods consolidated to 173% of the reactor density.

At emplacement, the total power output of the container with double-packed, 10-yr-old fuel is 4740 W (i.e., 360 W per BWR fuel canister and 1100 W per PWR fuel canister). That power per container with the given borehole spacing corresponds to a local power density (LPD) equal to 80 kW/acre. The power output in the case with the SCP layout spacing is 86.5% of the reference 10-yr-old fuel case. The

power output at emplacement from the container with the 5-yr-old fuel is 7392 W (i.e., 545 W per BWR fuel canister and 1737 W per PWR fuel canister), or a LPD equal to 125 kW/acre. The heat source in the 3-D model was defined as a volumetric heat generation rate with the assumption that the thermal contents are distributed over the borehole volume. For the 2-D analyses, the volumetric heat generation is based on a volume calculated from the cross section area of the individual fuel canisters and the length of the container. Table 1 documents the power output-time history of the individual fuel canisters and the respective power densities of the borehole and the fuel canisters.

Material Properties

Water-impregnated volcanic tuff was chosen as representing the host rock of the repository. The properties of the wetted tuff have changed substantially in the last few years and are still not settled. Current isotropic material thermal properties for volcanic tuff are given in Table 2. The thermal properties of the tuff are assumed to change from the normal in situ 80%-saturated conditions to perfectly dehydrated conditions at 100 $^\circ$C without any heat of vaporization. When the host rock cools below 100 $^\circ$C, thermal properties for 80%-saturated tuff are immediately in effect even though it would take years for the tuff to rehydrate. Even though phase change takes place at this level at 97 $^\circ$C, I used the existing 100 $^\circ$C data because this small variation makes no major difference in the predictions of the borehole wall temperature or the peak cladding temperature. The effects of ignoring the heat of vaporization and the time required for rehydration of the dried tuff will be studied at another time. Predicted borehole wall and peak cladding temperatures are likely to decrease when the heat of phase change is included. As mentioned previously, the analyses neglect thermal performance effects of voids in the tuff that arise from drift tunnels, of ventilation in these drift tunnels, and of migration of water/water vapor in the tuff induced by temperature gradients.

It has been proposed to pack the 0.05-m-thick annulus between the container and the borehole wall with loosely packed or firmly packed bentonite at emplacement. The bentonite backfill is supposed to improve long-term container containment by absorbing the local moisture and by suppressing diffusion of the radionuclides into the host rock after the container is breached. For the firmly packed bentonite backfill case, I assumed the properties of common bentonite deposits (25% water-saturated at temperatures below 100 ^{o}C). The properties used for the firmly packed bentonite are documented in Table 2. When these analyses were started, the actual thermal properties of the loosely packed bentonite backfill were unknown. For the current analyses I was asked to assume that the volumetric heat capacity of the loosely packed backfill is equal to two-thirds of the firmly packed condition and the thermal conductivity is equal to one-fourth of the firmly packed condition.[20]

Reference 5 looked at the effect of 0.15-m thickness of bentonite packing inside the container on thermal performance after vertical emplacement. It uses a value for bentonite thermal conductivity about equal to the value I use for the loosely packed backfill. Reference 7 looked at the performance effect of 0.15-m thickness of bentonite container packing for horizontal emplacement. The thermal conductivity of the packing, from measurements, is about equal to my value for firmly packed bentonite.

The materials for the structure of the container shell and fuel canister supports have not been chosen yet. For past thermal analyses we have assumed 304 stainless steel for these container components. In response to Project leadership suggestions for design analyses,[21] we have considered 7030 cupronickel and Incoloy 825 as well as the 304 stainless. The thermal properties for these three materials are also given in Table 2.

The actual heat transfer in the fuel canisters should be modeled in terms of individual fuel rods, the support basket, the gas fuel-canister fill, and the fuel-canister shell. The heat transfer

parallel to the fuel rod's axis can be significantly different from the heat transfer normal to the rods axis. Additional variations result dependent on the orientation of the fuel canister relative to gravity. To simplify these initial analyses, I assumed an homogeneous, isotropic material in place of the individual components and used an equivalent, or "effective," thermal conductivity to predict the thermal response of these fuel canisters. For most analyses, the effective conductivity is based only on conduction through the fuel canister gas fill and thermal radiation exchange between the fuel rods.[7]

Temperature measurements from recent experiments on doubly consolidated fuel canisters have suggested that natural convection of the storage gas within a vertically stored fuel canister may raise the effective thermal conductivity by as much as 35%.[18] An effective conductivity was determined from the reported steady-state temperature profiles by relating the test unit and its thermal response to a 2-D model with a closed-form solution for heat transfer in a rectangular canister with heat generation. The equivalent thermal properties for the double-packed spent fuel canisters used in these analyses are given near the end of Table 2. After the thermal properties of the proposed loosely packed backfill for the borehole annulus, the spent fuel canister equivalent conductivity has the least documentable support of the material thermal properties.

I assumed dry air properties where conduction through the gas fill inside the container is modeled. The properties of dry air are given in Table 2. Most other potential fill gases, e.g., argon, have slightly poorer thermal conductivity. In the case of a leak, an argon gas fill might be displaced by air from the borehole.

Initial and Boundary Conditions

The initial temperature for the 3-D, transient, f.e. heat transfer analyses of the tuff is 25 °C. Although the temperature of the undisturbed tuff is really a function of depth (around 22 °C at

ground level to 36 $^{\circ}$C at 350 m), assuming a constant 25 $^{\circ}$C does not alter the prediction of the heat flow significantly.[7] For all but one case, a constant 25 $^{\circ}$C temperature boundary condition is applied on the faces of the elements modeling the earth's surface (see Figure 1a). All other surfaces are assumed to be adiabatic. I ran one 3-D case to show the effect of assuming an adiabatic boundary condition on the earth's surface compared to a 25 $^{\circ}$C condition.

The initial temperature for the 2-D transient f.e. heat transfer analyses of the container is also 25 $^{\circ}$C. In actuality, the fuel-filled container has some initial steady-state temperature distribution that results from its pre-emplacement storage/ transportation conditions. Because this initial distribution affects only the thermal performance during the first few days after emplacement, an assumption of constant initial temperature made modeling sense.

For the cases with no backfill in the annulus, the heat-transfer model for the external surface of the container shell includes conduction through and convection in the water vapor/air-filled annulus to the borehole wall and thermal radiation from the container shell to the borehole wall. The model assumes no condensation on the outside of the container. Table 3 contains the borehole wall temperature-time history and the "convective" heat-transfer coefficient for this combined conduction/convection. This heat transfer coefficient was developed from correlations in Reference 19. I assumed natural convection and conduction in a vertical, constant-thickness annulus filled with saturated water vapor. The borehole wall temperature-time history is defined by the predicted temperatures from the 3-D analysis. The surface emissivities used for calculating thermal radiation heat transfer from the container and from the borehole wall are 0.8 and 1.0, respectively. The 0.8 value for the container's outside surface includes the effect of dust and corrosion on surface emissivity. These are historical values that have been used in all previous LLNL analyses, and are kept because no better values are available.

Inside the container, heat is transferred by conduction through the solid support structure, by thermal radiation between internal surfaces, by conduction across contact surfaces at support/fuel canister interfaces, by natural convection within the gas-filled cavities, and by conduction through the gas fill. Natural convection in oddly shaped cavities with non-uniform heating is difficult to model, and it has been left to a later study to check its contribution to the thermal performance. I expected, on the basis of previous work, that conduction and convection in the cavities would be a small contributor to the overall internal heat transfer. The reference case assumed the historically employed value of 0.8 for surface emissivity. While this value may be acceptable for the outside surface, recommended values of emissivity for the cleaner internal surfaces is somewhat lower.[22] Although I expected small increases in the predicted peak cladding temperature using the lower value of emissivity over those based on the 0.8 value, I ran an extra case to quantify the difference.

The contact thermal resistance between the fuel canisters and the support structure is assumed to be zero for all cases but one, where a more realistic value was used. Thermal radiation was expected to dominate the heat transfer; thus, the effect of modeling conduction through the gas was included in only three cases.

Analysis Codes

The f.e. mesh generator SLIC[23] was used to prepare the 3-D f.e. geometry model. The conduction heat-transfer code TACO3D[24] was used to calculate temperatures in the 3-D f.e. thermal model. The 2-D geometry mesh generator MAZE[25] was used to prepare the 2-D f.e. geometry model. TACO2D[26] was used to calculate temperatures in the 2-D f.e. thermal model. FACET[27] was used for the 2-D f.e. thermal model to calculate the view factors for thermal radiation heat transfer inside the container. Six 3-D thermal analyses and twelve 2-D thermal analyses were completed and are documented in this report. Table 4 describes each of these eighteen analyses.

NOTES:

ALL SURFACES ARE
ADIABATIC, EXCEPT
BOREHOLE WALL AND
EARTH'S SURFACE

ALL DIMENSIONS IN M

DIMENSIONS ARE FOR
1/8 OF A MODULE

(I) = NODE NO./LOCATION

EARTH'S SURFACE
AT 25 °C

CONTAINER CENTERLINE

350

VOLCANIC
TUFF

ADIABATIC PLANES
MIDWAY BETWEEN
BOREHOLES

1/2 BOREHOLE CAVITY
0.81 X 4.50/2
CONTAINING 4740/2 W

(THERMAL LOAD IS FOR
10-YR OLD FUEL AT
EMPLACEMENT)

13

56

11

4

15

CAVITY MIDPLANE
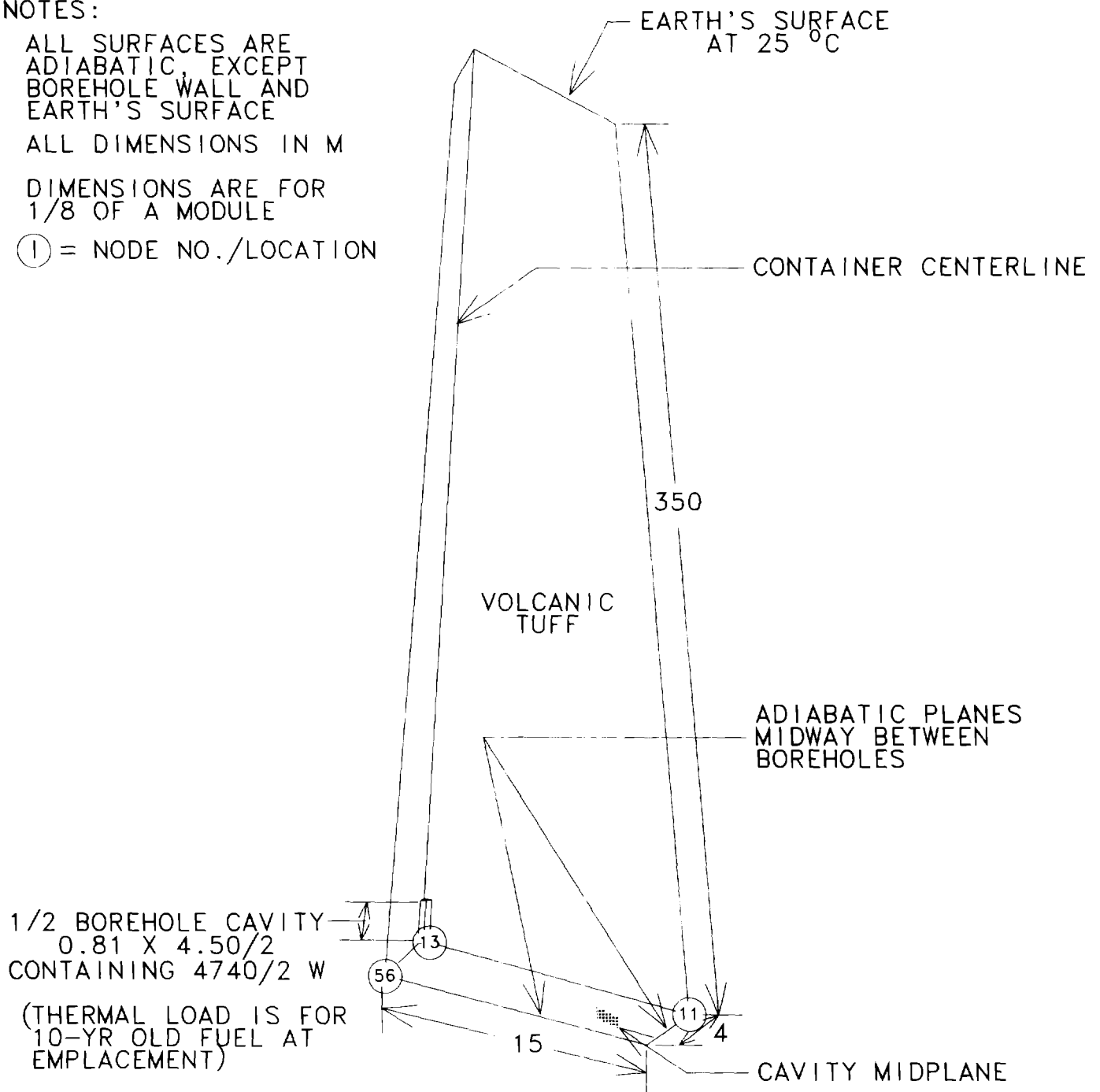
Figure 1a. Geometry model used for 3-D analysis of the tuff has
adiabatic planes at 4 and 15 m from the container axis.
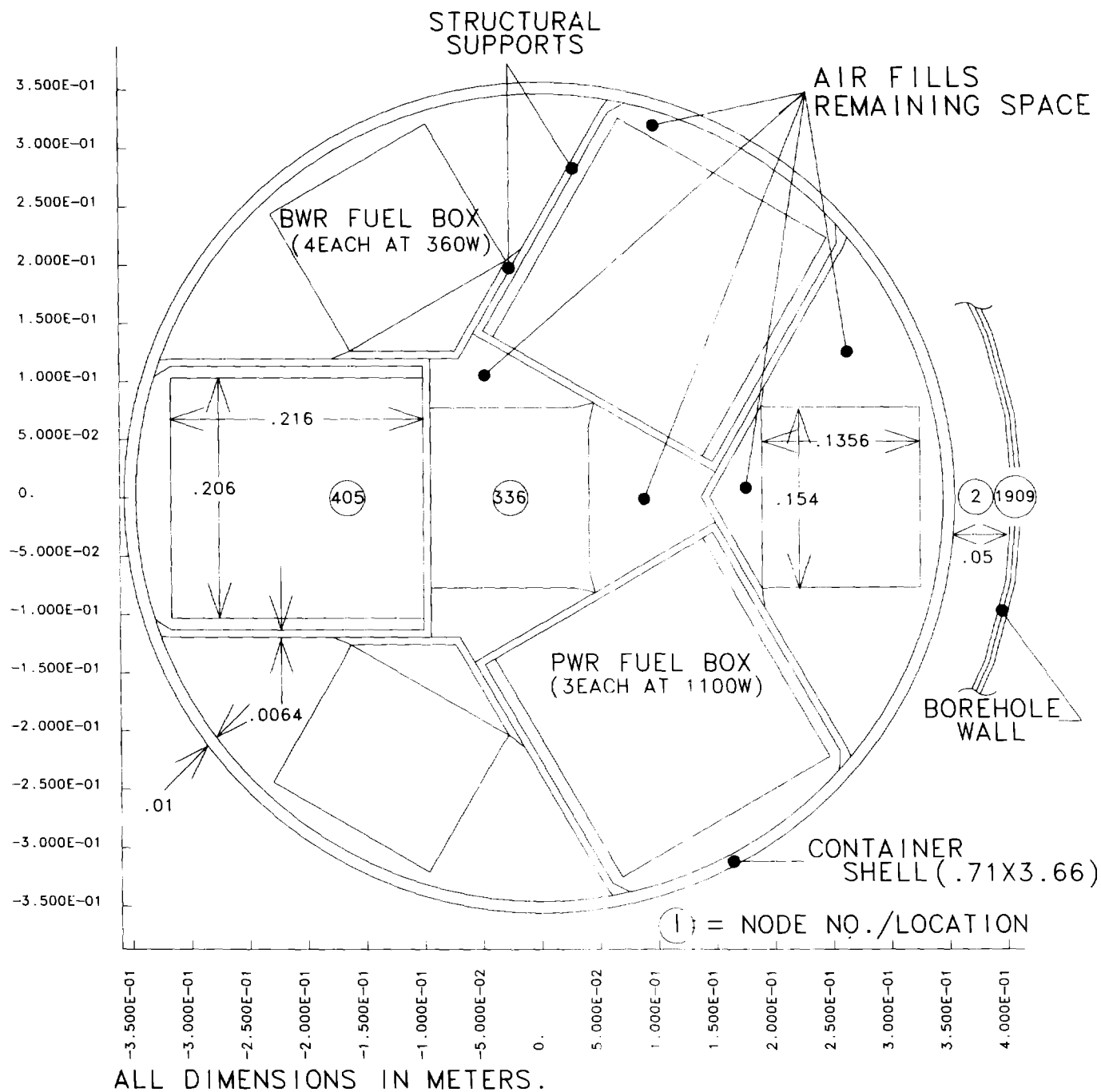
Geometry based on References 6-8.

Figure 1b. Geometry model used for 2-D analysis of container cross
section assumes uniform power generation in the PWR and BWR
fuel canisters over length of the container.

REFERENCE CASE (FULL VIEW)

FINITE ELEMENT
MODEL
(COARSE ZONING)

TUFF F.E. ZONING

CONTAINER

BOREHOLE CAVITY

(OBLIQUE VIEW)

TUFF

(SEE OBLIQUE VIEW)

CANISTER

Z

Y X

F.E. MODEL IS 1/8 OF REPRESENTATIVE FULL MODULE
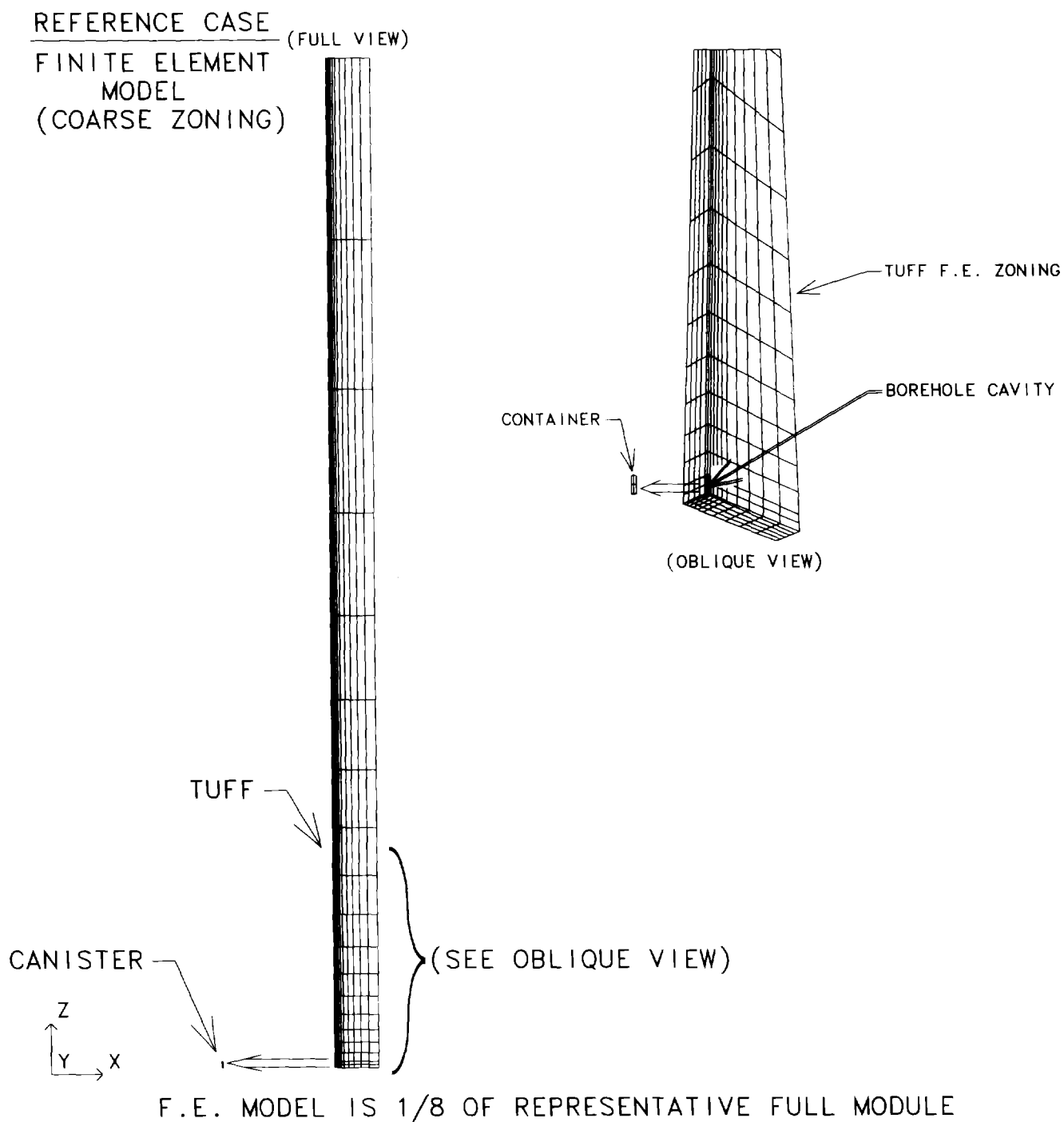
Figure 2a. Finite element model used for 3-D analysis of tuff
(coarsely zoned model used for the **3-D Reference Case**).
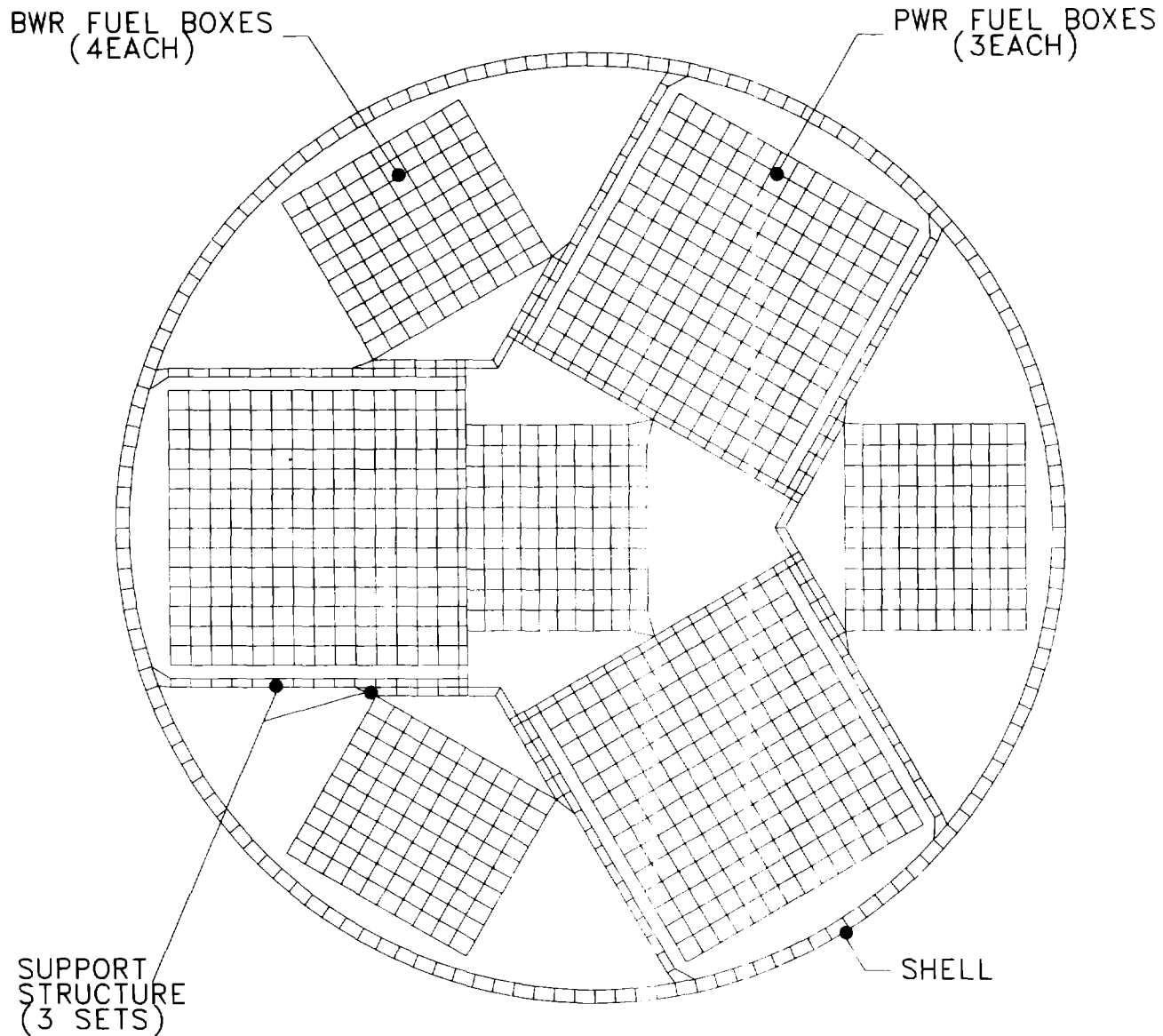
F.E. MODEL ASSUMES CONSTANT PROPERTIES ALONG LENGTH

Figure 2b. Finite element model used for 2-D analysis of container for the cases **without** gas fill elements.

BWR FUEL BOXES
(4EACH)

PWR FUEL BOXES
(3EACH)

AIR

SUPPORT
STRUCTURE
(3 SETS)

SHELL
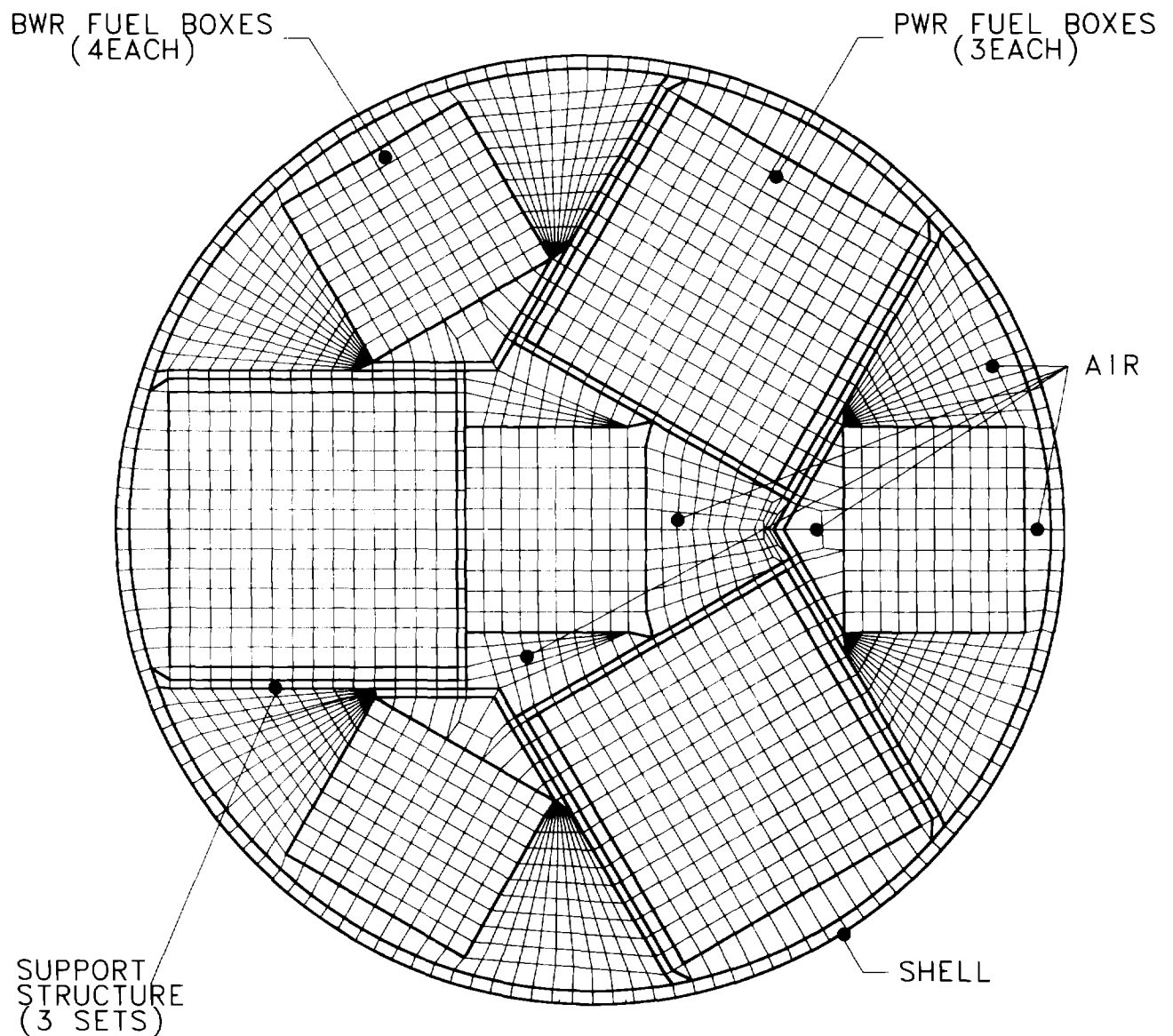
F.E. MODEL ASSUMES CONSTANT PROPERTIES ALONG LENGTH

Figure 2c. Finite element model used for 2-D analysis of container for the cases with gas fill elements.

III. 3-D Analysis Results

In review, the 3-D analyses model 350 m of tuff between the container midplane and the earth's surface for one quadrant of the 8 X 30-m rectangular section associated with one container. It has adiabatic planes at 4 and 15 m from the container centerline (Figure 1a). Volumetric heat generation based on the container thermal load and the borehole volume provides the heat source. A 25 $^{\circ}$C boundary condition at the earth's surface provides the heat sink. The analyses will be used to define the borehole wall temperature-time history for use by the 2-D analyses as well as define the time the borehole wall temperature falls below 97 $^{\circ}$C or tuff temperatures exceeds 200 $^{\circ}$C.

Figure 3 shows the predicted temperature-time histories for three nodes in the tuff for the **3-D Reference Case** [Case 1a/3-D:coarse mesh case]. The three nodes are located on the container midplane (Figure 1a). Node 13 is the location of the peak temperature on the borehole wall. Nodes 56 and 11 are on the adiabatic midplanes between adjacent boreholes and adjacent drifts, respectively. The node numbers identifying the curves are shown in parentheses. The minimum allowable borehole wall temperature, 97 $^{\circ}$C, is shown for reference. An expanded view of the temperature-time history for the first 50 yr is shown as an inset in the upper right hand corner of the figure. Figure 4 shows, for the time of maximum borehole wall temperature, lines of constant temperature (isotherms) on the borehole wall and on the surfaces of the tuff model radiating from the container axis. The borehole wall temperature-time history is documented in Table 3.

For the 3-D coarse mesh case, the maximum temperature of the borehole wall, 204 $^{\circ}$C, occurs at about 18 yr after emplacement. The temperature remains near the maximum value from 4 to 50 yr. The borehole wall stays above the 97 $^{\circ}$C minimum required temperature over the entire 1000-yr analysis period. Node 56, which is 4 m from the borehole axis, reaches a maximum temperature of about 149 $^{\circ}$C at approximately 50 yr after emplacement. Node 11 (15 m from the

borehole axis) reaches a maximum temperature of 125 $^{\circ}$C at about 75 yr. The tuff temperature 1 m from the borehole wall never exceeds 200 $^{\circ}$C. Figure 4 shows that at the time of peak temperature the heat flow in the tuff becomes one-dimensional about 20 borehole diameters above the container midplane.

Figure 5 compares the predicted temperature-time histories of the same three nodes for the case with the refined mesh and shorter calculative time step length [Case 1b/3-D:fine mesh case]. The histories for the same three nodes from the reference case are included for comparison. The peak temperature of the borehole wall, 211 $^{\circ}$C, is 7 $^{\circ}$C hotter than the reference case. Additional cases may be run during a later study to see if further refining the mesh increases the borehole wall temperature. The borehole temperature-time history for the 3-D fine mesh case is also documented in Table 3.

Figure 6 compares the isotherms near the borehole for these two cases. Note that the refined zoning/time step model results in larger temperature gradients near the borehole wall. Because this calculation was made near the end of the 2-D analysis series, I used the less conservative borehole wall temperature-time history from the 3-D coarse mesh case for all but the best model thermal analysis case. That case uses the the hotter time history resulting from the 3-D fine mesh analysis.

Figure 7 shows predicted temperature-time histories from the 3-D analysis of tuff surrounding a container with an equal weight of 5-yr-old fuel [Case 6/3-D:5-year fuel case]. The zoning and time step length correspond to that of the 3-D reference case. The plotted time histories are for the same three nodes previously documented. Figure 8 shows the isotherms for this case at the time of maximum borehole wall temperature.

For the 5-year fuel case the maximum temperature of the borehole wall, 248 $^{\circ}$C, occurs at about 1 yr after emplacement. This temperature stays above 120 $^{\circ}$C over the entire 1000 yr. The tuff

temperature 1 m into the tuff from the borehole wall reaches a maximum
of about 185 $^{\circ}$C after some 30 yr. Note the spacing of the isotherms
shown in Figure 8 indicates that for the time of maximum temperature
the heated region is concentrated to within 1 to 2 m of the borehole.
The borehole temperature-time history for the 5-year fuel case is
documented in Table 3.

Figure 9 shows borehole wall predicted temperature-time
histories for the model with the adiabatic ground surface
[Case 11/3-D:adiabatic surface case] and the 3-D reference case. The
effect of assuming an adiabatic upper surface is only slightly
noticeable near the end of the 1000-yr analysis period. Thus the heat
flow 350 m from the container midplane is significant only after the
first 1000 yr of the storage.

Figure 10 compares the results from the Case 12/3-D:700 m depth
case and the 3-D reference case (350-m model). Comparisons of the
isotherms indicate that because the heat flow is nearly symmetric
about the centerplane of the container. The borehole wall only senses
the non-symmetric boundary conditions after 700 yr of storage.

Finally, Figure 11 shows the temperature-time history for
Case 13a/3-D:SCP layout case. The peak borehole wall temperature,
237 $^{\circ}$C, is 30 $^{\circ}$C hotter than the corresponding case with 8 X 30 m
spacing. For a 20% increase in LPD over the reference case, the
difference between the peak temperature and the upper surface
temperature for this model increased by 16%.

At the close of this section on 3-D analyses, let me restate the
caveats for these results. These predictions assume that the tuff
section and container are modeled as if surrounded by an infinite
array of similarly sized tuff sections housing containers with the
same thermal loads emplaced nearly at the same time. Containers
storing this high a thermal load would more probably be dispersed
throughout the repository among containers with lower loads, thus
leading to lower temperatures. For a given fuel age, variations in

the LPD could be used to scale the expected change in the peak-borehole-wall to upper-surface temperature difference. In all cases the only heat sink is the earth itself (with its upper surface set to 25 $^{\circ}$C where the model permits). Perturbations in the heat flow patterns due to drift tunnels or heat transfer to ventilation air circulating in these tunnels are not included in the model. Addition of these effects would lower the temperatures even more.

The effects of various loading distributions and the presence of ventilated drift tunnels will be modeled in detail in other analytic tasks this year. Some earlier studies using linear superposition theory for multiple sources (Citations 7,8 of Appendix A) indicated that the maximum borehole wall temperature and its corresponding peak cladding temperature may be substantially lower than the infinite array value. These studies concluded that the effect of including the drift tunnel in the model would decrease these temperatures by 5 to 10 $^{\circ}$C. Including the drift tunnel and its associated humidity and heat removal by ventilation will also allow the analyst to determine if the barrier design could satisfy another project thermal limit. This limit requires that the temperature of the drift floor for the first 30 yr must remain cooler than the 50 $^{\circ}$C limit to provide for manned operations in the drift. Because the borehole wall temperature for arrays of highly loaded containers nears 200 $^{\circ}$C, these calculations become an absolute necessity.

HYBRIB(3PWR4BWR) WASTE CONTAINER/10YR-NORMAL BASE CASE 1 12/18/87 GLJ
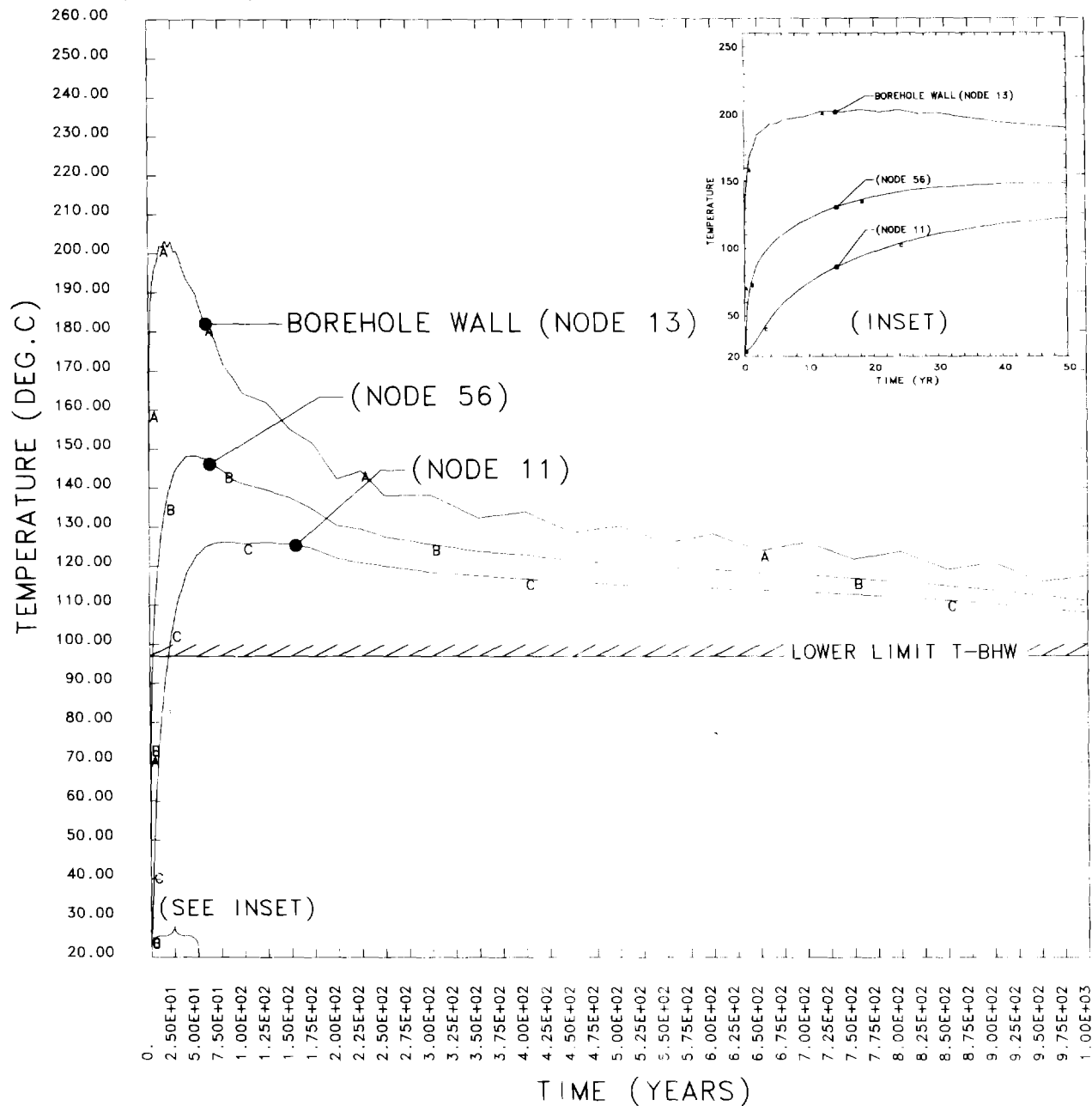
Figure 3. The temperature of the borehole wall for the reference case exceeds 204 °C at 18 yr after emplacement and remains above 97 °C for the entire 1000 yr.

HYBRIB(3PWR4BWR) WASTE CONTAINER/10YR—NORMAL BASE CASE 1 12/18/87 GLJ

TIME = 1.80000E+01 YEARS

MIN= 2.500E+01 AT NODE 1320
MAX= 2.040E+02 AT NODE 1

CONTOURS OF TEMPERATURE
(DEG.C)
A= 5.00E+01
B= 7.50E+01
C= 1.00E+02
D= 1.25E+02
E= 1.50E+02
F= 1.75E+02
G= 2.00E+02
H= 2.25E+02
I= 2.50E+02

BOREHOLE REGION ISOTHERMS

Z
Y X
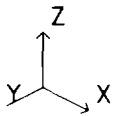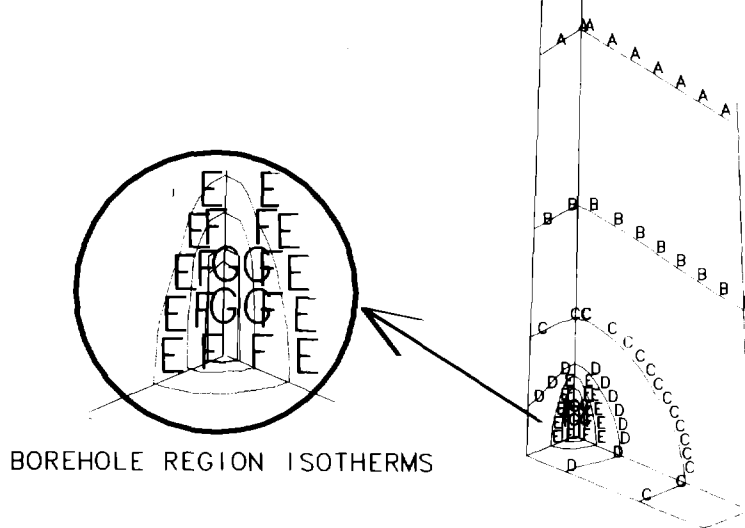
Figure 4. The heat flow in the tuff is one-dimensional above about
20 borehole diameters from the container midplane.

HYBRIB(3PWR4BWR) WASTE CONTAINER/10YR-NORMAL BASE CASE 1 12/18/87 GLJ
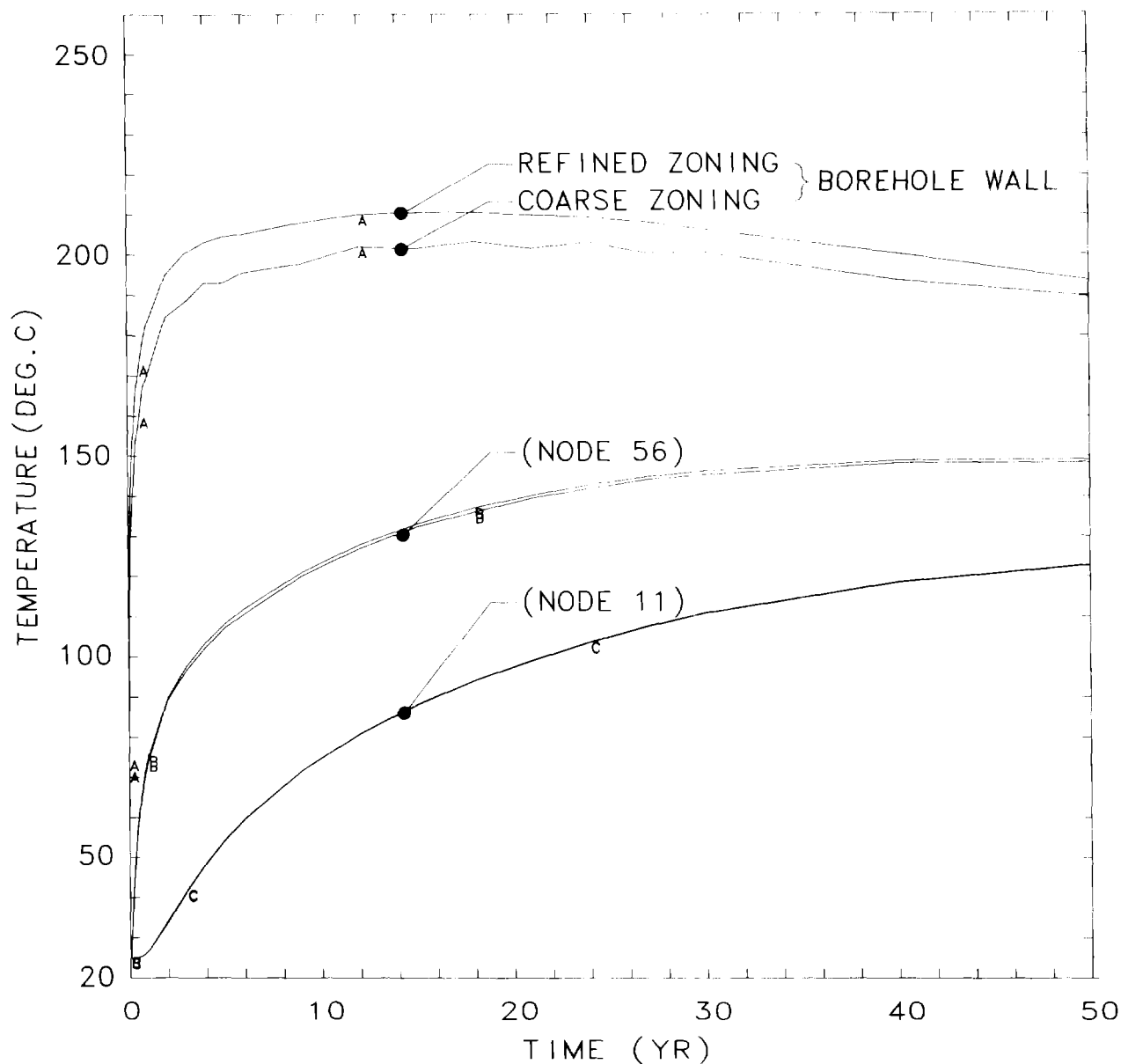
Figure 5.   The predicted peak temperature of the borehole wall is 7 °C
            hotter for the f.e. model with refined zoning and time step
            length than the 3-D reference case with its coarser zoning
            and time step.

HYBRIB(3PWR4BWR) WASTE CONTAINER/10YR—NORMAL BASE CASE 1 12/18/87 GLJ

CONTOURS OF TEMPERATURE

TIME = 1.80000E+01 YEARS

(DEG.C)

TIME = 1.80000E+01 YEARS

A=	5.00E+01
B=	7.50E+01
C=	1.00E+02
D=	1.25E+02
E=	1.50E+02
F=	1.75E+02
G=	2.00E+02
H=	2.25E+02
I=	2.50E+02

MIN= 2.500E+01 AT NODE   1320
MAX= 2.040E+02 AT NODE   1

MIN= 2.500E+01 AT NODE   2640
MAX= 2.107E+02 AT NODE   13
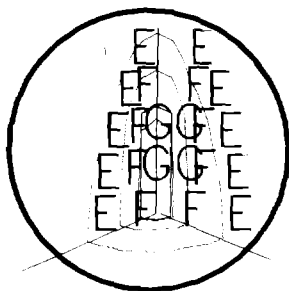
BOREHOLE REGION ISOTHERMS
COARSE ZONING
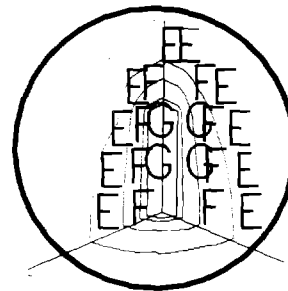
BOREHOLE REGION ISOTHERMS
REFINED ZONING

Figure 6. The near-field temperature gradient in the tuff increases
somewhat in the case with the refined zoning and time step
length.

HYBRIB(3PWR4BWR) WASTE CONTAINER/ 5YR-NORMAL BASE CASE 6 12/18/87 GLJ
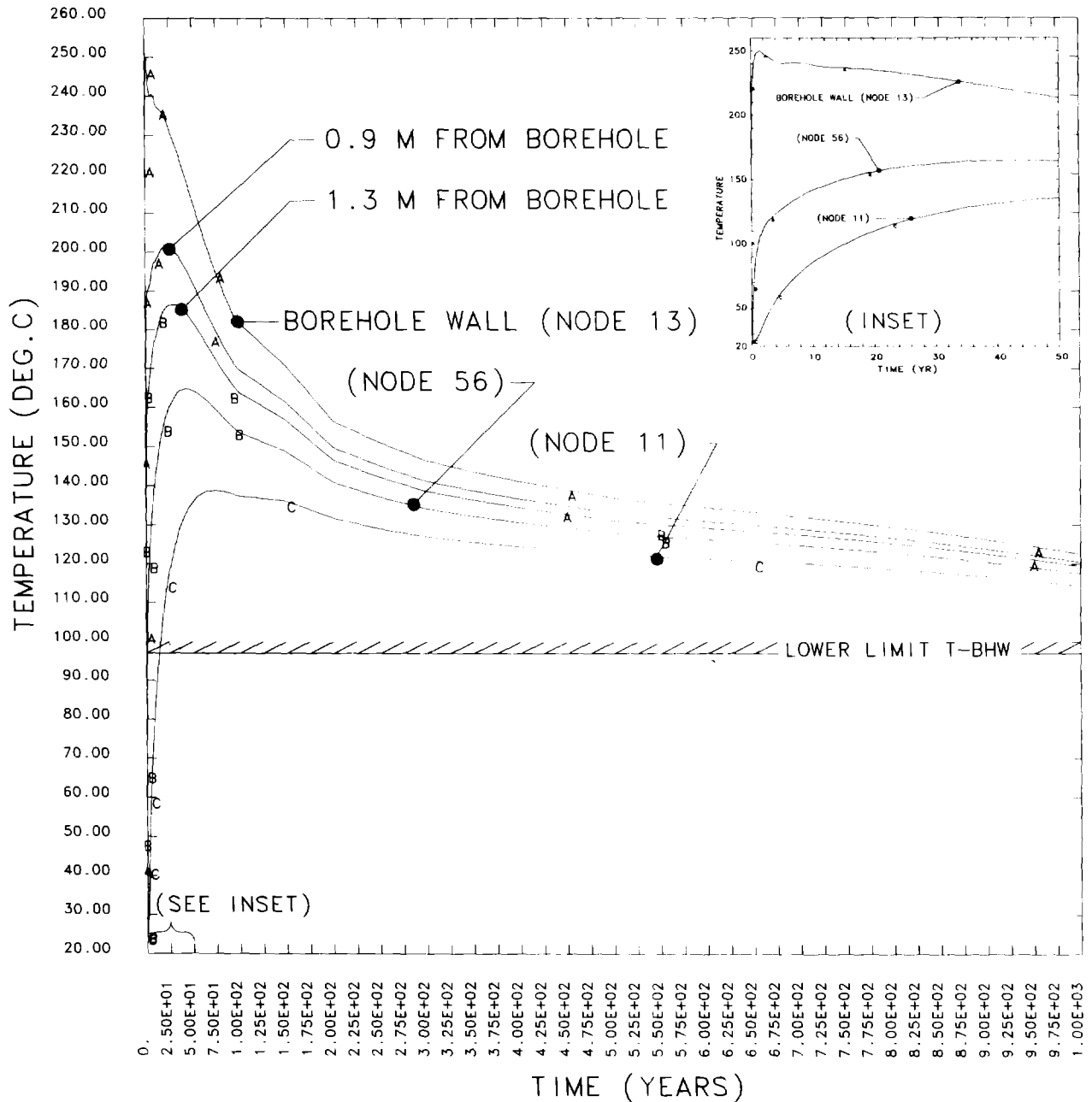
Figure 7. The maximum temperature of the borehole wall for the f.e.
model with 5-yr-old fuel nears 250 $^{\circ}$C at about 1 yr after
emplacement. The tuff at 1 m never exceeds 200 $^{\circ}$C.

HYBRIB(3PWR4BWR) WASTE CONTAINER/ 5YR-NORMAL BASE CASE 6 12/18/87 GLJ

TIME = 1.05000E+00 YEARS

MIN= 2.500E+01 AT NODE 2266
MAX= 2.483E+02 AT NODE   13

CONTOURS OF TEMPERATURE
(DEG.C)
A= 5.00E+01
B= 7.50E+01
C= 1.00E+02
D= 1.25E+02
E= 1.50E+02
F= 1.75E+02
G= 2.00E+02
H= 2.25E+02
I= 2.50E+02

BOREHOLE REGION ISOTHERMS

Z
Y   X
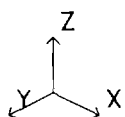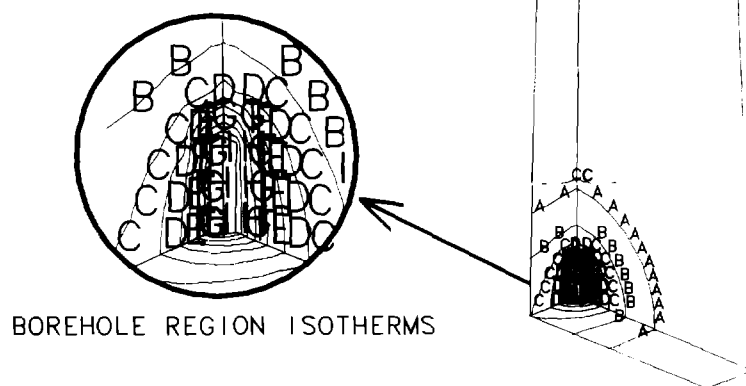
Figure 8.   The near-field temperature gradient in the tuff at the time
of peak borehole wall temperature is very large. The tuff
at 1 m never exceeds 200 °C.

HYBRIB(3PWR4BWR) WASTE CONTAINER/10YR-NORMAL BASE CASE 1 VS CASE 11
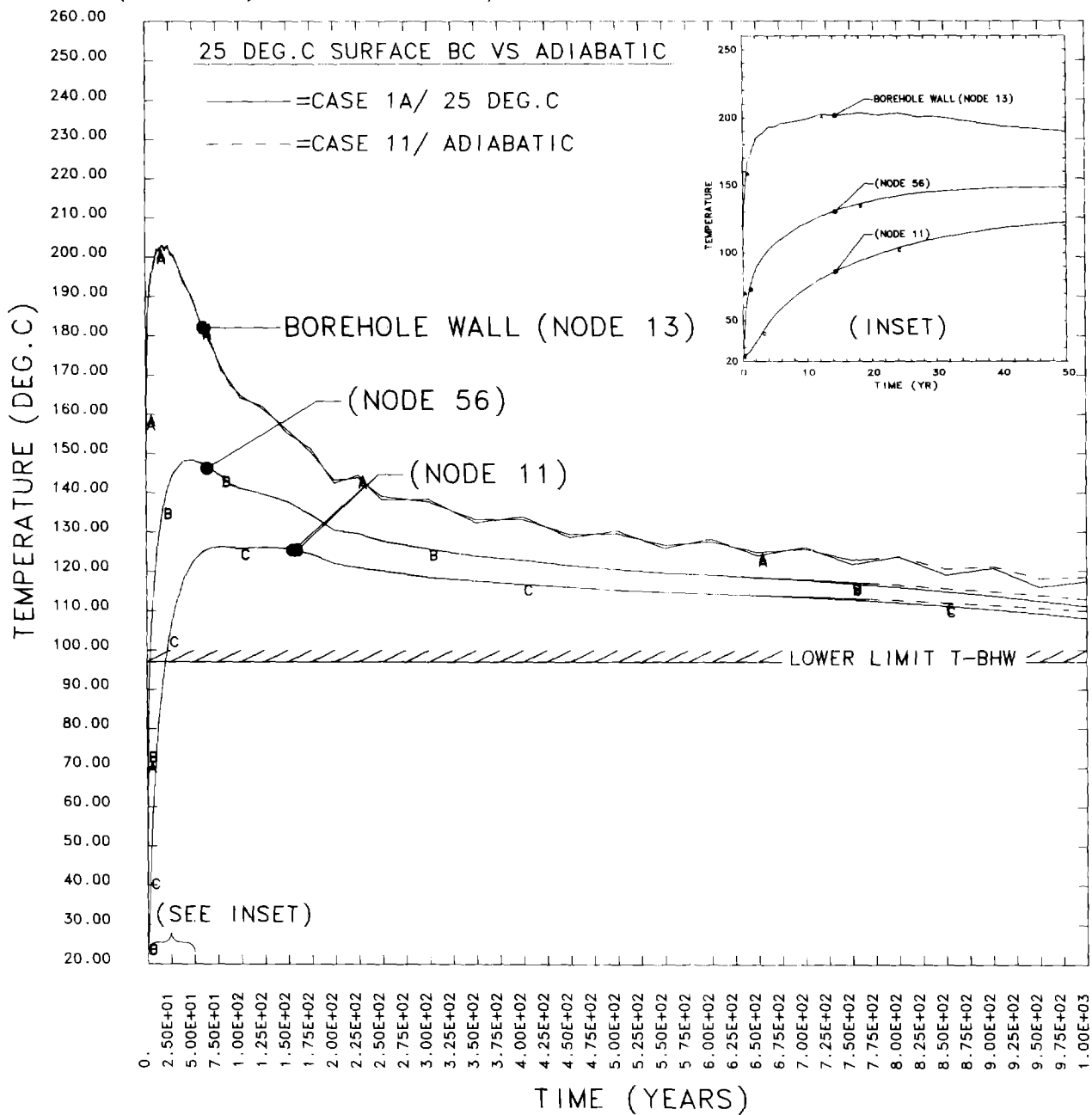
Figure 9. The predicted temperature of the tuff depends on the boundary condition at the earth's surface only at times nearing 1000 yr.

HYBRIB(3PWR4BWR) WASTE CONTAINER/10YR-NORMAL BASE CASE 1 12/18/87 GLJ

350 M MODEL VS 700 M MODEL

——— =CASE 1A/ 350 M

- - - =CASE 12/ 700 M

BOREHOLE WALL (NODE 13)

(NODE 56)

(NODE 11)

(INSET)

LOWER LIMIT T-BHW

(SEE INSET)

HYBRIB(3PWR4BWR) WASTE CONTAINER/10YR-NORMAL
TIME WORD = 1.80000E+01 YEARS

MIN= .250E+02 AT NODE 1322
MAX= .204E+03 AT NODE 1

CONTOURS OF TEMPERATURE
(DEG.C)

A= 5.00E+01
B= 7.50E+01
C= 1.00E+02
D= 1.25E+02
E= 1.50E+02
F= 1.75E+02
G= 2.00E+02
H= 2.25E+02
I= 2.50E+02

BOREHOLE REGION ISOTHERMS

Figure 10. Differences in thermal performance between the 350 m case
and the 700 m case only become noticable after 800 yr.
Isotherms for the 700 m case show that the heat flow is
nearly symmetric about the container's centerplane.

HYBRID(3PWR4BWR) WASTE CONTAINER/10YR—NORMAL SCP CASE 13A
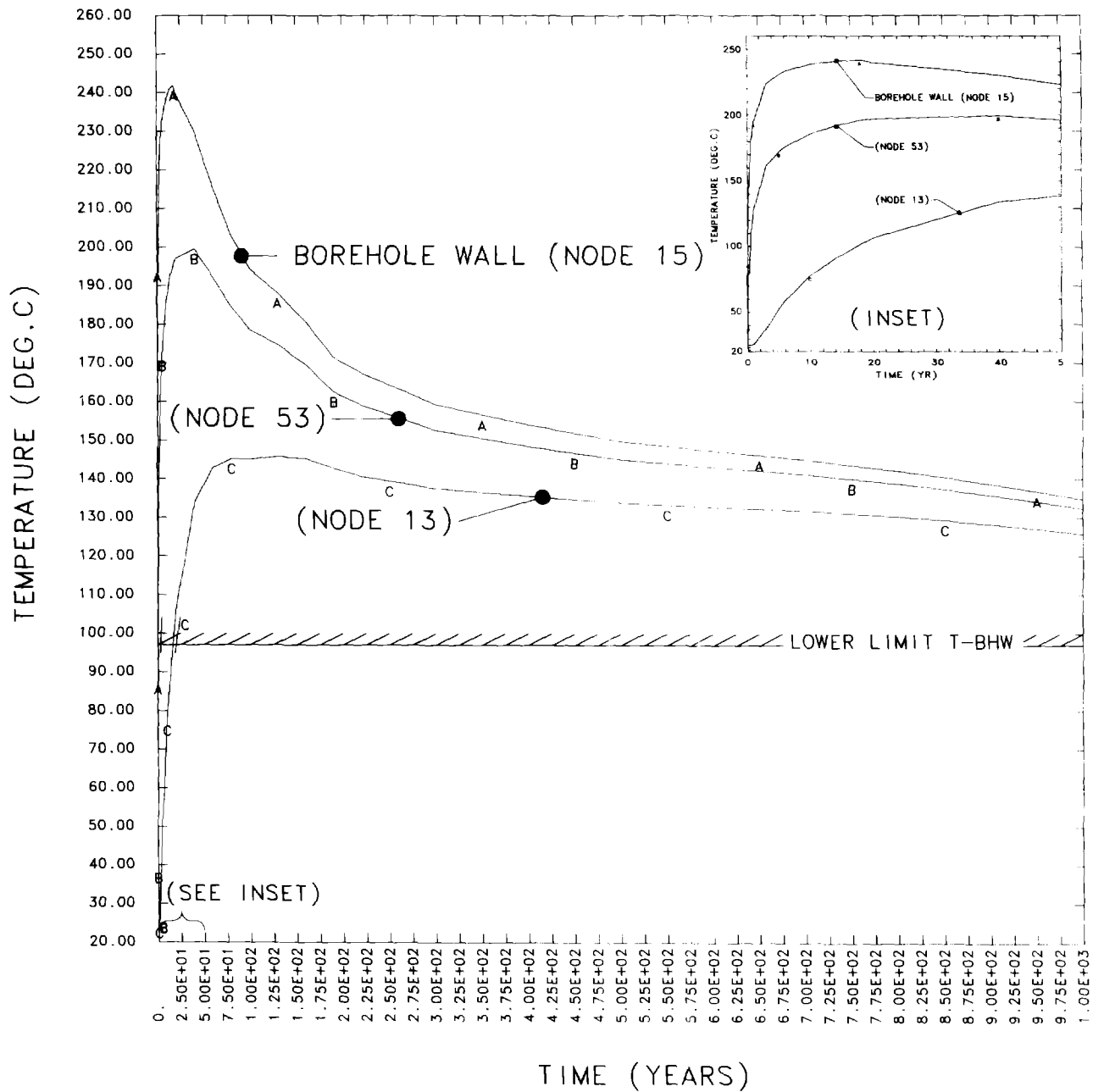
Figure 11. Storing 10-yr-old fuel at a 1.73:1 consolidation with the
15 X 126 ft spacings defined in the SCP results in a peak
borehole wall temperature of 237°C.

IV.   2-D Analysis Results

In review, the 2-D analyses model a mean cross section of the container midplane (Figure 1b). The heat source from the container thermal load is modeled as volumetric heat generation referenced to the PWR and BWR fuel-can volumes. The appropriate borehole wall temperature-time history from the 3-D analyses provides the heat sink. The analyses will determine if the fuel cladding temperature exceeds 350 $^{\circ}$C and the prediction's sensitivity to various model parameters.

Figure 12 shows the predicted temperature-time histories of four nodes from the 2-D analysis of a container whose shell and internal support structure are made of 304 stainless steel [Case 1:304SS]. The node numbers identifying the curves are shown in parentheses. Node 2 is on the external surface of the container, and Node 1909 is on the borehole wall (see Figure 1b). Node 403 is near the center of the leftmost PWR fuel canister, and Node 336 is near the center of the central BWR fuel canister. These nodes were chosen as locations near the peak fuel temperatures after a review of the isotherm plots for times of peak cladding temperature (see Figure 13). These same nodes will be used consistently for documenting the peak temperatures, although the location of the actual peak shifts slightly with the thermal model. Because the local temperature profile near the center of the fuel canister is nearly flat, the variation in temperature between the plotted node and the actual peak temperature location should be less than 2 $^{\circ}$C. The temperatures at these nodes are assumed to represent an upper bound on the fuel cladding temperature. The maximum allowable cladding temperature is shown for reference in the time history plots where needed. An expanded view of the temperature-time history for the first 50 yr is shown as an inset in the upper right-hand corner.

The maximum temperature of the PWR fuel (i.e., cladding) for the 304SS case is 329 $^{\circ}$C. It occurs at about 3 yr after emplacement. The maximum temperature of the BWR cladding for the 304SS case is 313 $^{\circ}$C,

which also occurs about 3 yr after emplacement. These peak cladding
temperatures are substantially warmer than those of many of the
previous analyses. In fact they approach the 350 $^{\circ}$C maximum allowed
value. The cladding temperature remains near the peak value for only
about 5 yr.

Outside surface temperatures of the container shell are used to
evaluate the corrosion rate. For this container the temperature
around the outside diameter of the container shell may vary by as much
as 10 $^{\circ}$C (see Figure 18). The warmest portion of the external surface
of the container comes within 2 to 5 $^{\circ}$C of the uniform borehole wall
temperature over the 1000-yr analysis period. The coolest portion
stays about 5 to 15 $^{\circ}$C warmer than the borehole wall. A 3-D analysis
of the container and tuff would show variations in the borehole wall
temperature giving a more uniform variation in the temperature
difference between the container surface and the borehole wall.

A heat balance on the predicted heat transfer from the container
shell to the borehole wall indicates that only 20% of the heat is
transferred by conduction/convection through the air/water vapor
layer, and the remaining portion is transferred by thermal radiation.
This 1:4 ratio is characteristic of past analyses.

Figure 14 shows the predicted temperature-time histories of the
same four key nodes for the analysis modeling the design with
7030 cupronickel container/support materials [Case 2:7030 case].
Isotherms at the time of peak temperatures are shown in Figure 15.

The maximum temperature of the PWR cladding for the 7030 case is
325 $^{\circ}$C and the maximum temperature of the BWR cladding is 304 $^{\circ}$C.
Note that because of the improved conduction through the support
structure the central BWR canister (with its smaller heat source)
stays much cooler than the hottest PWR canister. They reach a common
peak temperature after 100 yr.

Figure 16 shows the predicted temperature-time histories of the

Incoloy 825 container/support model [Case 3:IN825 case]. This is my **2-D Reference Case**. Isotherms at the time of peak temperatures are shown in Figure 17. Figure 18 shows a characteristic temperature profile around half of the container perimeter at the time peak cladding temperature occurs.

The maximum temperature of the PWR cladding for the IN825 case is 336 $^{\circ}$C. It also occurs at about 3.5 yr after emplacement. The corresponding maximum temperature of the BWR cladding is 323 $^{\circ}$C. I have used this case as the reference for the remaining studies because it gives the highest cladding temperature of the three cases testing the effect of material choice. Figure 19 contains a synopsis of these three cases in terms of the peak cladding temperatures of the PWR fuel. Because the effect of structural material choice is small (<12 $^{\circ}$C between the poorest heat conductor, IN825, and the best conductor, 7030), it suggests that most of the decay heat is transferred to the shell by thermal radiation.

Figure 20 shows results of the 2-D analysis of the Incoloy 825 container with loosely packed bentonite backfill surrounding the container [Case 4:loose backfill]. Nodes 2, 403, and 336 are the same as before, but Node 2195 now defines the borehole wall temperature (i.e., edge of backfill). Figure 21 shows the isotherms in the container and tuff backfill.

The maximum temperature of the PWR cladding for the loose backfill case is 391 $^{\circ}$C, while the maximum temperature of the BWR cladding is 383 $^{\circ}$C. The loose bentonite backfill is a significantly poorer conductor for the thermal load to the borehole wall than the combined conduction, convection, and thermal radiation across the humid air layer when no backfill is installed. Analyses documented in References 5 and 7 on the effect of backfill installed within the container resulted in similar increases in peak cladding temperature.

Figure 22 shows the predicted temperature-time histories of the 2-D analysis of the Incoloy 825 container with firmly packed bentonite

backfill surrounding the container [Case 14:firm backfill]. Figure 23 shows the isotherms in the container and backfill at the time of peak cladding temperature.

The maximum temperature of the PWR cladding for the firm backfill case is 341 $^{\circ}$C while the maximum temperature of the BWR cladding is 329 $^{\circ}$C. While the firmly packed bentonite's thermal conductivity is only three to four times higher than the loosely packed bentonite, it lowers the peak cladding temperature back to nearly the value predicted for the case with the unfilled annulus.

Figure 24 shows a time history comparison of the IN825 case (no backfill), the loose backfill case, and the firm backfill case in terms of the peak cladding temperatures of the PWR fuel. These results are very similar to those of previously reported analyses. It is not possible to conclude that the thermal performance of firmly packed bentonite backfill is acceptable because these results are so sensitive to the assumed thermal conductivities of the backfill, which are not necessarily representative of conditions in the repository.

Figure 25 compares the peak cladding temperatures of the PWR fuel of the IN825 case (no contact thermal resistance between the support structure) with the case using calculated contact thermal resistances based on a 100-psi contact pressure and an air interface heat transfer medium (Case 5:contact resistance case). The resultant order-of-magnitude change in contact resistance does not have an observable effect in the temperature history of the PWR or BWR fuel canisters. Again, this is due to the dominance of the thermal radiation heat transfer mode inside the container.

Figure 26 contains temperature-time histories from the 2-D analysis of the Incoloy 825 container loaded with an equal number of 5-yr-old fuel rods replacing the 10-yr-old fuel [Case 6:5-year fuel case]. Isotherms at the time of peak temperatures are shown in Figure 27.

The maximum temperature of the PWR cladding for the 5-year fuel case is 411 $^\circ$C. It occurs at about <u>8 months</u> after emplacement. The maximum temperature of the BWR cladding is 399 $^\circ$C. I included this case in the hybrid thermal performance study to give a feeling for the effect of storing 5-yr-old fuel in a contiguous repository array. High-burnup 10-yr-old fuel would give a similar response.

Figure 28 and Figure 29 document the thermal response of the Incoloy 825 container if a surface emissivity of 0.5 is assumed on inside surfaces [Case 7:emissivity case] rather than the 0.8 value that was used in previous analyses. The thermal resistance to radiative heat transfer is inversely proportional to the surface emissivity. Thus I expected an increase in peak cladding temperature because the heat transfer inside the container is dominated by thermal radiation.

The maximum temperature of the PWR cladding for the altered emissivity case is 346 $^\circ$C, and the maximum temperature of the BWR cladding is 339 $^\circ$C. As with the highly conductive 7030 container, the smaller difference between the BWR and PWR peak temperatures primarily results from the increased dependence of heat transfer through the structural supports. Figure 30 compares the PWR and BWR thermal responses for the two values of surface emissivity. The lower (and more realistic) emissivity raises the peak temperature by about 10 $^\circ$C. This puts it just about on the maximum allowed cladding temperature.

The temperature-time histories shown in Figure 31 and the isotherms in Figure 32 model the thermal response of an Incoloy 825 container with thermal conductivities for the spent fuel canisters derived from measured temperature profiles [Case 8:fuel conductivity case].

The maximum temperatures of the PWR and BWR cladding for the fuel conductivity case are 322 and 315 $^\circ$C, respectively. The comparison with the reference case in Figure 33 shows the higher fuel

pack thermal conductivity lowers the peak temperature by 8 to 15 ^{o}C. This change substantially increases the thermal performance margin because the peak cladding temperature in the reference case is so near the maximum allowable.

The 2-D analysis of the Incoloy 825 container including the effect of heat conduction through the gas fill [Case 9:gas conduction] gives predicted temperature-time histories shown in Figure 34 and isotherms like those shown in Figure 35.

The maximum temperature of the PWR cladding for the gas conduction case is 335 ^{o}C, and the maximum temperature of the BWR cladding is 322 ^{o}C. The net 1 ^{o}C change in peak temperature between this case and the reference case implies that total heat conduction through the gas fill is minimal, and thermal radiation between inside surfaces remains the dominant heat transfer mode. Comparison of the isotherms in the structure and fuel for the gas conduction case with those for the reference case show no obvious differences. Including natural convection in the cavity heat transfer model would decrease the peak temperature further, but probably not enough to overwhelm the dominance of the thermal radiation.

Concluding these parametric studies, Figures 36 and 37 document the predicted temperature-time histories from a "best model" 2-D thermal analysis of an Incoloy 825 container incorporating information gained from the earlier analyses of this study. It uses the borehole wall time history of the fine-zoned tuff for the 10-yr-old fuel load (from the 3-D fine mesh case), a more accurate surface thermal emissivity for the internal surfaces equal to 0.5 (from Case 7), a fuel canister thermal conductivity derived from the Battelle-measured data (from Case 8), and internal heat conduction through the gas fill (from Case 9).

The maximum temperature of the PWR cladding for the best model case is 336 ^{o}C and the maximum temperature of the BWR cladding is 334 ^{o}C. The near equality of these peak temperatures results from the

combination of assumed higher thermal conductivity in the fuel pack, inclusion of heat transfer through the gas fill, and reduced heat transfer by thermal radiation.

To put these results in the context of the current repository borehole layout, Figures 38 and 39 show a prediction of the thermal performance of a container filled with 4100 W PWR and BWR fuel distributed among the same seven canisters [Case 13a:SCP layout]. The container is surrounded with similarly loaded containers on 15 X 126 ft borehole spacings (4.6 X 38.4 m). Except for the thermal load and borehole spacing, the model uses the same assumptions as the best model discussed previously.

The maximum temperatures of the PWR and BWR cladding for SCP layout case are 335 and 334 $^\circ$C, respectively. Thus, using the SCP-defined spacing would be acceptable with only a 15% decrease in the thermal load.

Because the 2-D results are driven by the borehole wall temperature-time history generated in the 3-D analyses, the caveats to the 3-D results are pertinent here also. Some additional cautions pertain just to the 2-D analyses. The models used for these temperature predictions assume that the mean section of the container analyzed is representative of the response of the whole container. Axial variations in geometry, material properties, and thermal load may cause temperatures to vary by 11 to 33 $^\circ$C from the mean section values (Reference 1 in Appendix B). Values assumed for the material properties, like the fuel canisters' thermal conductivity and structure's surface emissivity, may be off by 30 to 50%, thus significantly altering the container's predicted thermal performance. Finally, the large cavities between fuel canisters probably experience significant heat transfer from natural convection. This would reduce the fuel temperatures.

HYBRIB(3PWR4BWR) SS304 CONTAINER/10YR-NORMAL BASE CASE 1 12/18/87 GLJ
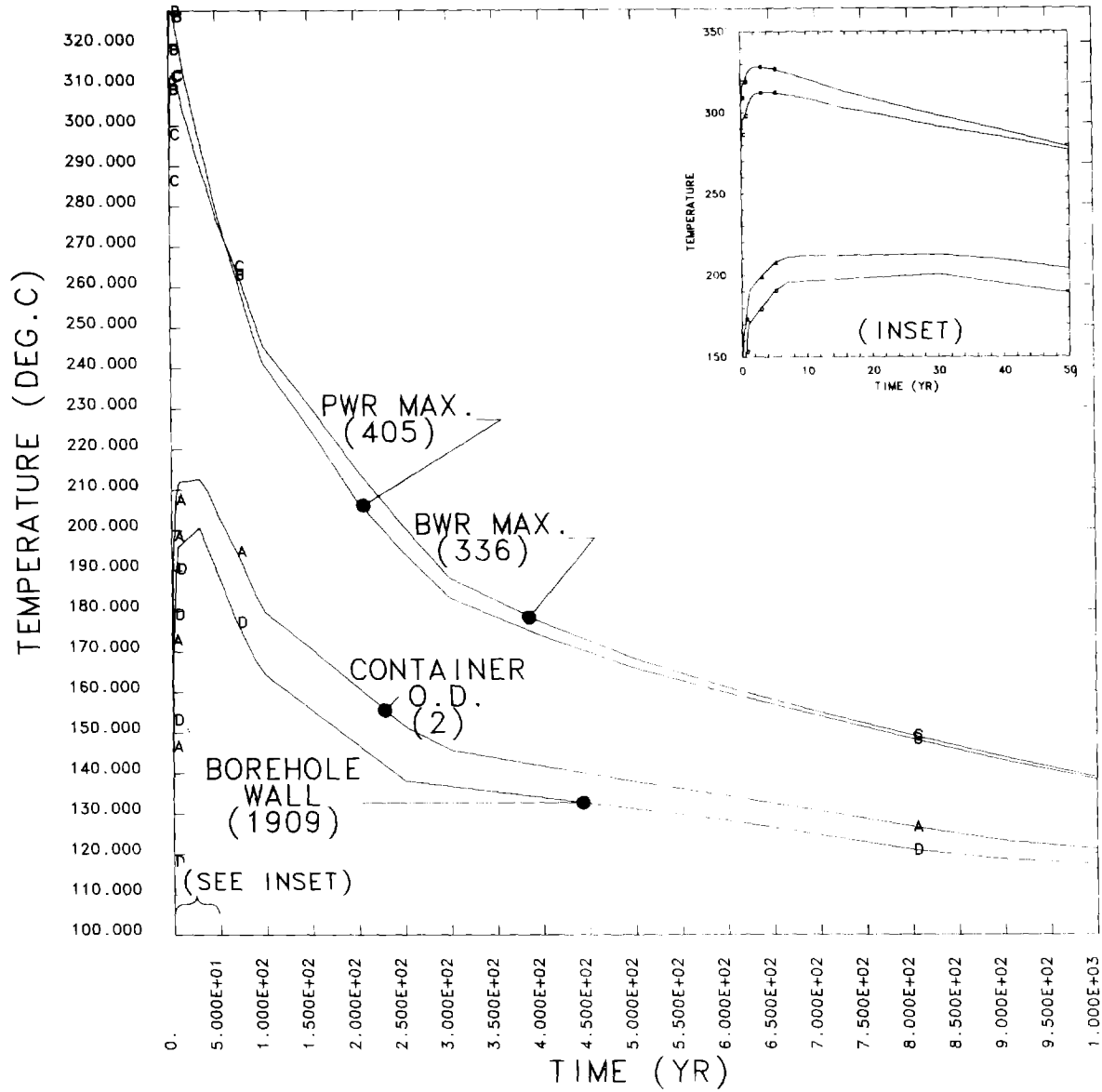
Figure 12. The peak temperature of the fuel cladding for the 304SS structure case is 329 °C. It occurs at about 3 yr after emplacement.

NNWSI HYB(3PWR4BWR) SS304 CONTAINER/10YR—NORMAL BASE CASE 1 12/18/87 GLJ
TIME=   3.80000E+00 YEARS
T—BOREHOLE WALL = 190 DEG.C

MIN(−)= 1.84E+02
MAX(+)= 3.28E+02
CONTOUR LEVELS
TEMPERATURE (DEG.C)

A= 2.00E+02

B= 2.20E+02

C= 2.40E+02

D= 2.60E+02

E= 2.80E+02

F= 3.00E+02

G= 3.20E+02

H= 3.40E+02

I= 3.60E+02

● = HOTTEST FUEL SPOTS
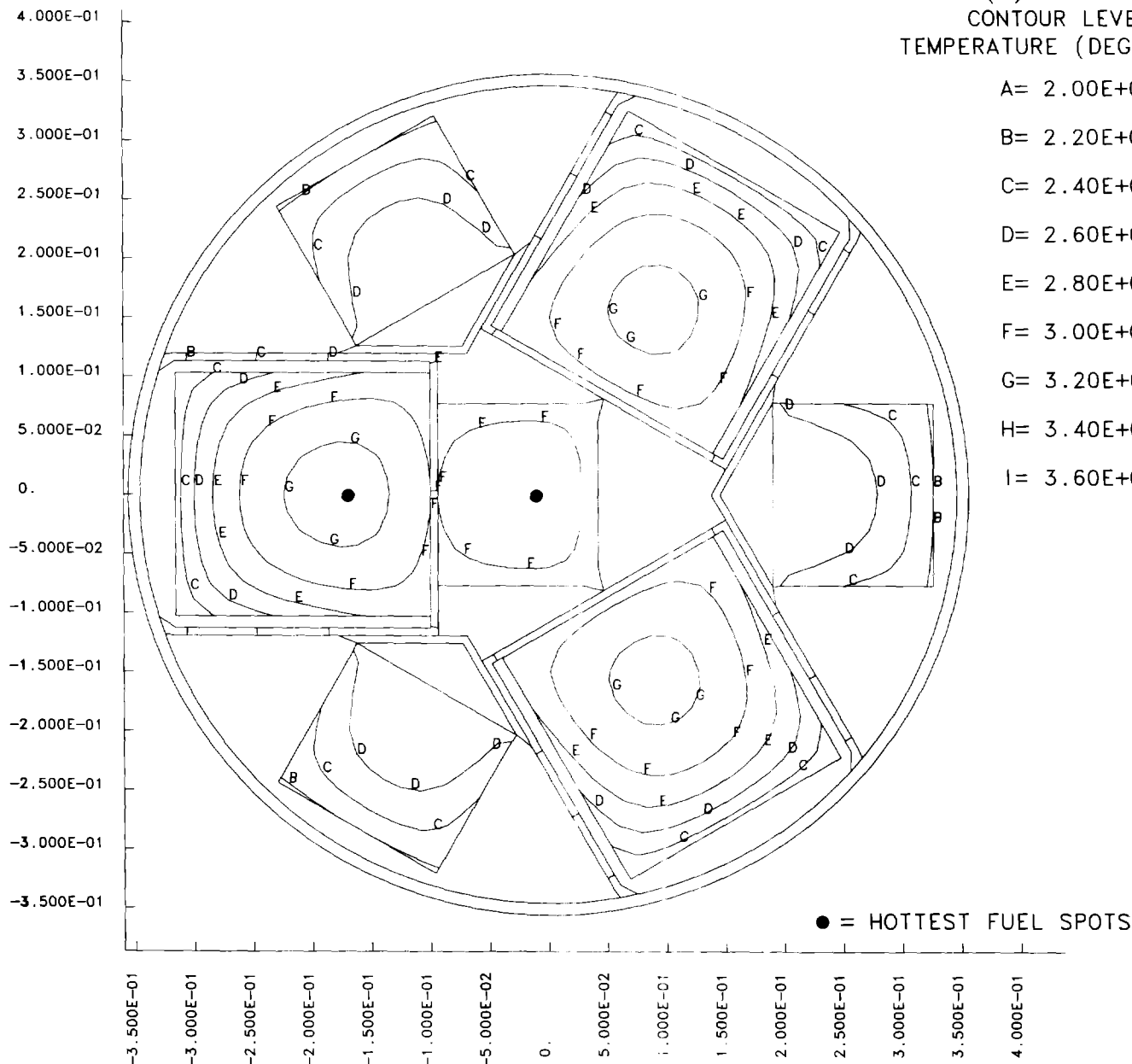
Figure 13. Isotherms for the 304SS case at about 3 yr after
emplacement show the peak cladding temperatures occur near
the center of the leftmost PWR and central BWR fuel
canisters.

NNWSYB(3PWR4BWR) 7030 CUNI CONT./10YR-NORMAL BASE CASE 2 12/18/87 GLJ
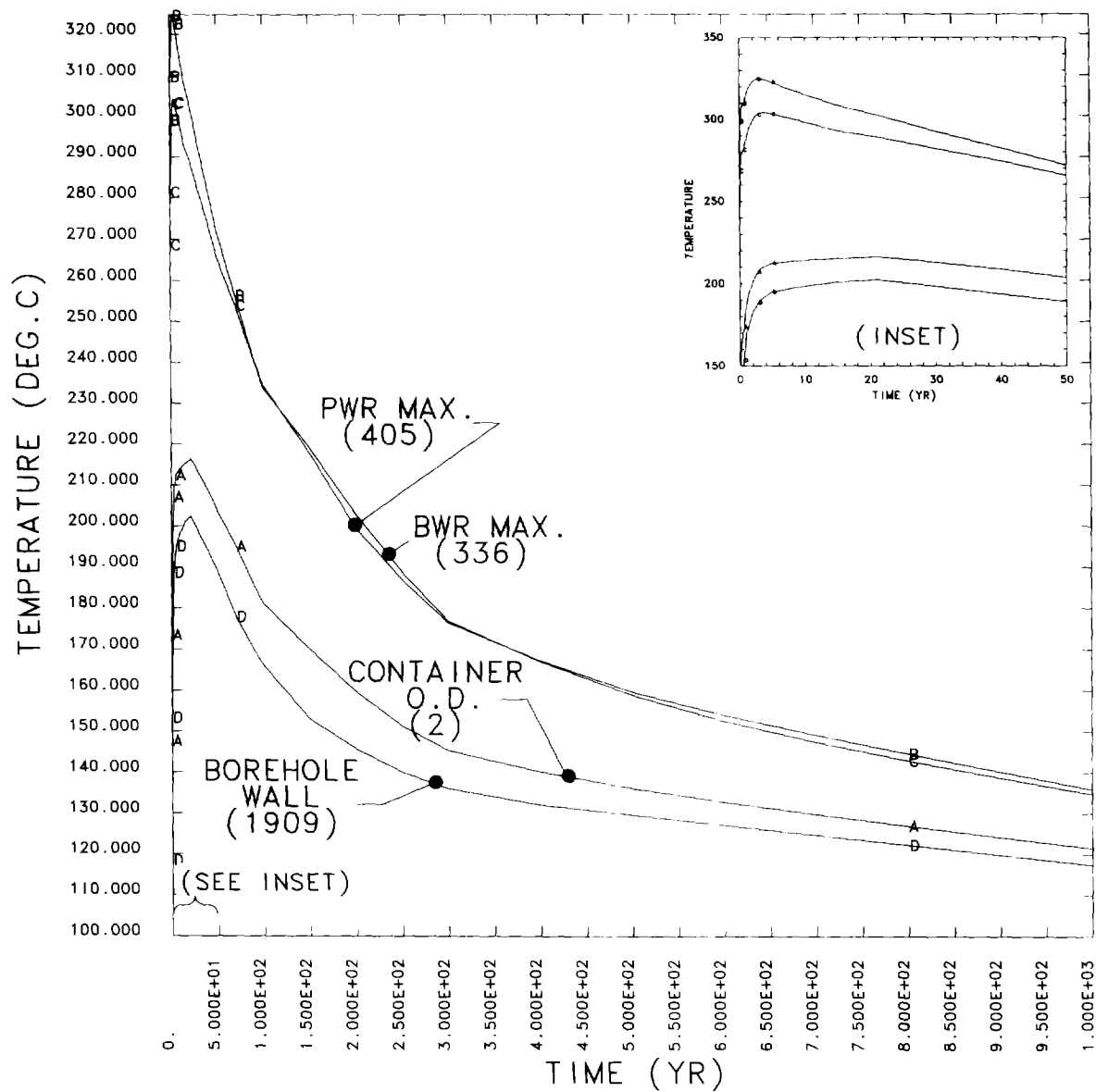
Figure 14. The peak temperature of the fuel cladding for the 7030 structure case, 325 °C, occurs about 3 yr after emplacement.

NNWSI HYB(3PWR4BWR) 7030 CUNI CONT./10YR-NORMAL BASE CASE 2 12/18/87 GLJ
TIME=   3.80000E+00 YEARS
T-BOREHOLE WALL = 190 DEG.C

MIN(-)= 1.92E+02
MAX(+)= 3.25E+02
CONTOUR LEVELS
TEMPERATURE (DEG.C)

A= 2.00E+02

B= 2.20E+02

C= 2.40E+02

D= 2.60E+02

E= 2.80E+02

F= 3.00E+02

G= 3.20E+02

H= 3.40E+02

I= 3.60E+02

● = HOTTEST FUEL SPOTS
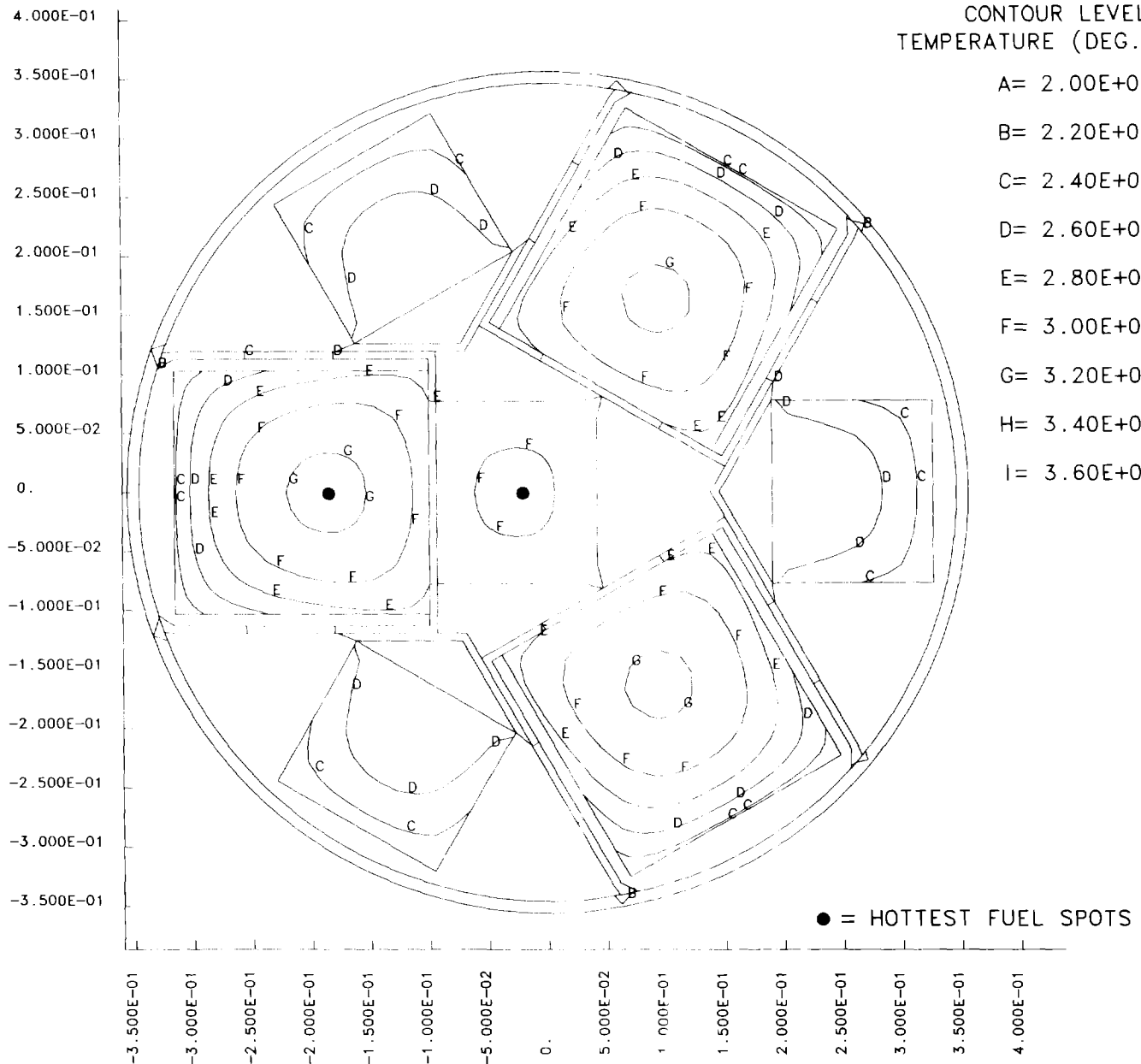
Figure 15. Isotherms for the 7030 case at about 3 yr after emplacement
show the central BWR canister is much cooler than the 304SS
case.

HYBRIB(3PWR4BWR) INCOLOY 825 CON/10YR-NORMAL BASE CASE 3 12/18/87 GLJ
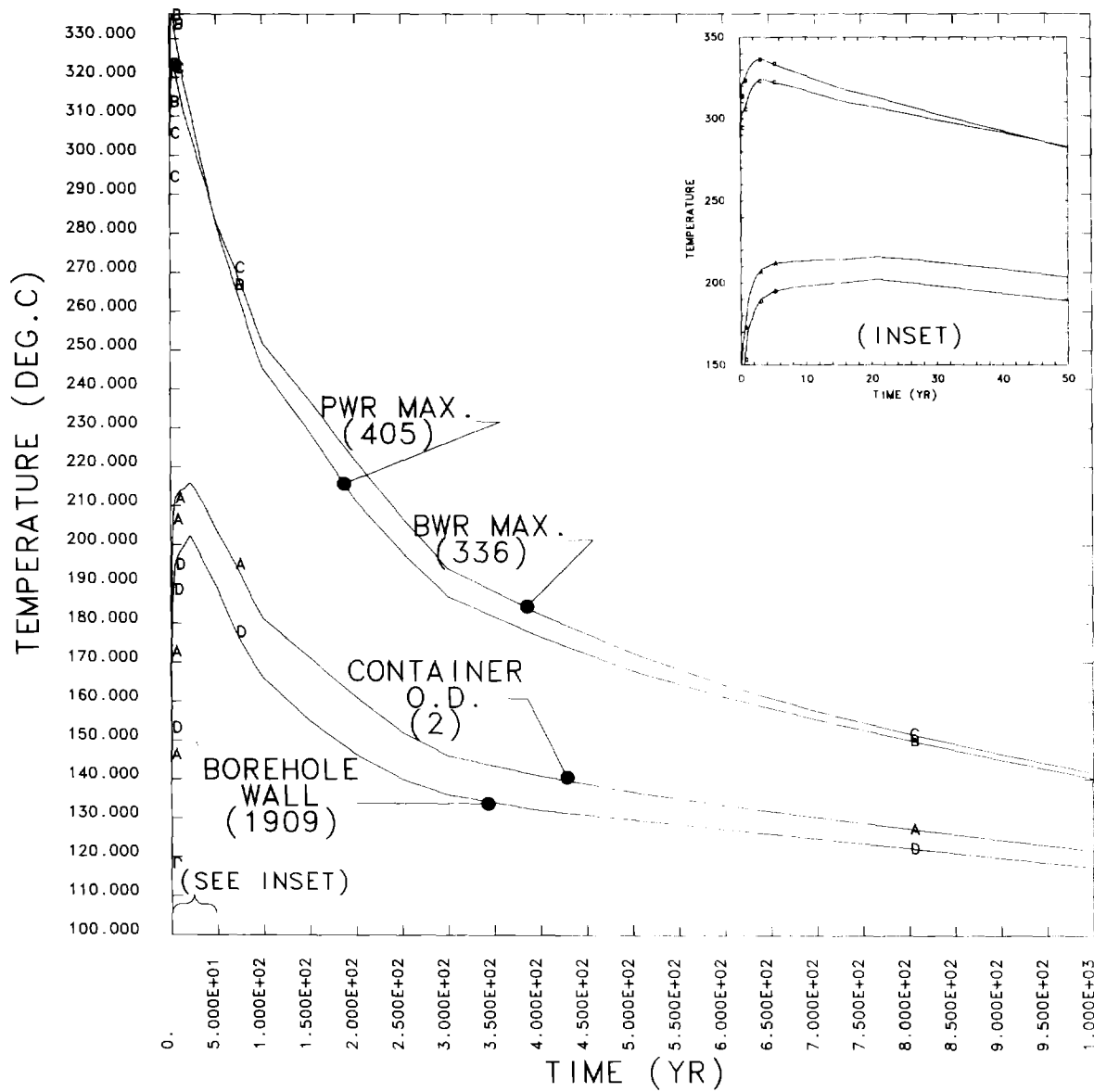
Figure 16. The peak temperature of the fuel cladding for the IN825
structure case (2-D Reference Case) is 336 °C.

NNWSI HYB(3PWR4BWR) INCOLOY 825 CON/10YR-NORMAL BASE CASE 3 12/18/87 GLJ
TIME=   3.80000E+00 YEARS
T-BOREHOLE WALL = 190 DEG.C

MIN(-)= 1.92E+02
MAX(+)= 3.36E+02
CONTOUR LEVELS
TEMPERATURE (DEG.C)

A= 2.00E+02

B= 2.20E+02

C= 2.40E+02

D= 2.60E+02

E= 2.80E+02

F= 3.00E+02

G= 3.20E+02

H= 3.40E+02

I= 3.60E+02

● = HOTTEST FUEL SPOTS
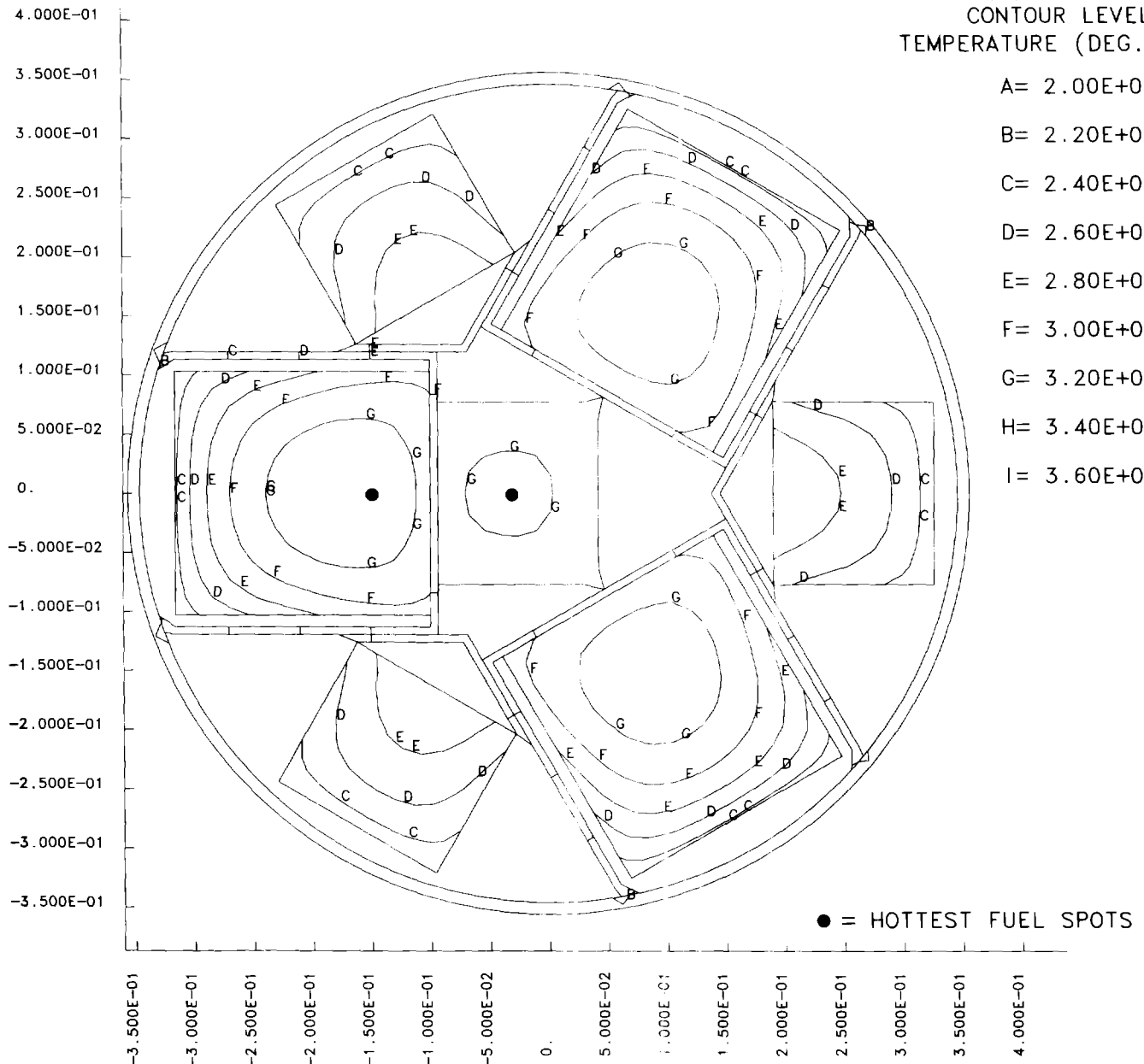
Figure 17. Isotherms for the IN825 case at about 3 yr after
emplacement.

NNWSI HYB(3PWR4BWR) INCOLOY 825 CON/10YR—NORMAL BASE CASE 3 12/18/87 GLJ
TIME= 3.80000E+00 PROFILE OF TEMPERATURE ALONG PATH
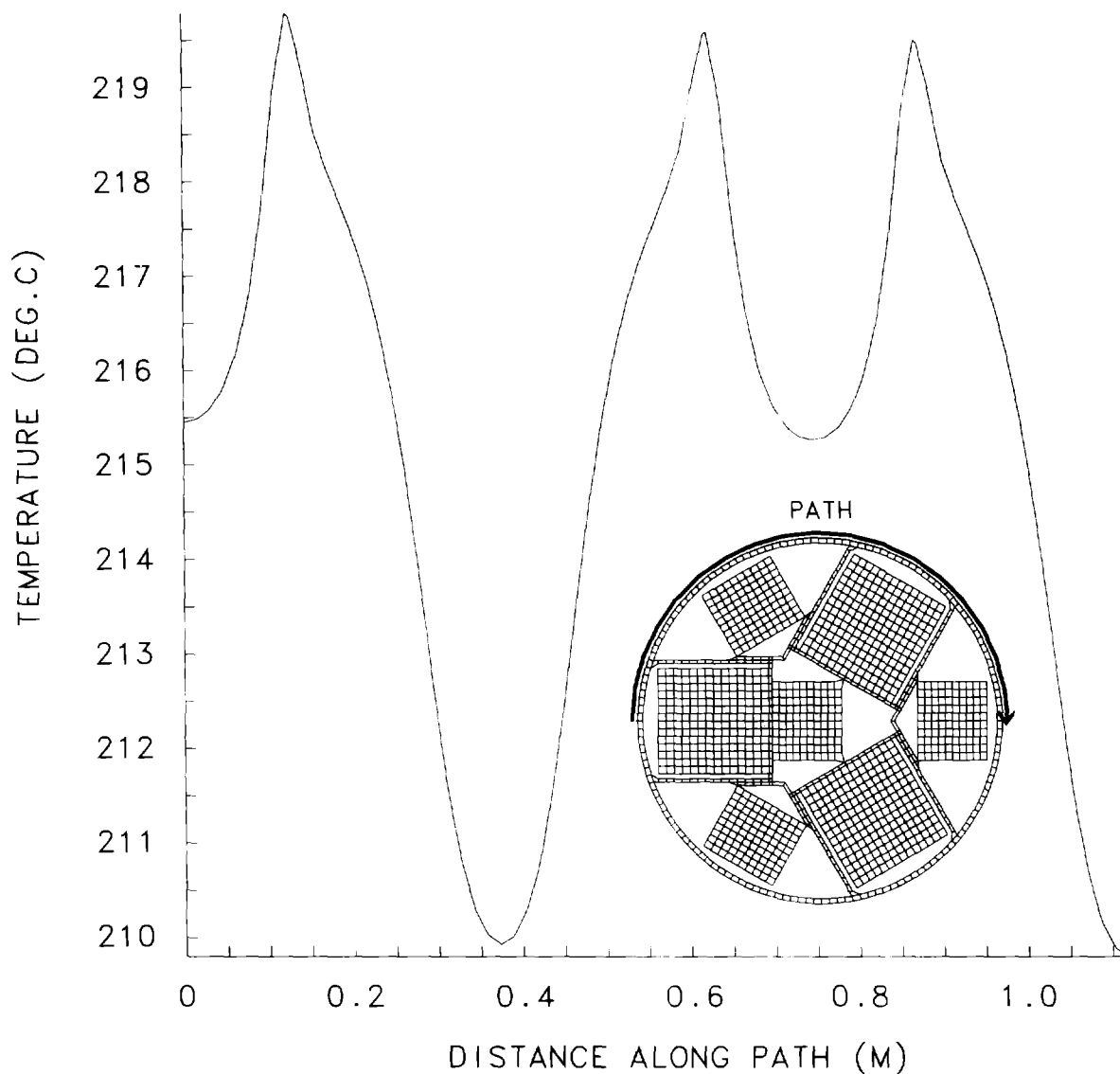
Figure 18. The surface temperature of the container may vary by as much as 10 $^{\circ}$C between adjacent hot and cool spots.
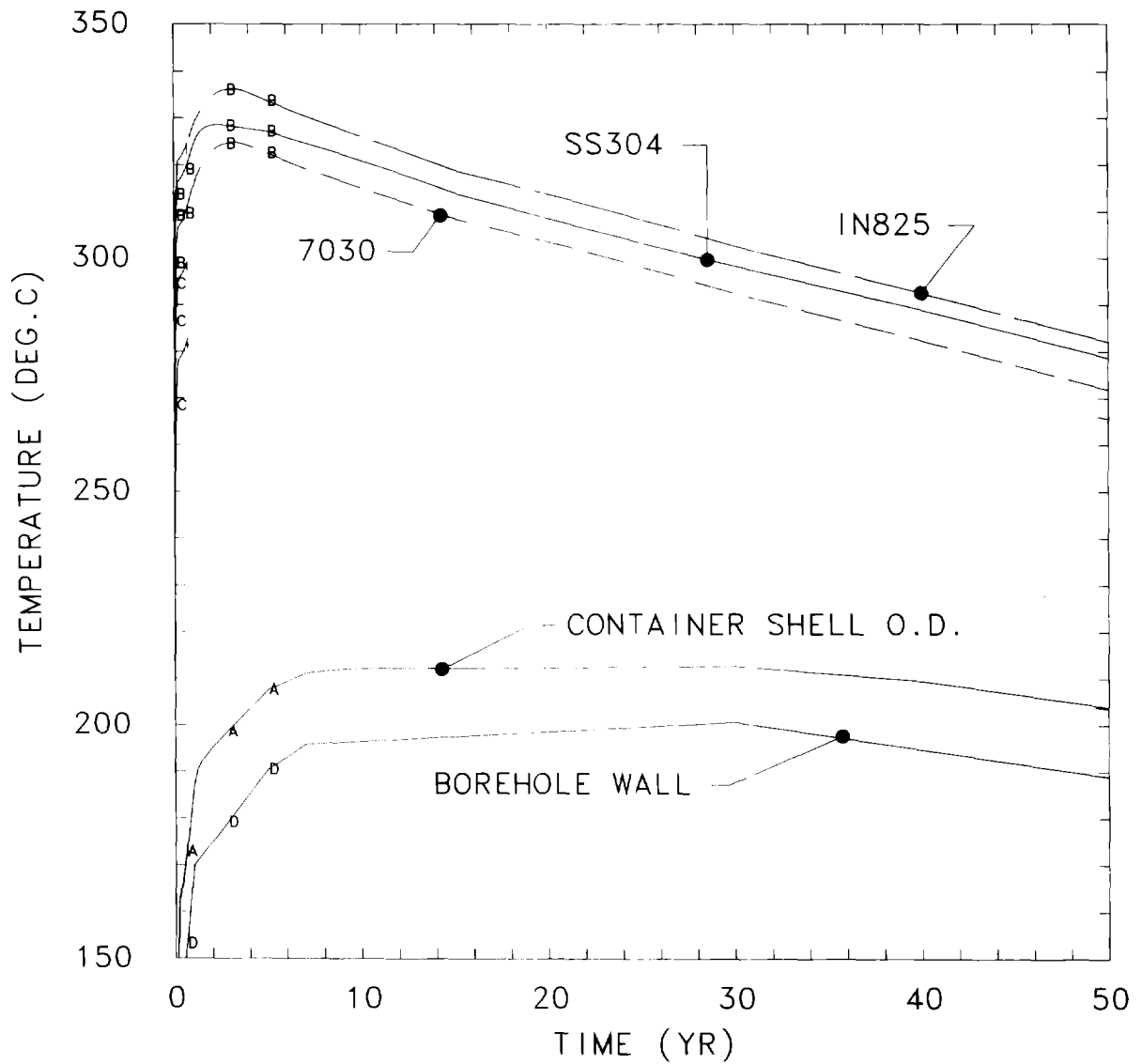
Figure 19. The effect of structural material choice is small, indicating that most of the heat is transferred to the shell by thermal radiation.

NWSI HYB(3PWR4BWR) INCOLOY 825 CONT/10YR—OVERPK BASE CASE 4 12/18/87 GL

Figure 20. The peak temperature of the fuel cladding for the loose backfill case in annulus is 391 °C, occurring about 5 yr after emplacement.

NWSI HYB(3PWR4BWR) INCOLOY 825 CONT/10YR-OVERIPK BASE CASE 4 12/18/87 GL
TIME= 5.05000E+00 YEARS
T-BOREHOLE WALL = 204 DEG.C

MIN(-)= 1.95E+02
MAX(+)= 3.92E+02
CONTOUR LEVELS
(TEMPERATURE-°C)

A= 2.40E+02

B= 2.60E+02

C= 2.80E+02

D= 3.00E+02

E= 3.20E+02

F= 3.40E+02

G= 3.60E+02

H= 3.80E+02

I= 4.00E+02

—BOREHOLE WALL

● =HOTTEST FUEL SPOTS

Figure 21. Isotherms for the loose backfill case at about 4 yr after
emplacement.

NNWSYB(3PWR4BWR) INCOLOY 825 CONT/10YR-BETNPK BASE CASE14 12/18/87 GL
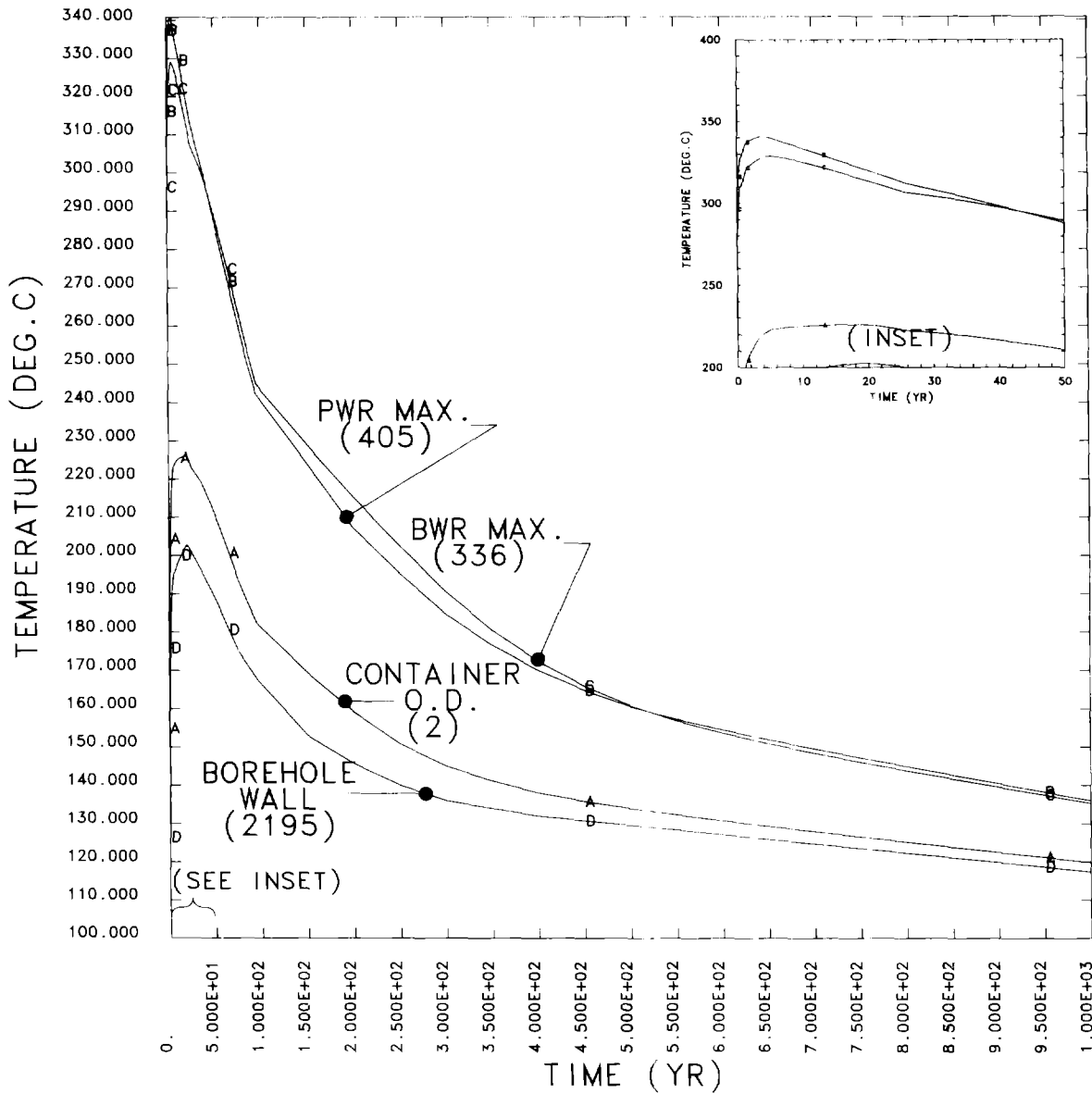
Figure 22. The peak temperature of the fuel cladding for the firm
backfill case is 341 °C, occurring about 4 yr after
emplacement.

NNWSI HYB(3PWR4BWR) INCOLOY 825 CONT/10YR–BETNPK BASE CASE14 12/18/87 GL
TIME=   5.05000E+00 YEARS
T–BOREHOLE WALL = 196 DEG.C

MIN(−)= 1.95E+02
MAX(+)= 3.40E+02
CONTOUR LEVELS
(TEMPERATURE–°C)

A= 2.40E+02

B= 2.60E+02

C= 2.80E+02

D= 3.00E+02

E= 3.20E+02

F= 3.40E+02

G= 3.60E+02

H= 3.80E+02

I= 4.00E+02

● =HOTTEST FUEL SPOTS
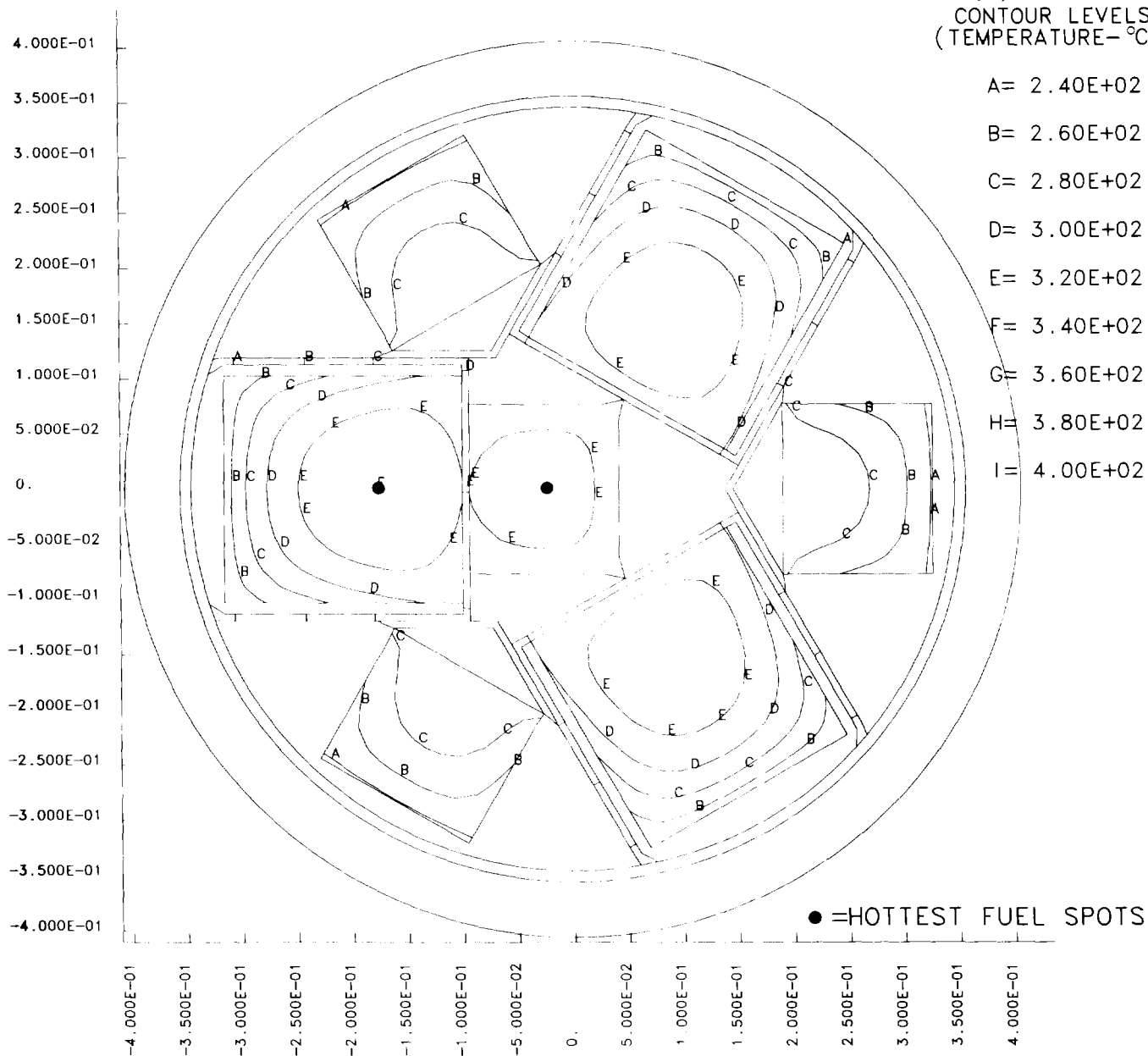
Figure 23. Isotherms for the firm backfill case at about 5 yr after
emplacement.
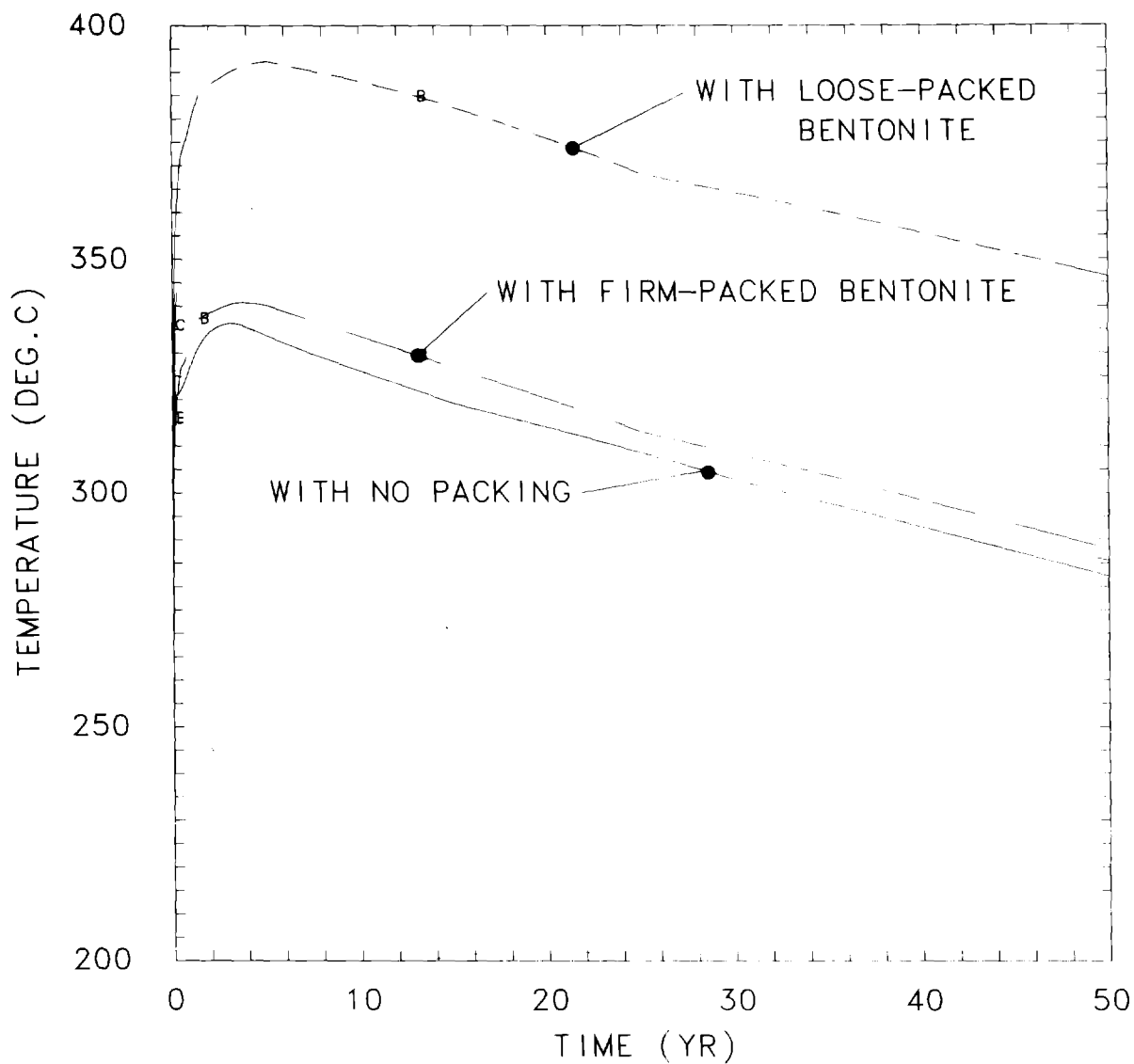
Figure 24. Backfilling the annulus with loosely packed bentonite
raises the peak temperatures over 50 °C above the case with
no backfill. Backfilling the annulus with firmly packed
bentonite only raises the peak temperatures by about 5 °C.
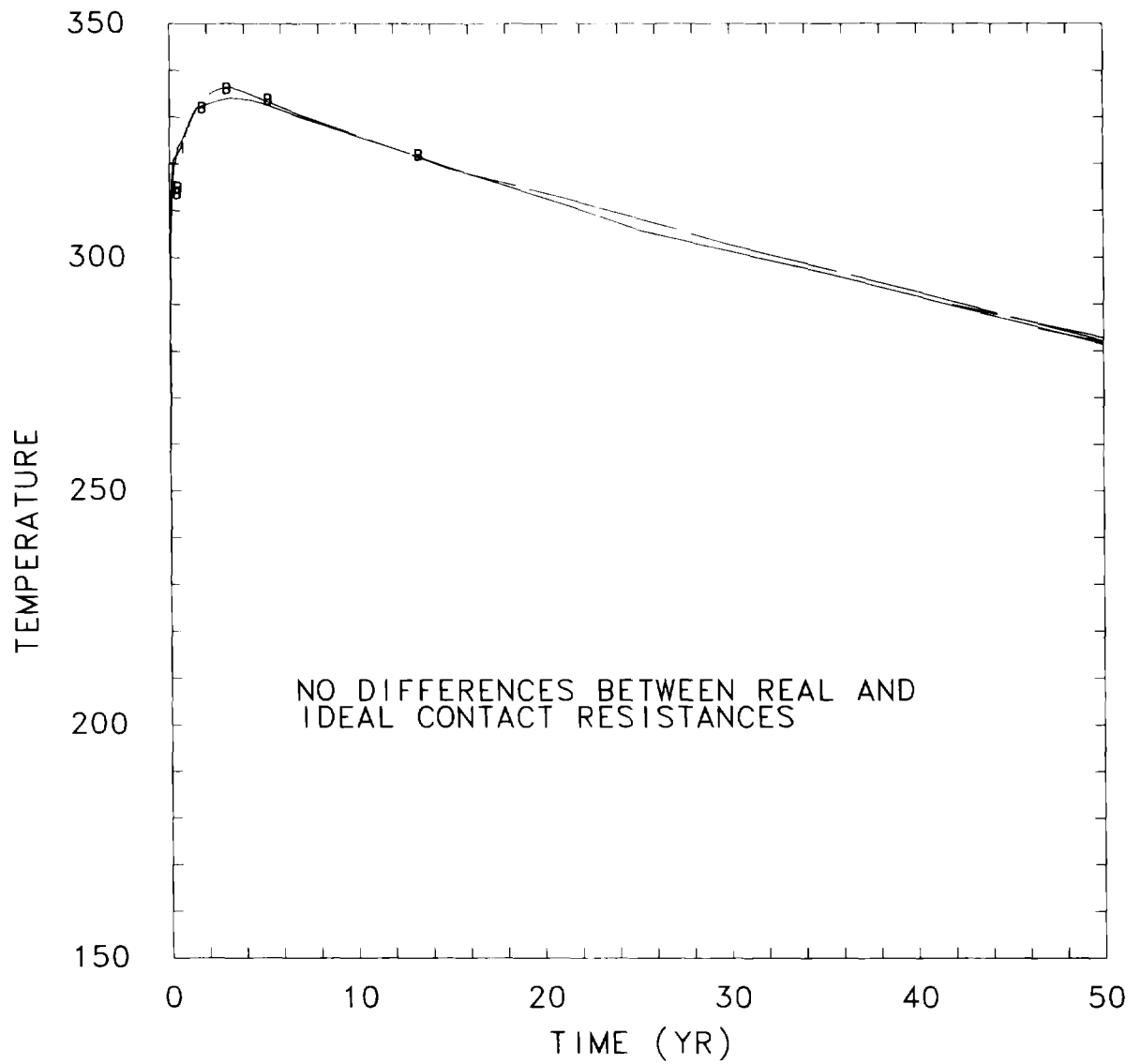
Figure 25. Using realistic contact thermal resistances rather than
ideal values does not change the peak temperatures.

HYBRIB(3PWR4BWR) INCOLOY 825 CONT./5YR-NORMAL CASE 6 1/18/88 GLJ-TACO
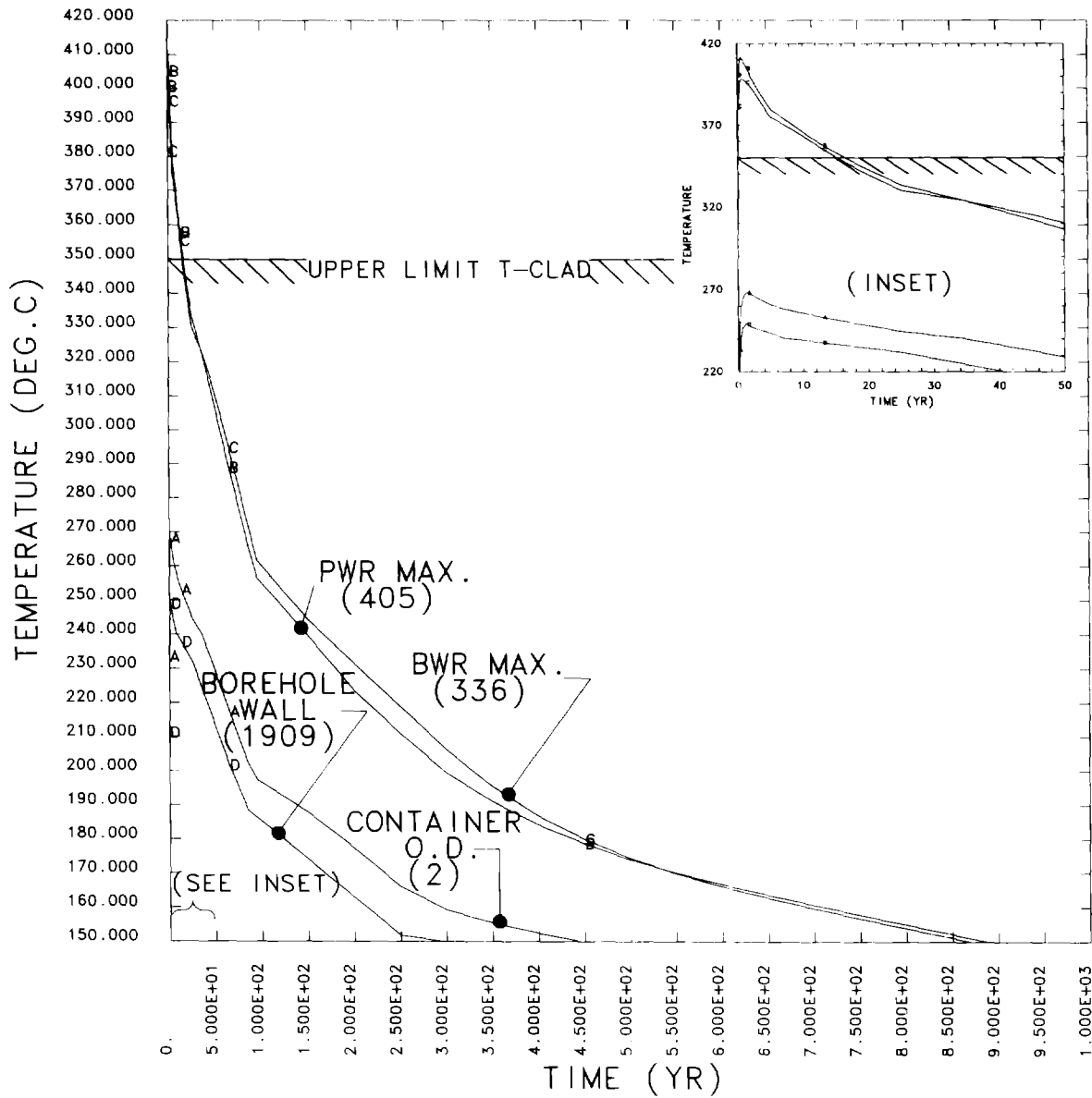
Figure 26. The peak temperature of the fuel cladding for the 5-year
fuel case, 411 °C, occurs about <u>8 months</u> after emplacement.

NNWSI HYB(3PWR4BWR) INCOLOY 825 CONT./5YR-NORMAL CASE 6 1/18/88 GLJ-TACO
TIME=   6.50000E-01 YEARS
T-BOREHOLE WALL = 248 DEG.C

MIN(-)= 2.46E+02
MAX(+)= 4.11E+02
CONTOUR LEVELS
TEMPERATURE (DEG.C)

A= 2.00E+02

B= 2.20E+02

C= 2.40E+02

D= 2.60E+02

E= 2.80E+02

F= 3.00E+02

G= 3.20E+02

H= 3.40E+02

I= 3.60E+02

J= 3.80E+02

K= 4.00E+02

● = HOTTEST FUEL SPOTS
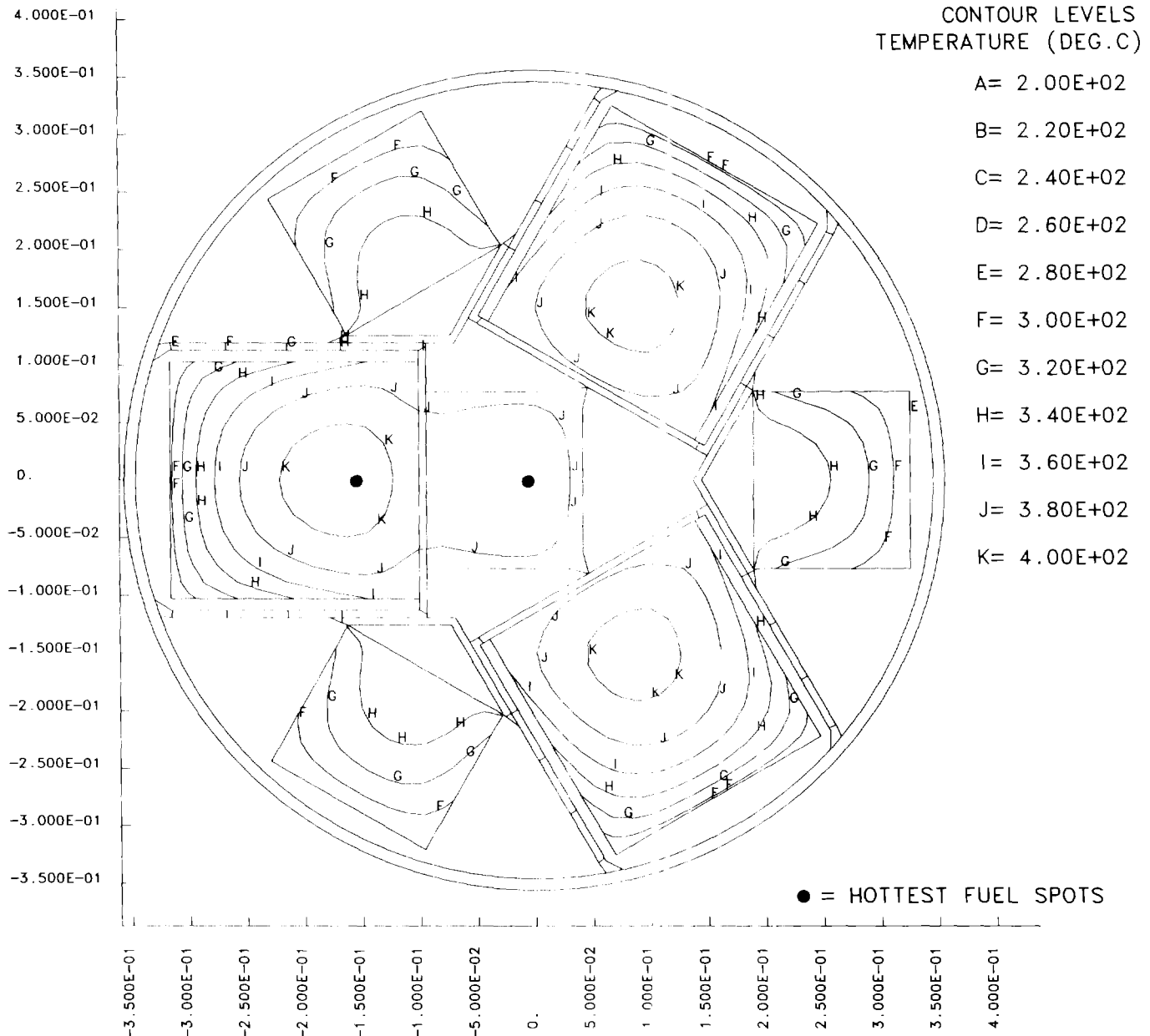
Figure 27. Isotherms for the 5-year fuel case at about 8 months after emplacement.

HYBRIB(3PWR4BWR) INCOLOY 825 CON/10YR-0.5 EMISSIV CASE 7 12/18/87 GLJ
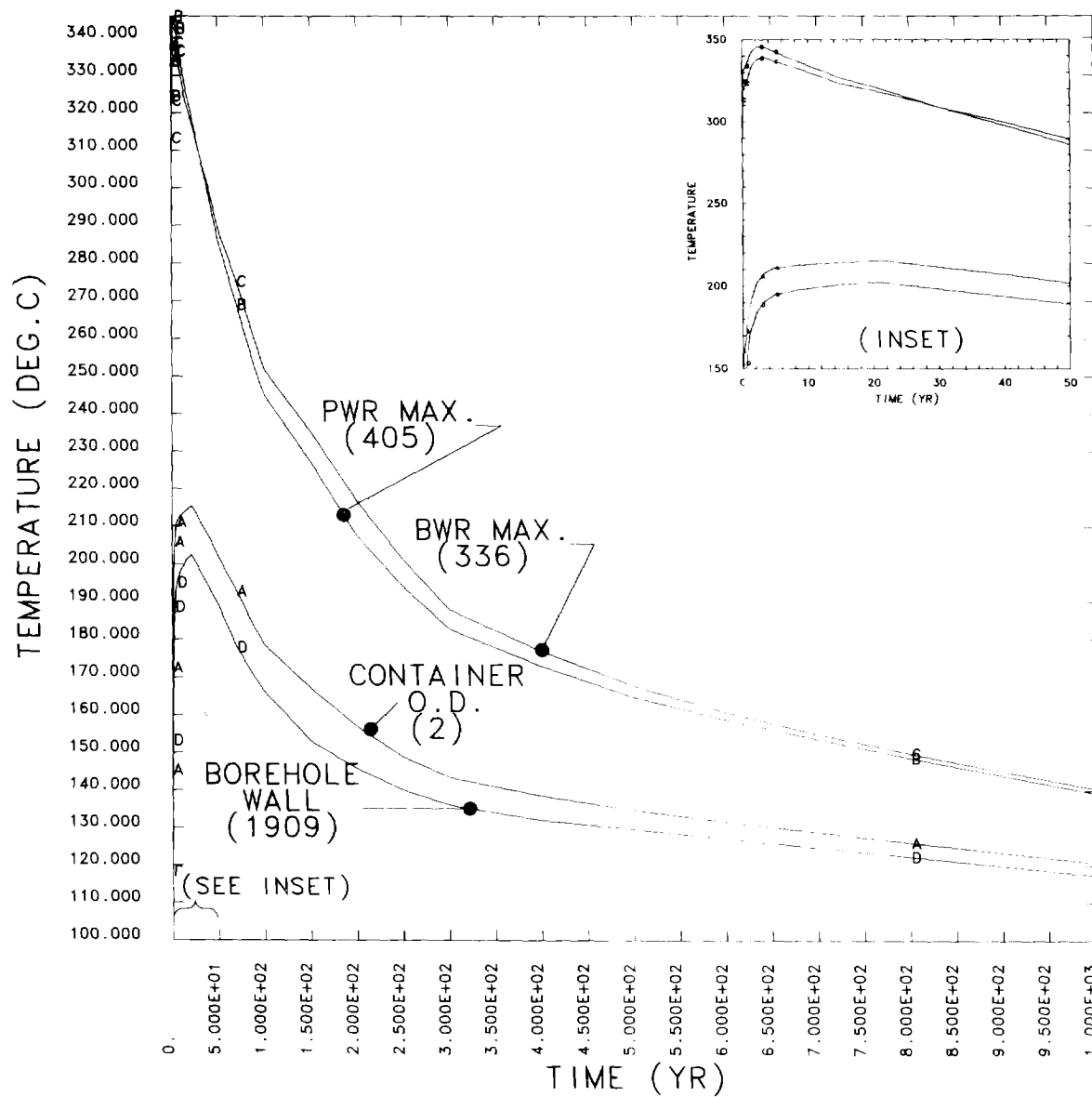
Figure 28. The peak temperature of the fuel cladding for the
emissivity case with its lower emissivity on the inside
surfaces is 346 °C.

NNWSI HYB(3PWR4BWR) INCOLOY 825 CON/10YR-0.5 EMISSIV CASE 7 12/18/87 GLJ
TIME=   3.80000E+00 YEARS
T-BOREHOLE WALL = 190 DEG.C

MIN(-)= 1.92E+02
MAX(+)= 3.45E+02
CONTOUR LEVELS
TEMPERATURE (DEG.C)

A= 2.00E+02

B= 2.20E+02

C= 2.40E+02

D= 2.60E+02

E= 2.80E+02

F= 3.00E+02

G= 3.20E+02

H= 3.40E+02

I= 3.60E+02

● = HOTTEST FUEL SPOTS
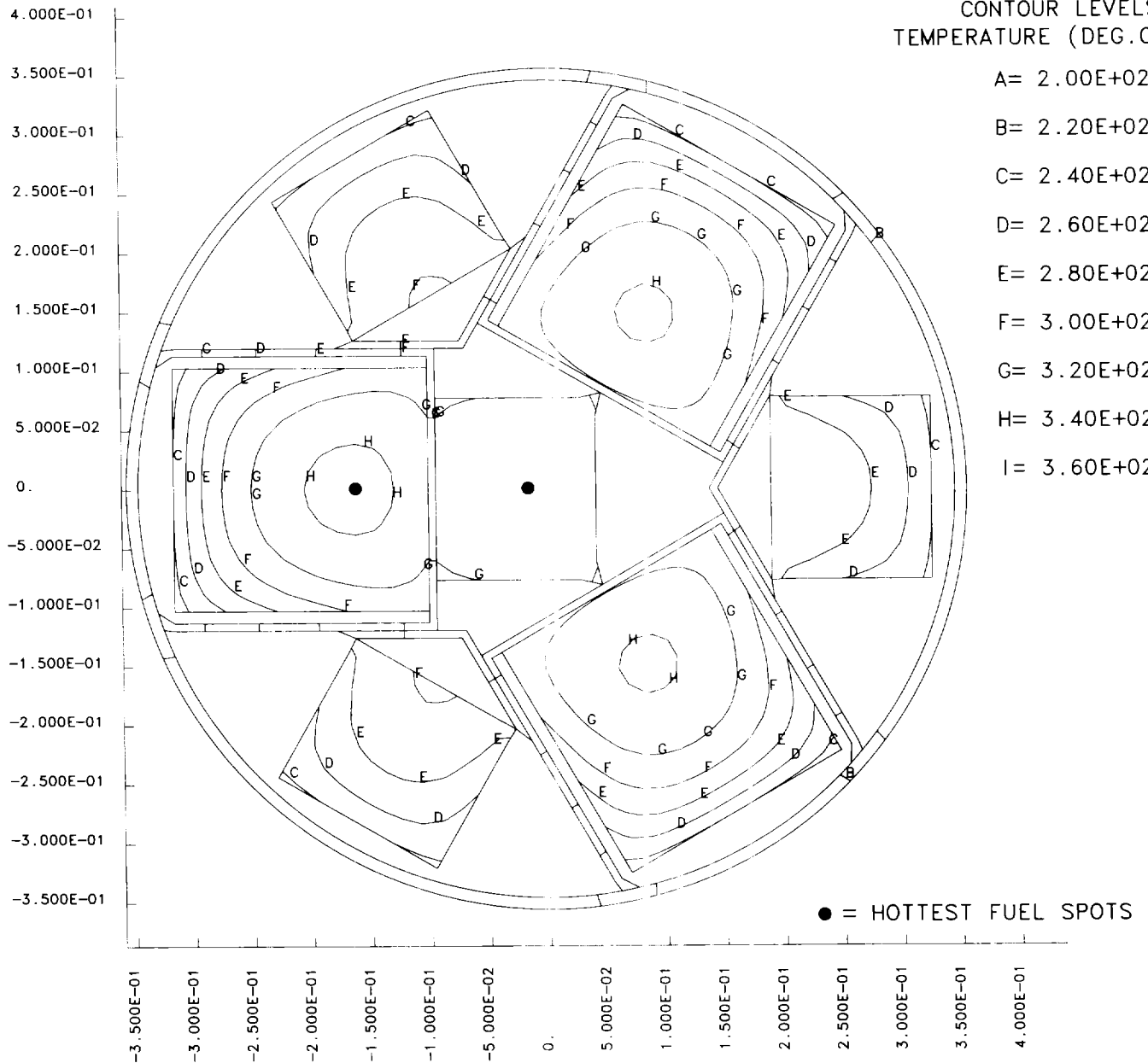
Figure 29. Isotherms for the emissivity case near the time of peak
temperature show sharper gradients in structure than in the
reference case.
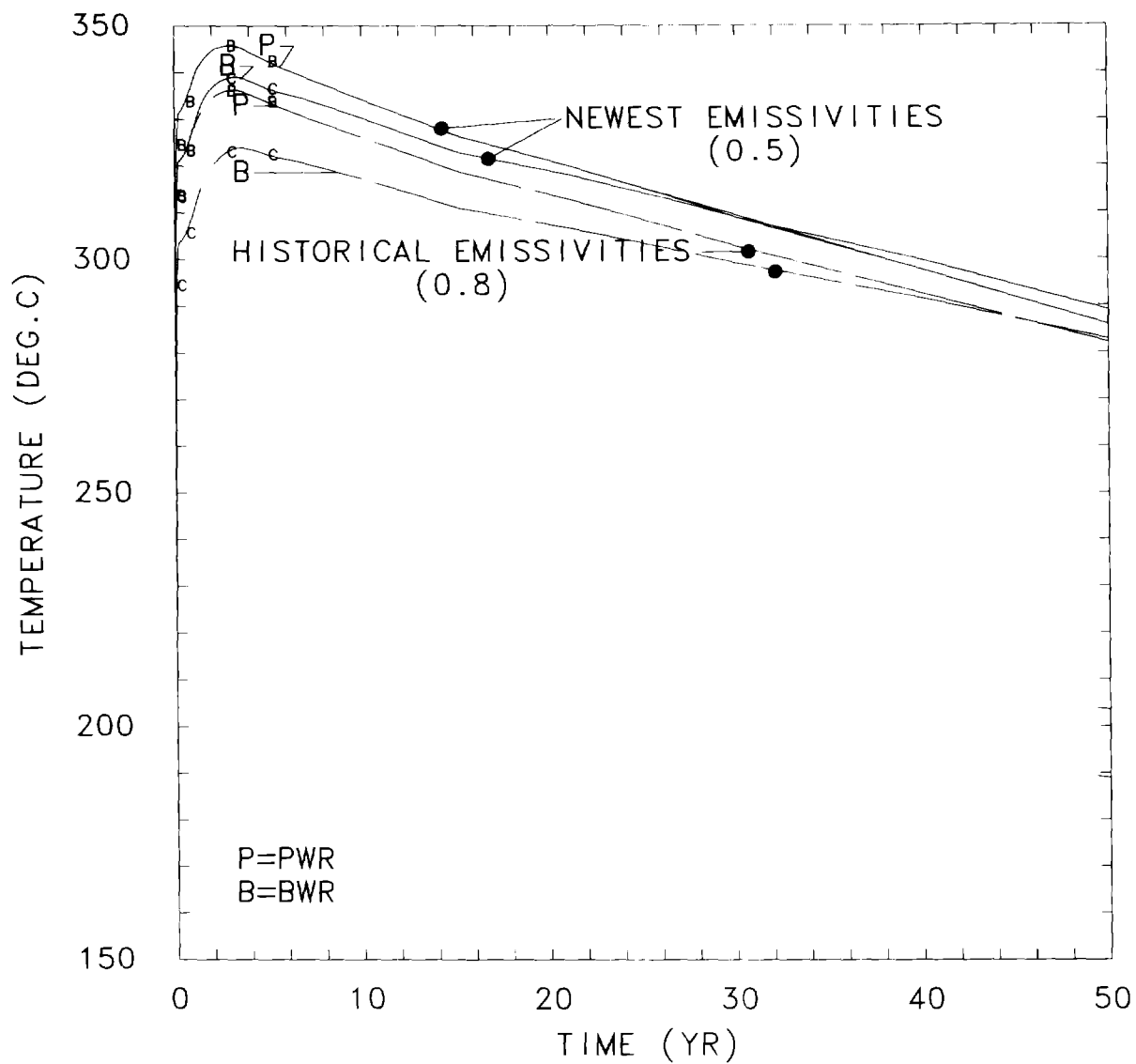
Figure 30. When compared with the reference case, the peak
temperatures increase by as much as 10 $^{\circ}$C by assuming the
lower emissivity for the inside surfaces.

NNWSYB(3PWR4BWR) INCOLOY 825 CON/10YR-RED.FUEL.K CASE 8 12/18/87 GLJ
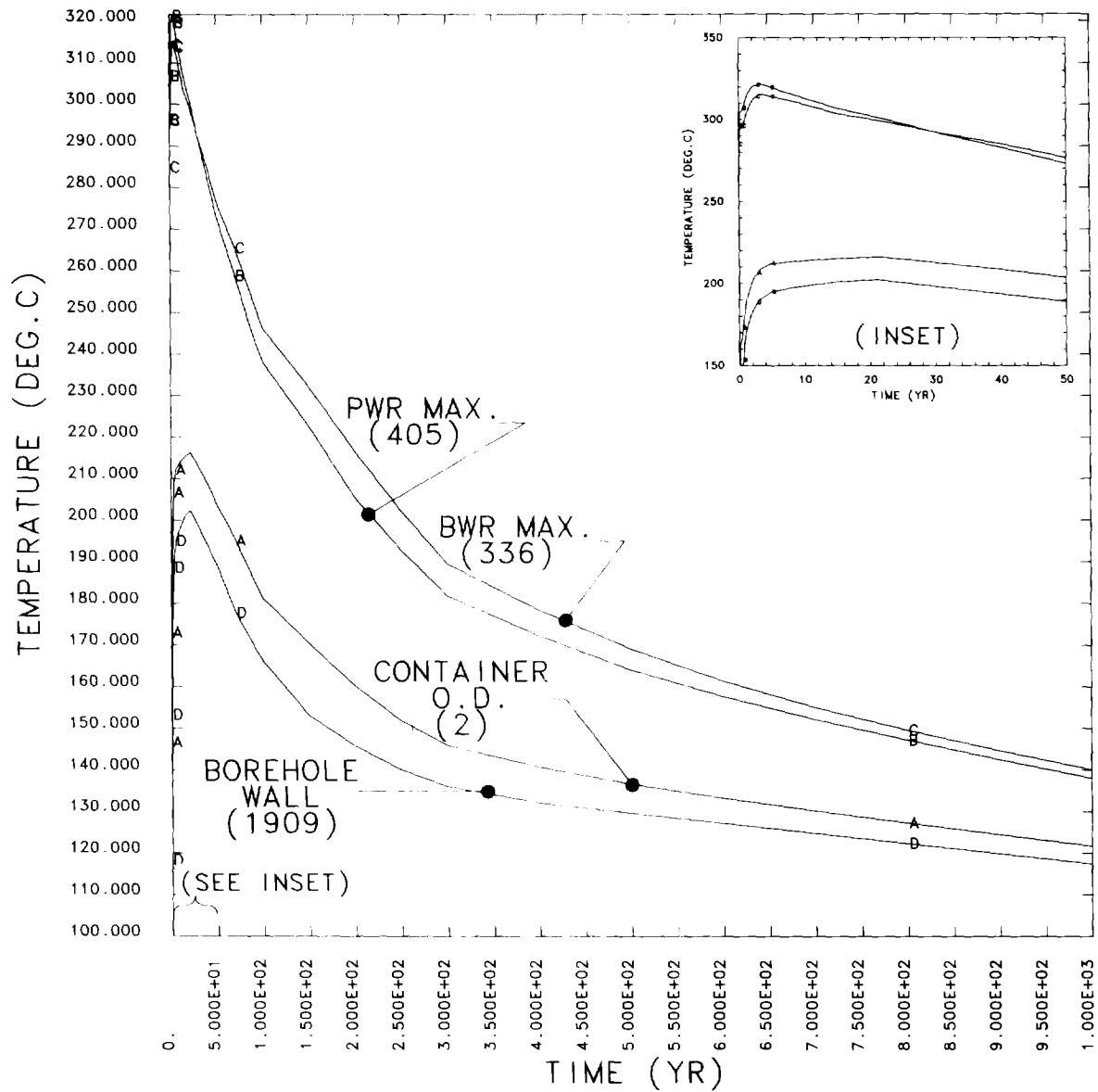
Figure 31. The peak temperature of the fuel cladding for the case with increased fuel conductivity is 322 °C.

NNWSI HYB(3PWR4BWR) INCOLOY 825 CON/10YR-RED.FUEL.K CASE 8 12/18/87 GLJ
TIME=   3.80000E+00 YEARS
T-BOREHOLE WALL = 190 DEG.C

MIN(−)= 1.92E+02
MAX(+)= 3.22E+02
CONTOUR LEVELS
TEMPERATURE (DEG.C)

A= 2.00E+02

B= 2.20E+02

C= 2.40E+02

D= 2.60E+02

E= 2.80E+02

F= 3.00E+02

G= 3.20E+02

H= 3.40E+02

I= 3.60E+02

● = HOTTEST FUEL SPOTS
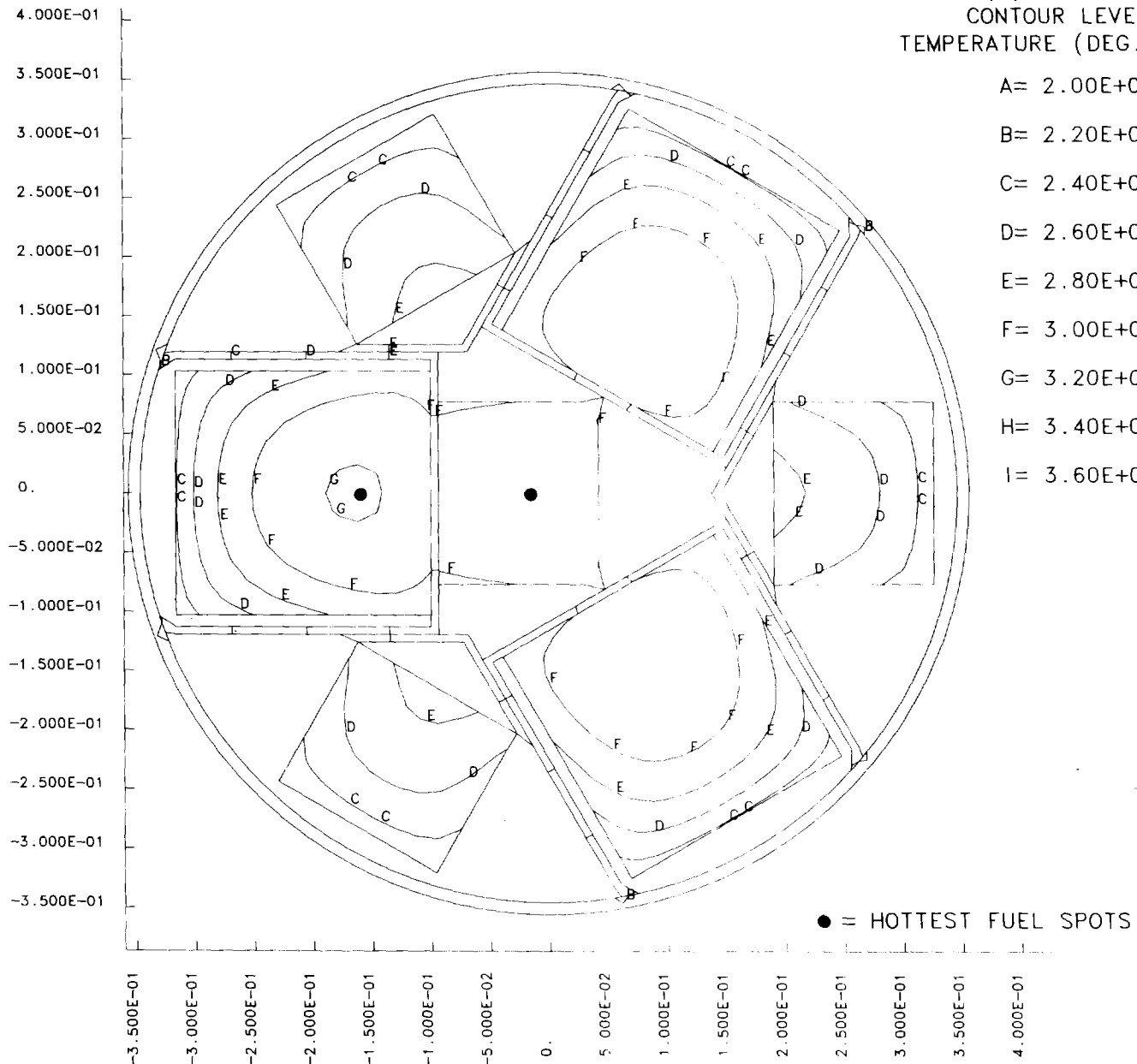
Figure 32. Isotherms for the fuel conductivity case show much less
temperature gradient in the fuel canisters.
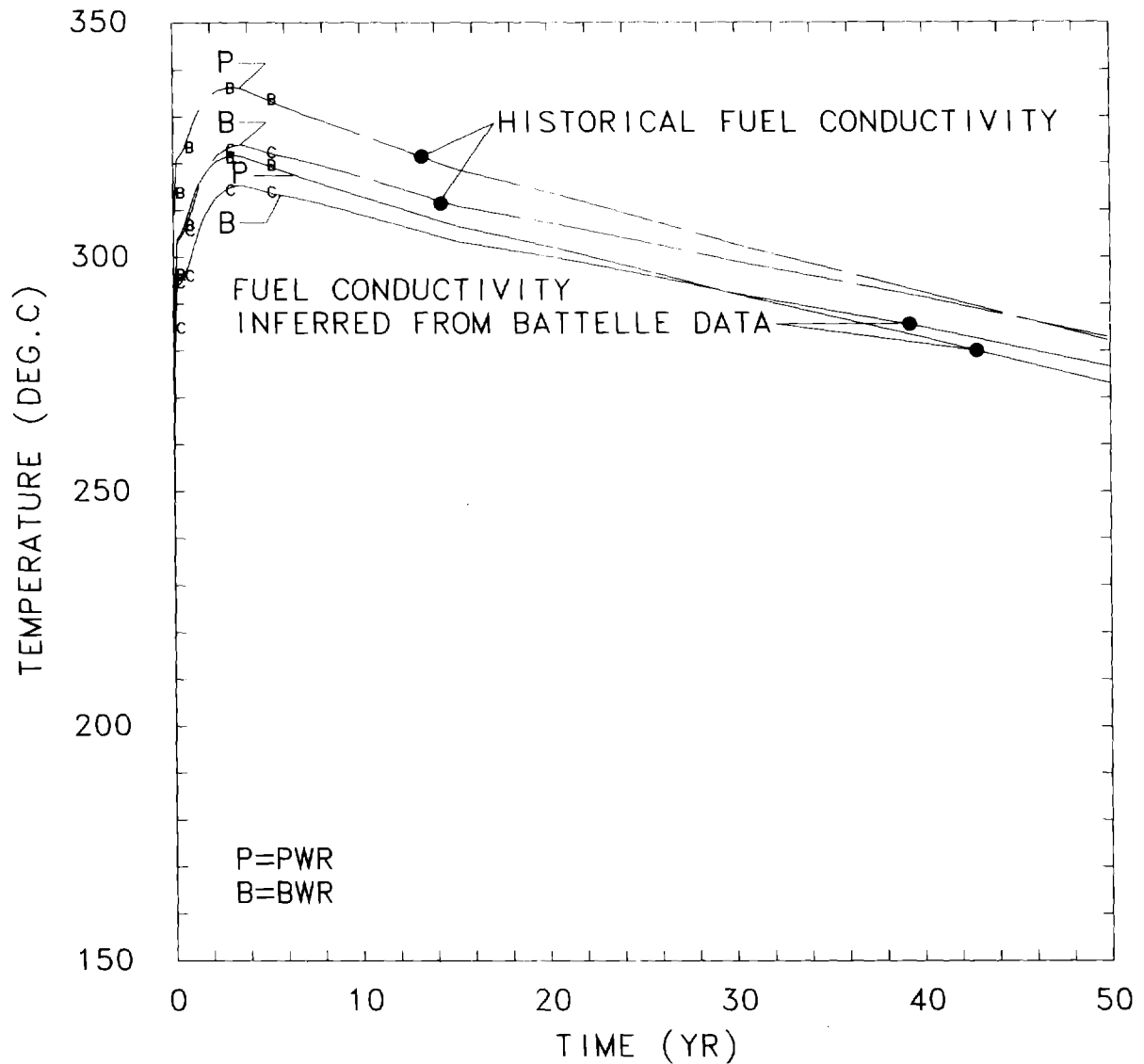
Figure 33. The use of fuel pack thermal conductivities derived from Battelle's measured fuel bundle temperature profiles lowers the peak cladding temperatures by 8 to 15 ^{o}C.

NNWSYB(3PWR4BWR) INCOLOY 825 CON/10YR-NORMAL GASFL CASE 9 2/15/88 GLJ
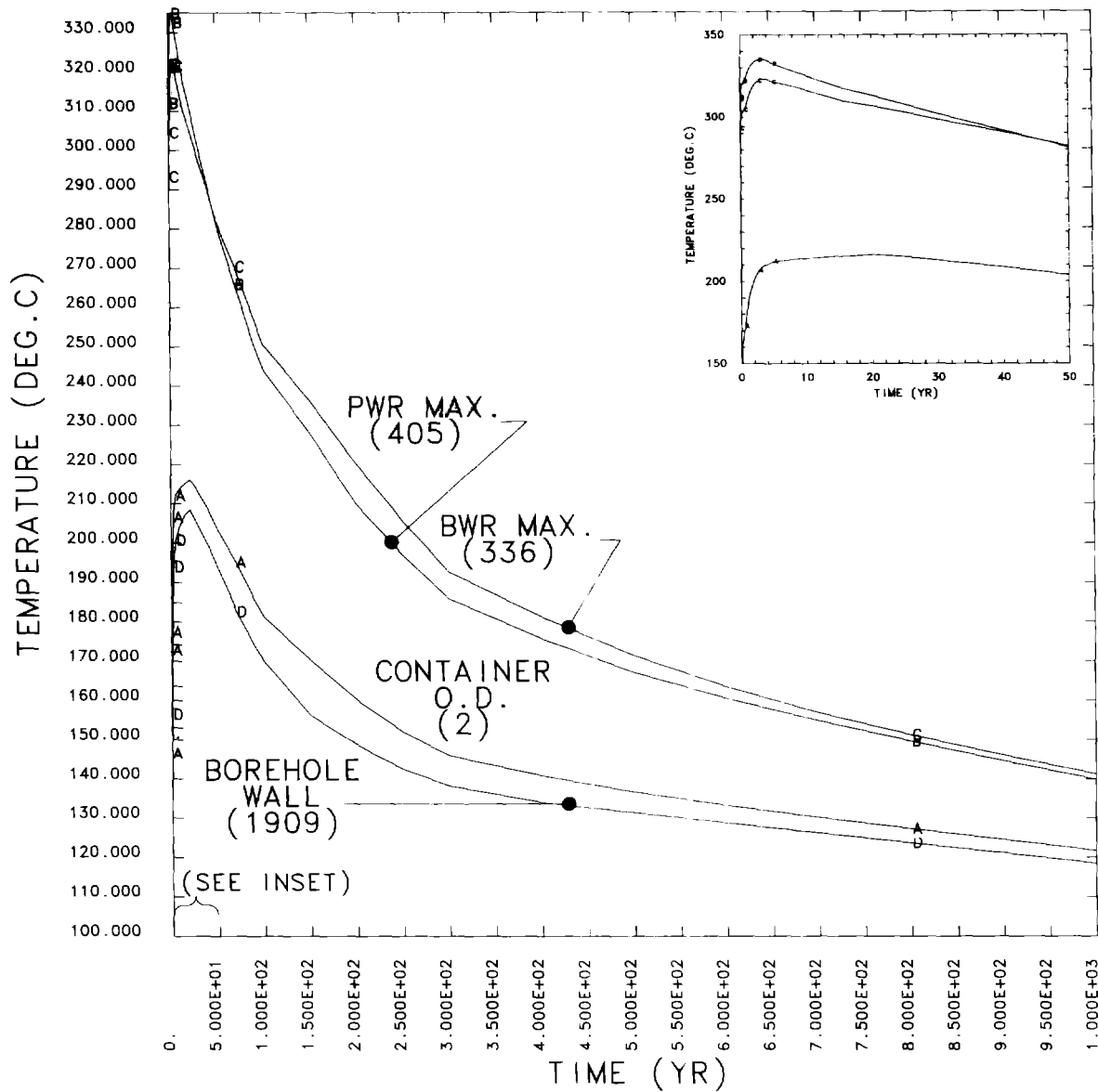
Figure 34. The peak temperature of the fuel cladding for the gas fill
case is 335 °C. Thermal radiation is still the predominant
heat transfer mode.

NNWSI HYB(3PWR4BWR) INCOLOY 825 CON/10YR-NORMAL GASFL CASE 9 2/15/88 GLJ
TIME=   3.80000E+00 YEARS
T-BOREHOLE WALL = 190 DEG.C

MIN(-)= 2.10E+02
MAX(+)= 3.35E+02
CONTOUR LEVELS
TEMPERATURE (DEG.C)

A= 2.00E+02

B= 2.20E+02

C= 2.40E+02

D= 2.60E+02

E= 2.80E+02

F= 3.00E+02
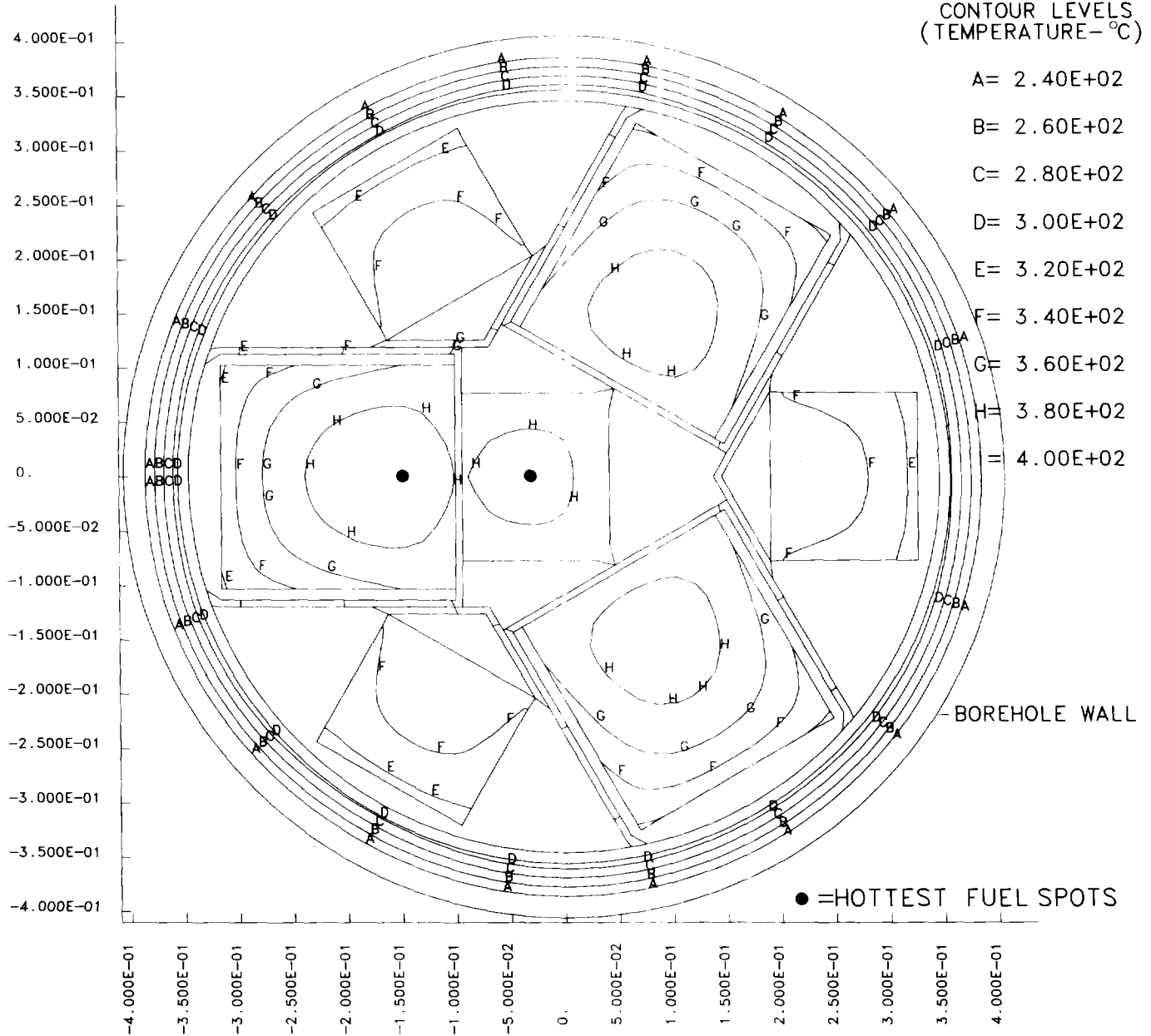
G= 3.20E+02

H= 3.40E+02

I= 3.60E+02

● = HOTTEST FUEL SPOTS
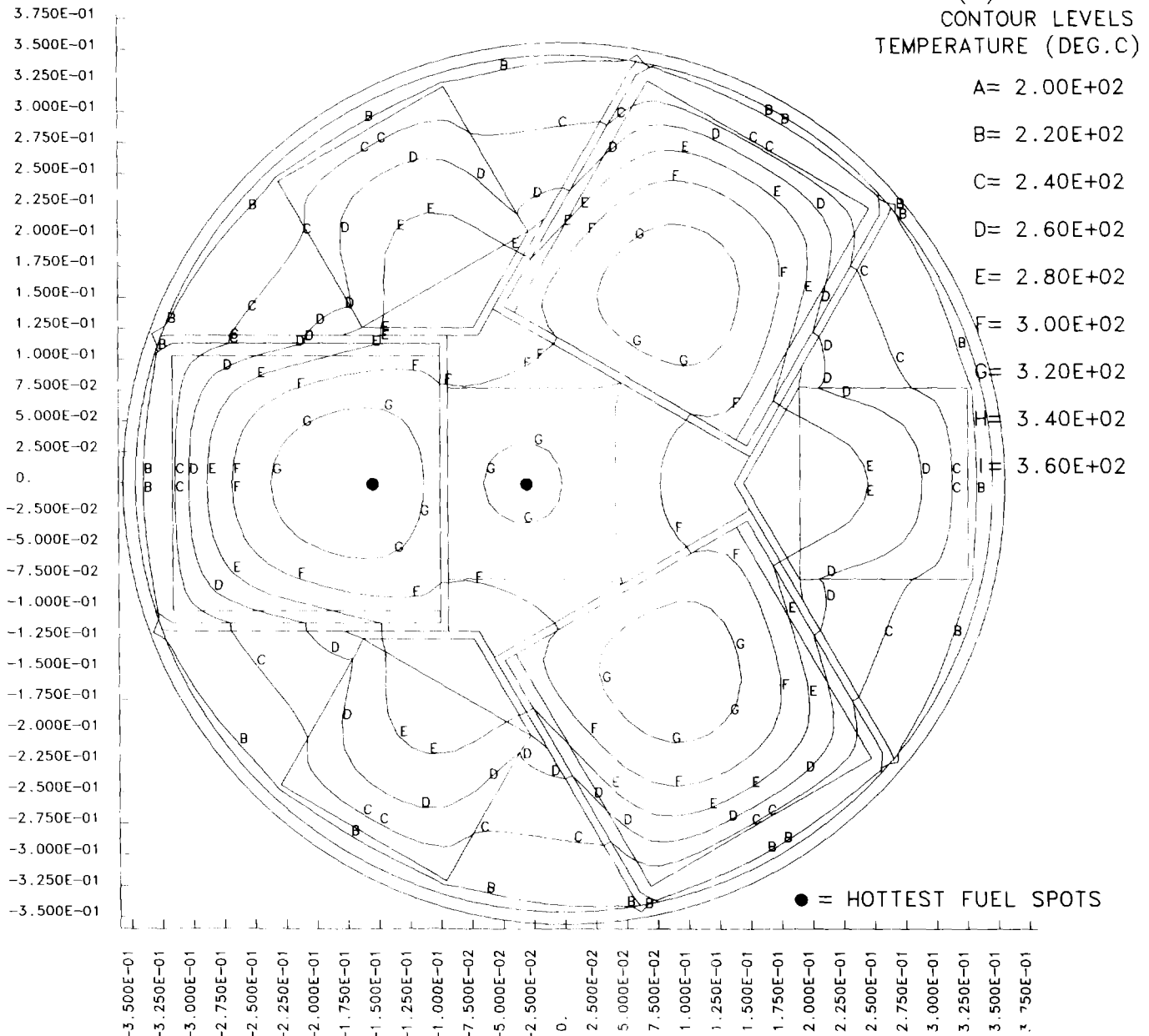
Figure 35. Isotherms for the gas fill case at about 3 yr after
emplacement.

NNWSYB(3PWR4BWR) INCOLOY 825 CON/10YR-NORMAL BEST CASE 10 2/15/88 GLJ
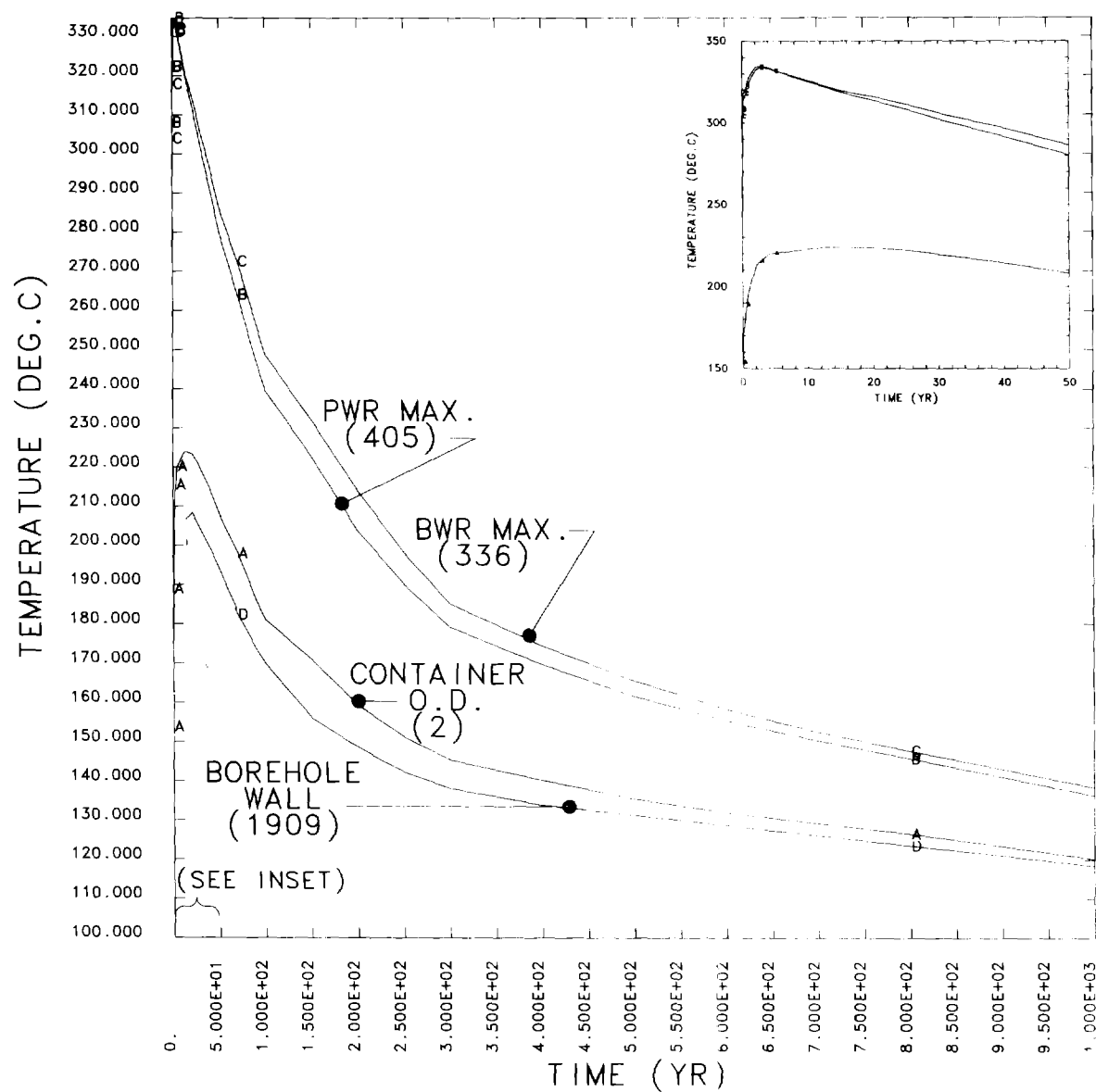
Figure 36. The peak temperature of the fuel cladding for the "best
model" analysis including: fine-zoned mesh of tuff,
improved fuel conductivity, 0.5 internal surface
emissivity, and gas-fill conduction is 336 °C.

NNWSI HYB(3PWR4BWR) INCOLOY 825 CON/10YR-NORMAL BEST CASE 10 2/15/88 GLJ
TIME=   3.20000E+00 YEARS
T-BOREHOLE WALL = 198 DEG.C

MIN(−)= 2.17E+02
MAX(+)= 3.36E+02
CONTOUR LEVELS
TEMPERATURE (DEG.C)

A= 2.00E+02

B= 2.20E+02

C= 2.40E+02

D= 2.60E+02

E= 2.80E+02

F= 3.00E+02

G= 3.20E+02

H= 3.40E+02

I= 3.60E+02

● = HOTTEST FUEL SPOTS
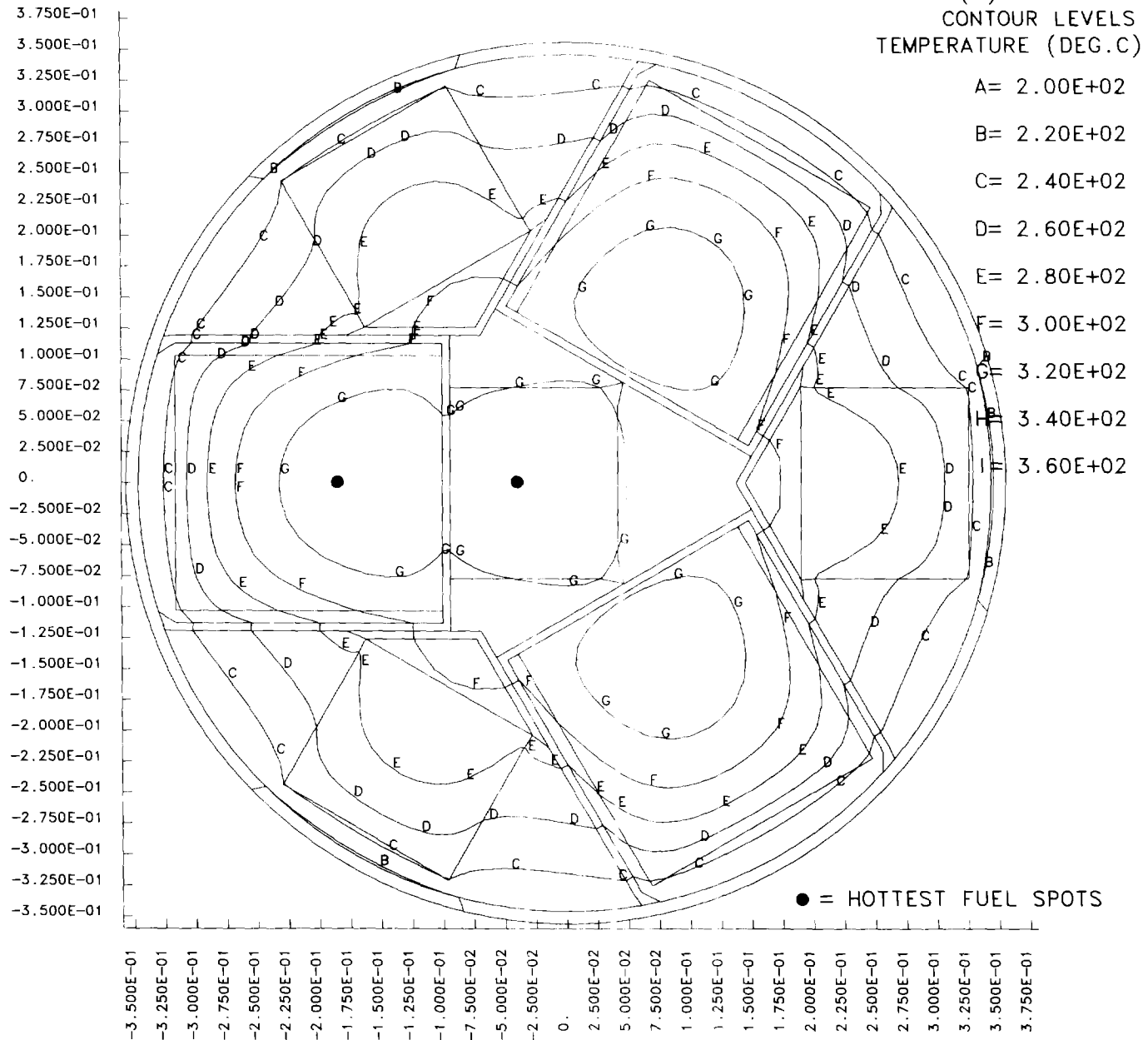
Figure 37. Isotherms for the best model analysis at about 3 yr after
emplacement.

NNWSYB(3PWR4BWR) INCOLOY 825 CON/10YR-1.73:1 SCPCHK CS13A 4/8/88 GLJ
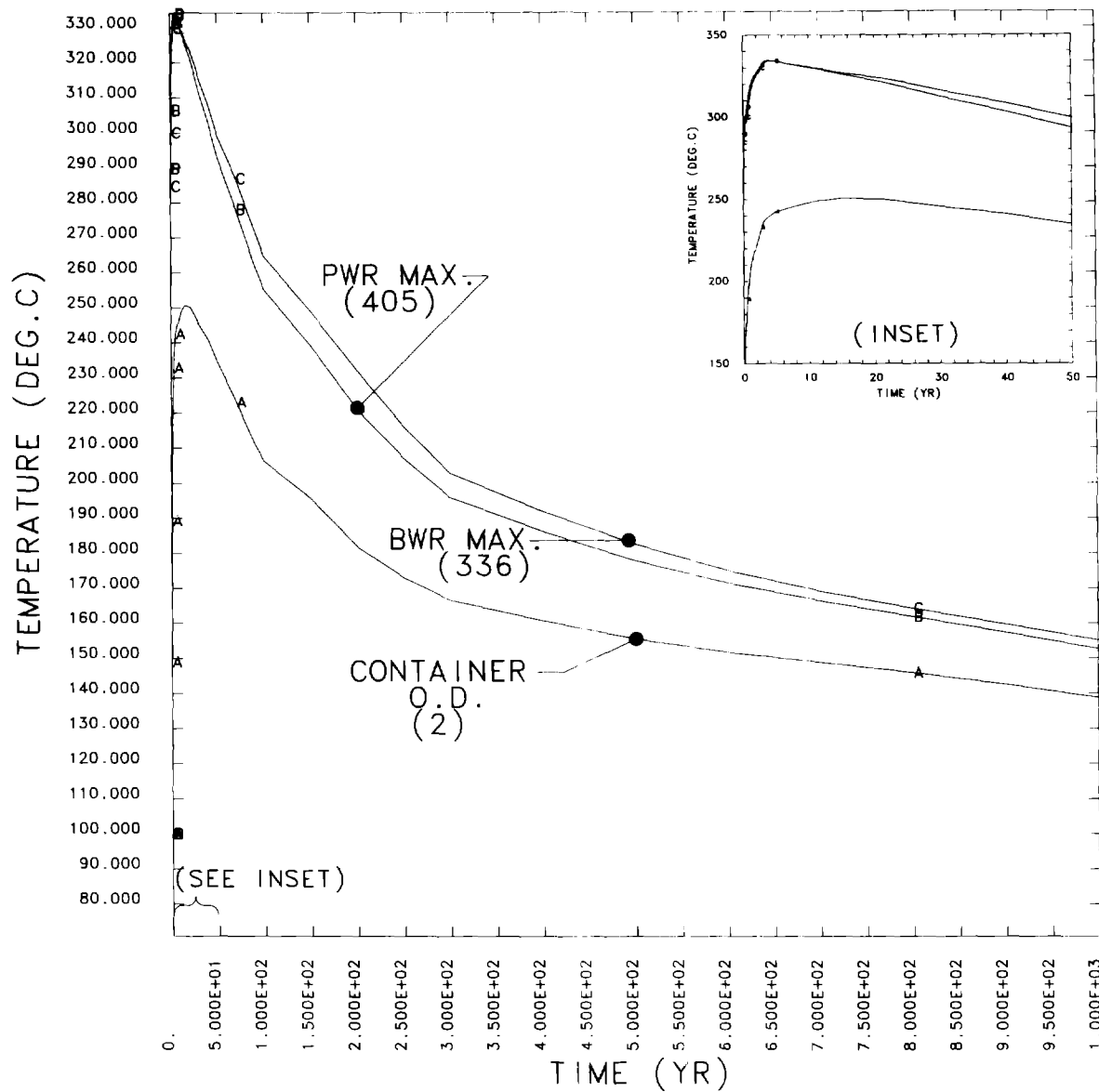
Figure 38. The peak temperature of the fuel cladding for the SCP
layout case, with its 28% decrease in repository area per
borehole and 15% decrease in thermal load, is 335 $^{\circ}$C.

NNWSI HYB(3PWR4BWR) INCOLOY 825 CON/10YR-1.73:1 SCPCHK CS13A 4/8/88 GLJ
TIME=   5.00000E+00 YEARS
T-BOREHOLE WALL = 227 DEG.C

MIN(-)= 2.43E+02
MAX(+)= 3.35E+02
CONTOUR LEVELS
(TEMPERATURE- °C)

A= 2.00E+02

B= 2.20E+02

C= 2.40E+02

D= 2.60E+02

E= 2.80E+02

F= 3.00E+02

G= 3.20E+02

H= 3.40E+02

I= 3.60E+02

● =HOTTEST FUEL SPOTS
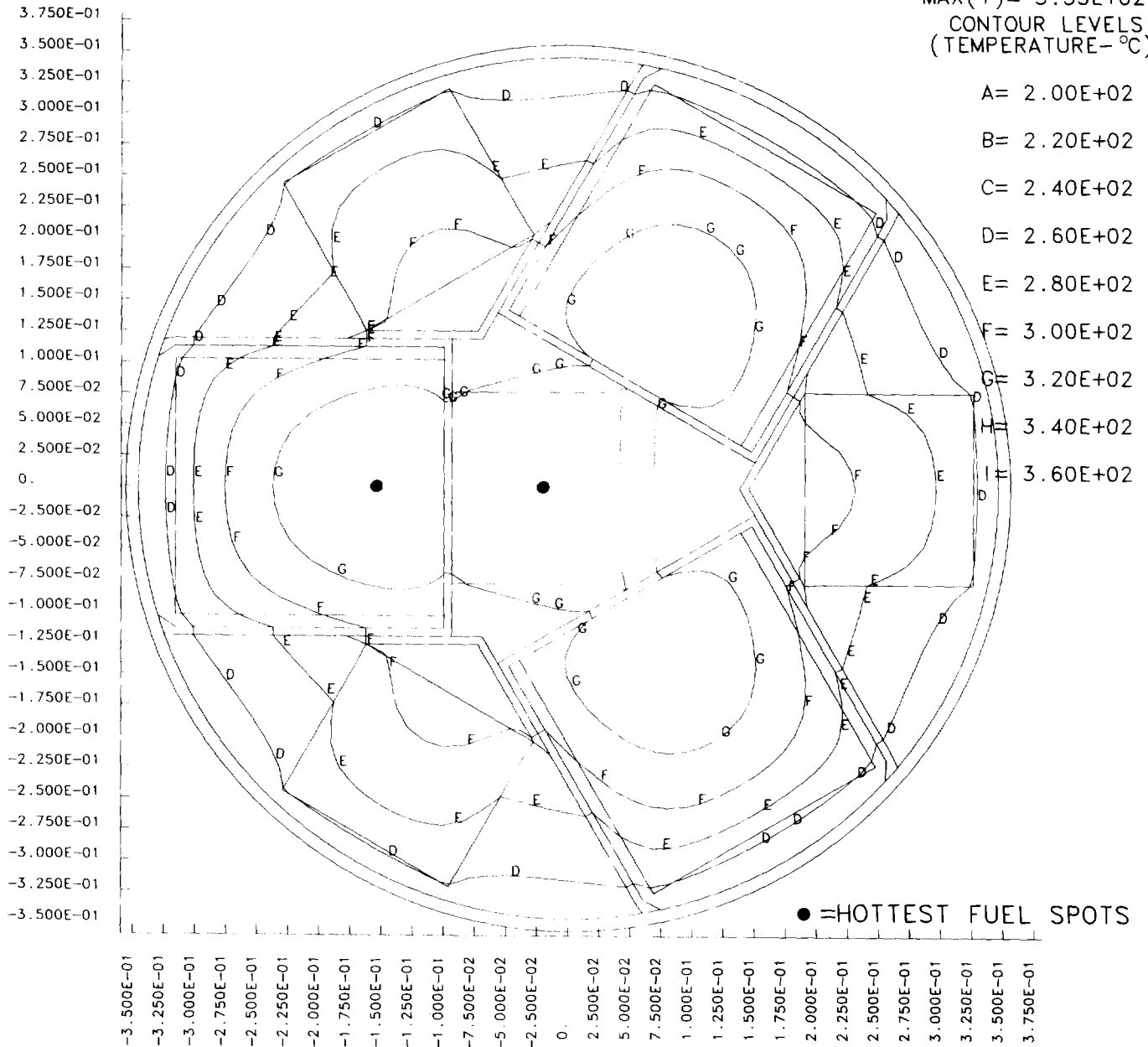
Figure 39. Isotherms for the SCP layout case at about 4 yr after
emplacement.

V.   Conclusions

The following conclusions can be made from these analyses of a hybrid-filled container surrounded by an infinite array of equivalently loaded containers on 8 X 30-m spacings. (See Figure 40 and Table 5.) For 4.74-kW load or greater, the borehole wall stays above 97 ^{o}C for the full 1000-yr analysis period. This load corresponds to a local power density of 80 kW/acre. The tuff 1 m from the borehole wall never exceeds 200 ^{o}C. Because the borehole wall surface temperature nears 200 ^{o}C, it is possible that the floor of the drift tunnel near these containers might surpass the 50 ^{o}C maximum allowable temperature set by repository manned-use requirements. For all but the case with 5-yr-old fuel and the case with loosely packed bentonite backfill, the peak cladding temperature remains below, but near, the 350 ^{o}C limit. The best model thermal analysis with 10-yr-old fuel and no backfill results in a 336 ^{o}C peak cladding temperature occurring 3 yr after emplacement. Thus, this thermal load (approximately 5 kW) is the largest acceptable under the defined emplacement geometry and container design constraints. Under the SCP spacing constraints, the maximum allowable thermal load would be approximately 4 kW. Table 6 lists some other thermal load possibilities for comparison. With the peak cladding temperature nearly equal to the maximum allowable, it will be critical to evaluate the axial temperature gradients in a full 3-D model of the container before finalizing container design guidelines.

The two cases that do not satisfy the cladding temperature limit requirement, 5-year fuel and loosely packed backfill, result in peak cladding temperatures 40 to 60 ^{o}C hotter than the maximum allowable. Firmly packing the bentonite in the borehole annulus results in a peak temperature of 341 ^{o}C. Because these backfill results are highly sensitive to the assumed thermal properties of the backfill, use of accurately measured values of these properties is crucial in further analyses guiding design decisions.

In addition to these specific conclusions, some general comments can be added. The small effect of the conductivity of the container assembly structural material on predicted peak cladding temperatures, its sensitivity to the value of the surface emissivity for the surfaces inside the container, and minor effect of modeling heat conduction through (and probably even convection in) the gas fill suggests that radiative heat transfer is the dominant mode inside the container. Variations in the "effective" thermal conductivity of the fuel rods/fuel canister is the other material parameter to which predictions of peak cladding temperatures are very sensitive. While conduction through the gas fill is small, the effect of heat transfer from natural convection in the cavities between the fuel canisters and the container shell may turn out to be more significant. For boreholes with no backfill, heat balance calculations on heat transferred from the container to the borehole wall also show that most of the external heat flow results from thermal radiation. Finally, analysis results show that lack of accurate values for the thermal resistances between surfaces in contact does not affect a good prediction of a peak cladding temperature.

On the basis of these conclusions and an overall view of the repository layout and expected container emplacement history, I make the following recommendations for thermal performance evaluations:

a.   Establish accurate values for the effective thermal conductivity of the homogenized fuel canisters for all possible fuel packing configurations. Determine the relationship between the actual peak cladding temperature and that predicted by the homogenized model.

b.   Add natural convection in the gas fill to the internal-heat-transfer model of the vertical container.

c.   Determine the surface emissivity of the tuff and the materials to be used in the waste package designs for various expected surface conditions.

d.   Establish more accurate values for the thermal conductivity of potential container backfills at various densities.

e.   Using a best model, complete a 3-D analysis of the vertical container including axial variations in power output, material geometries, and thermal properties.

f.   Do transient, 3-D thermal analysis of various combinations of emplaced packages and emplacement histories for whole sections of the repository using the planned waste delivery scenario (e.g., Ref. 2).

g.   Model the presence of ventilated drift tunnels in detail, including the drift tunnel and its associated humidity and heat removal by ventilation.

A) ACTUAL REPOSITORY LAYOUT

B) 3-D TUFF MODEL AND 2-D CONTAINER MODEL

C) • MINIMUM BOREHOLE TEMPERATURE ALWAYS GREATER THAN 97 DEG.C
  • MAXIMUM FUEL CLADDING TEMPERATURE LESS THAN 350 DEG.C
        FOR THERMAL LOADS LESS THAN 4740W
  • BACKFILL MAY RAISE CLADDING TEMPERATURE ABOVE 350 DEG.C
  • CONTAINER MODEL RESULTS MOST SENSITIVE TO THERMAL
        RADIATION PARAMETERS
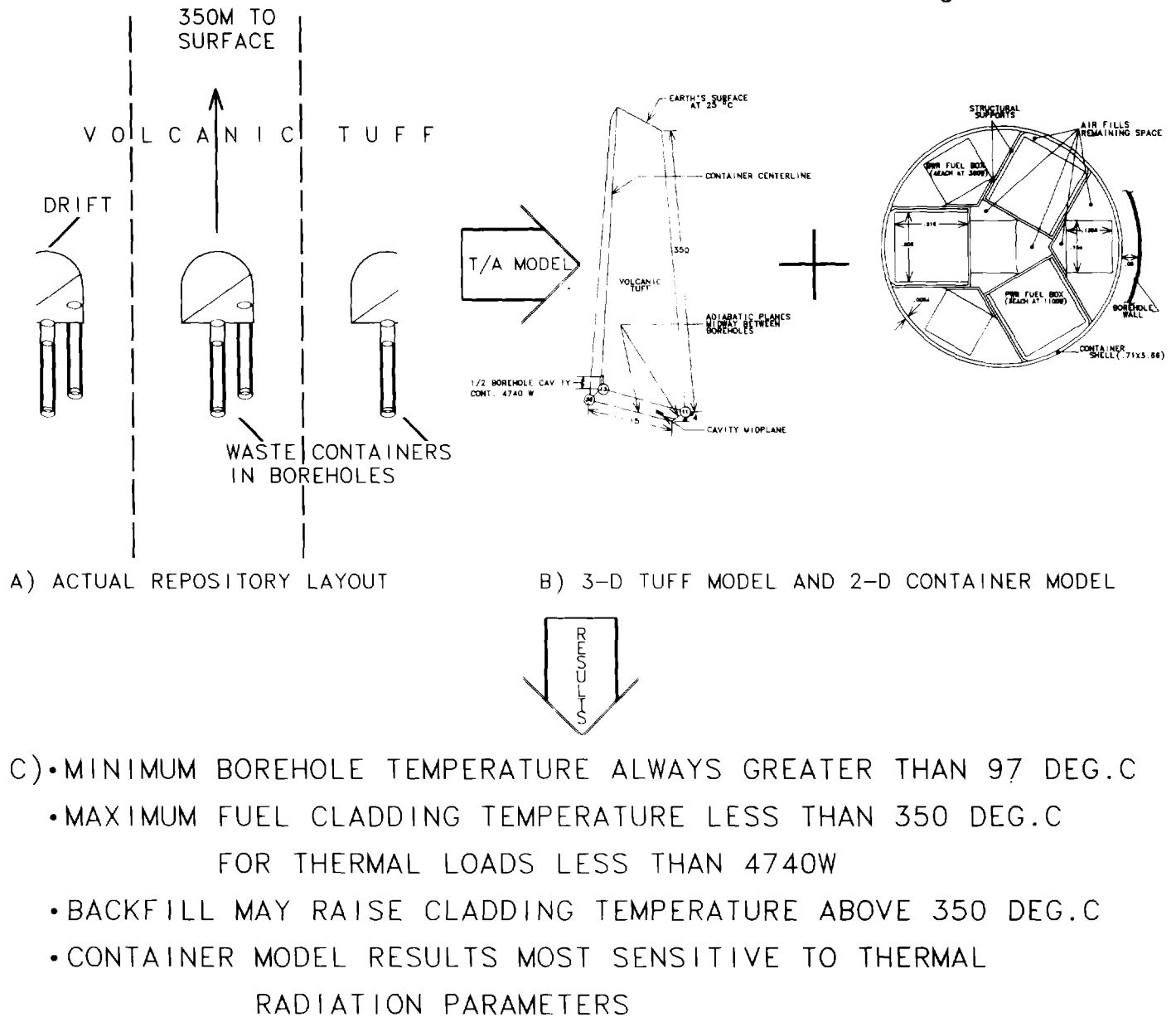
Figure 40. The best model thermal analysis of the container shows that
the hybrid-loaded container satisfies the thermal design
criteria.

REFERENCES

1. *Nuclear Waste Policy Act (Section 113), Site Characteristic Plan, Yucca Mountain Site, Nevada Research and Development Area, Nevada,* Volume III, U. S. Department of Energy, Office of Civilian Radioactive Waste Management, DOE/RW-0160, 1988.

2. DOE (U.S. Department of Energy), *Generic Requirements in a Mined Geologic Disposal System,* DOE/NE/44301-1, Washington, D.C., 1984.

3. J.R. Schornhorst et al., *Conceptual Waste Package Designs for Disposal of Nuclear Waste in Tuff,* Westinghouse Electric Corp., Advanced Energy Systems Division, Rept. No. ONWI-439, 1983.

4. W.C. O'Neal et al., *Nuclear Waste Package Design for the Vadose Zone in Tuff,* Lawrence Livermore National Laboratory, UCRL-89830, 1984.

5. J.N. Hockman and W.C. O'Neal, *Thermal Modeling of Nuclear Waste Package Designs for Disposal in Tuff,* Lawrence Livermore National Laboratory, UCRL-89820, Rev.1, 1984.

6. W. Stein, J.N. Hockman, and W.C. O'Neal, *Thermal Analysis of NNWSI Conceptual Waste Package Designs,* Lawrence Livermore National Laboratory, UCID-20291, 1984.

7. W.C. O'Neal et al., *Preclosure Analysis of Conceptual Waste Package Designs for a Nuclear Waste Repository in Tuff,* Lawrence Livermore National Laboratory, UCRL-53595, 1984.

8. W.E. Glassily, *Reference Waste Package Environment Report,* Lawrence Livermore National Laboratory, UCID-53726, 1986.

REFERENCES (cont'd.)

9. D.H. Zeuch and M.J. Eatough, *Reference Interface Base for the Nevada Nuclear Waste Storage Investigations Project* (DRAFT), Sandia National Laboratories, Albuquerque, SLTR 86-5005, April 1986.

10. D.W. Gregg and W.C. O'Neal, *Initial Specification for Nuclear Waste Package External Dimensions and Materials*, Lawrence Livermore National Laboratory, UCID-19926, 1984.

11. L.W. Scully, *Reference Waste Emplacement Geometries*, Sandia National Laboratories, Albuquerque, Keystone Document 6310-83-1, 1983.

12. Developed using the National Waste Terminal Storage Data Base-ORNL "Repository Waste Characteristics-I. Commercial LWR Spent Fuel," Oak Ridge National Laboratory, ORNL/TM-9591.

13. F.C. Nimic et al., *Recommended Matrix and Rock Mass Bulk, Mechanical, and Thermal Properties for Thermal-Mechanical Stratigraphy of Yucca Mountain*, Sandia National Laboratory-Albuquerque, Keystone Document 6310-85-11, 1985.

14. Memorandum from M.A. Molecke to Distribution, "Thermal Conductivity of Bentonite Backfills," Sandia National Laboratories, Albuquerque, December 7, 1981.

15. *Aerospace Structural Metals Handbook*, Volume 5 (Material #1303), 1985.

16. A.L. Edwards, *A Compilation of Thermal Property Data for Computer Heat Conduction Calculations*, Lawrence Livermore National Laboratory, UCRL-50589, 1969.

<u>REFERENCES</u> (cont'd.)

17. F.J. Jelinek, Contract Report on Literature Survey, *Properties and Microstructure of AISI Stainless Steel, Types 304, 204L, 316L, 321, and Incoloy 825*, Battelle Columbus Laboratory, Metal and Ceramics Information Center, 1985 (I have a copy).

18. J.M. Cuta, D.R. Rector, and J.M. Creer, *Thermal Hydraulic Analysis of Consolidated Spent PWR Fuel Rods*, Battelle, Pacific Northwest Laboratory, EPRI NP-3764, 1984.

19. J.P. Holman, *Heat Transfer*, 4th Edition, McGraw-Hill Book Company, New York, 1976.

20. Memorandum from J. Kass to T.A. Nelson and G. L. Johnson, "Thermal Analysis Work for 1988," December 9, 1987.

21. Memorandum from T.A. Nelson to Distribution, "Metal Barrier Update," December 2, 1987

22. Memorandum from R. Van Konynenburg to D.A. Lappa, "Hemispherical Total Emissivities of Candidate Waste Package Materials," August 4, 1987. (NOTE densities given in the memo are low by a factor of 1000.)

23. M.A. Gerhard, *SLIC, An Interactive Graphic Mesh Generator*, Lawrence Livermore National Laboratory, UCRL-52823, Rev. 4, 1985.

24. W.E. Mason, Jr., *TACO3D, A Three-Dimensional Finite Element Heat Transfer Code*, Lawrence Livermore National Laboratory, Unpublished.

25. J.O. Halquist, *MAZE-An Input Generator for NIKE2D and DYNA2D*, Lawrence Livermore National Laboratory, UCID-19029, Rev. 2, 1983.

REFERENCES (cont'd.)

26. P.J. Burns, *TACO2D, A Finite Element Heat Transfer Code*, Lawrence
    Livermore National Laboratory, UCRL-17980, Rev. 2, 1982.

27. A.B. Shapiro, *FACET, A Radiation View Factor Computer Code for
    Axisymmetric, 2-D Planar, and 3-D Geometry with Shadowing*,
    Lawrence Livermore National Laboratory, UCID-19887, 1982.

28. F.C. Nimic et al., *Bulk Thermal and Medium Properties of the
    Tonopah Spring Member of the Paintbrush Tuff, Yucca Mountain,
    Nevada*, Sandia National Laboratory-Albuquerque, SAND85-762, 1987.

TABLE 1

<u>SPENT FUEL UNIT THERMAL OUTPUT</u>

BWR 10-yr-old, Normal Burnup Fuel (27500 MWD/MTIHM)[***]

2:1 At-Reactor-Consolidation

Volume/canister (m^3)	Metric ton per canister
0.0756	0.3952

Time since emplacement (yr)	Power[*] (W/metric ton)	Power (W/canister)	2-D model[**] heat generation (J/yr-m^3)	Normalized power
0	911.0	360.0	1.5018E+11	1.00000
6	773.0	305.5	1.2743E+11	0.84852
8	741.0	292.8	1.2215E+11	0.81339
10	713.0	281.8	1.1754E+11	0.78266
15	652.0	257.7	1.0748E+11	0.71570
20	599.0	236.7	9.8744E+10	0.65752
30	511.0	201.9	8.4237E+10	0.56092
40	440.0	173.9	7.2533E+10	0.48299
50	383.0	151.4	6.3137E+10	0.42042
60	338.0	133.6	5.5719E+10	0.37102
70	300.0	118.6	4.9454E+10	0.32931
80	270.0	106.7	4.4509E+10	0.29638
90	245.0	96.8	4.0388E+10	0.26894
190	142.0	56.1	2.3408E+10	0.15587
290	114.0	45.0	1.8793E+10	0.12514
390	97.2	38.4	1.6023E+10	0.10670
490	85.0	33.6	1.4012E+10	0.09330
1000	49.9	19.7	8.2259E+09	0.05477

[*] Reference 12

[**] [For power/canister distributed in volume defined by canister cross section and container length]

[***] MWD/MTIHM=megawatt days per metric ton-irradiated heavy metal

TABLE 1 (cont'd.)

SPENT FUEL UNIT THERMAL OUTPUT

BWR 10-yr-old, Normal Burnup Fuel (27500 MWD/MTIHM)

2:1 At-Reactor-Consolidation

Time since emplacement (yr)	3-D model heat generation[*] (J/yr-m^3)
0	5.4110E+09
6	4.5913E+09
8	4.4013E+09
10	4.2350E+09
15	3.8726E+09
20	3.5578E+09
30	3.0351E+09
40	2.6134E+09
50	2.2749E+09
60	2.0076E+09
70	1.7819E+09
80	1.6037E+09
90	1.4552E+09
190	8.4343E+08
290	6.7712E+08
390	5.7733E+08
490	5.0487E+08
1000	2.9639E+08

[*] [For power of one canister spread over volume of one borehole]

TABLE 1 (cont'd.)

SPENT FUEL UNIT THERMAL OUTPUT

PWR 10-yr-old, Normal Burnup Fuel (33000 MWD/MTIHM)
2:1 At-Reactor-Consolidation

Volume/canister (m^3)	Metric ton per canister
0.1629	0.9649

Time since emplacement (yr)	Power[*] (W/metric ton)	Power (W/canister)	2-D model[**] heat generation (J/yr-m^3)	Normalized power
0	1140.0	1100.0	2.1301E+11	1.00000
6	949.0	915.7	1.7732E+11	0.83246
8	908.0	876.1	1.6966E+11	0.79649
10	871.0	840.4	1.6275E+11	0.76404
15	791.0	763.2	1.4780E+11	0.69386
20	723.0	697.6	1.3509E+11	0.63421
30	612.0	590.5	1.1435E+11	0.53684
40	525.0	506.6	9.8096E+10	0.46053
50	455.0	439.0	8.5017E+10	0.39912
60	398.0	384.0	7.4366E+10	0.34912
70	353.0	340.6	6.5958E+10	0.30965
80	316.0	304.9	5.9045E+10	0.27719
90	286.0	276.0	5.3439E+10	0.25088
190	160.0	154.4	2.9896E+10	0.14035
290	126.0	121.6	2.3543E+10	0.11053
390	108.0	104.2	2.0180E+10	0.09474
490	93.8	90.5	1.7527E+10	0.08228
1000	54.7	52.8	1.0221E+10	0.04798

[*] Reference 12

[**] [For power/canister distributed in volume defined by canister cross section and container length]

TABLE 1 (cont'd.)

SPENT FUEL UNIT THERMAL OUTPUT

PWR 10-yr-old, Normal Burnup Fuel (33000 MWD/MTIHM)

2:1 At-Reactor-Consolidation

Time since emplacement (yr)	3-D model heat generation* (J/yr-m³)
0	1.6534E+10
6	1.3763E+10
8	1.3169E+10
10	1.2632E+10
15	1.1472E+10
20	1.0486E+10
30	8.8759E+09
40	7.6142E+09
50	6.5989E+09
60	5.7723E+09
70	5.1196E+09
80	4.5830E+09
90	4.1479E+09
190	2.3205E+09
290	1.8274E+09
390	1.5663E+09
490	1.3604E+09
1000	7.9332E+08

* [For power of one canister spread over volume of one borehole]

TABLE 1 (cont'd.)

SPENT FUEL UNIT THERMAL OUTPUT

BWR 5-yr-old, Normal Burnup Fuel (27500 MWD/MTIHM)
2:1 At-Reactor-Consolidation

Time since emplacement (yr)	Power* (W/metric ton)	Power (W/canister)	2-D model** heat generation (J/yr-m^3)	Normalized power
0	1380.0	545.3	2.2749E+11	1.00000
1	1190.0	470.3	1.9617E+11	0.86232
2	1080.0	426.8	1.7804E+11	0.78261
3	1000.0	395.2	1.6485E+11	0.72464
4	951.0	375.8	1.5677E+11	0.68913
5	911.0	360.0	1.5018E+11	0.66014
11	773.0	305.5	1.2743E+11	0.56014
13	741.0	292.8	1.2215E+11	0.53696
15	713.0	281.8	1.1754E+11	0.51667
20	652.0	257.7	1.0748E+11	0.47246
25	599.0	236.7	9.8744E+10	0.43406
35	511.0	201.9	8.4237E+10	0.37029
45	440.0	173.9	7.2533E+10	0.31884
55	383.0	151.4	6.3137E+10	0.27754
65	338.0	133.6	5.5719E+10	0.24493
75	300.0	118.6	4.9454E+10	0.21739
85	270.0	106.7	4.4509E+10	0.19565
95	245.0	96.8	4.0388E+10	0.17754
195	142.0	56.1	2.3408E+10	0.10290
295	114.0	45.0	1.8793E+10	0.08261
395	97.2	38.4	1.6023E+10	0.07043
495	85.0	33.6	1.4012E+10	0.06159
1000	49.9	19.7	8.2259E+09	0.03616

* Reference 12

** [For power/canister distributed in volume defined by canister cross section and container length]

TABLE 1 (cont'd.)

SPENT FUEL UNIT THERMAL OUTPUT

BWR 5-yr-old, Normal Burnup Fuel (27500 MWD/MTIHM)
2:1 At-Reactor-Consolidation

Time since emplacement (yr)	3-D model heat generation[*] $(J/yr\text{-}m^3)$
0	8.1967E+09
1	7.0682E+09
2	6.4148E+09
3	5.9396E+09
4	5.6486E+09
5	5.4110E+09
11	4.5913E+09
13	4.4013E+09
15	4.2350E+09
20	3.8726E+09
25	3.5578E+09
35	3.0351E+09
45	2.6134E+09
55	2.2749E+09
65	2.0076E+09
75	1.7819E+09
85	1.6037E+09
95	1.4552E+09
195	8.4343E+08
295	6.7712E+08
395	5.7733E+08
495	5.0487E+08
1000	2.9639E+08

[*] [For power of one canister spread over volume of one borehole]

TABLE 1 (cont'd.)

SPENT FUEL UNIT THERMAL OUTPUT

PWR 5-yr-old, Normal Burnup Fuel (33000 MWD/MTIHM)
2:1 At-Reactor-Consolidation

Time since emplacement (yr)	Power* (W/metric ton)	Power (W/canister)	2-D model** heat generation (J/yr-m^3)	Normalized power
0	1800.0	1736.8	3.3633E+11	1.00000
1	1530.0	1476.3	2.8588E+11	0.85000
2	1370.0	1321.9	2.5598E+11	0.76111
3	1270.0	1225.4	2.3730E+11	0.70556
4	1200.0	1157.9	2.2422E+11	0.66667
5	1140.0	1100.0	2.1301E+11	0.63333
11	949.0	915.7	1.7732E+11	0.52722
13	908.0	876.1	1.6966E+11	0.50444
15	871.0	840.4	1.6275E+11	0.48389
20	791.0	763.2	1.4780E+11	0.43944
25	723.0	697.6	1.3509E+11	0.40167
35	612.0	590.5	1.1435E+11	0.34000
45	525.0	506.6	9.8096E+10	0.29167
55	455.0	439.0	8.5017E+10	0.25278
65	398.0	384.0	7.4366E+10	0.22111
75	353.0	340.6	6.5958E+10	0.19611
85	316.0	304.9	5.9045E+10	0.17556
95	286.0	276.0	5.3439E+10	0.15889
195	160.0	154.4	2.9896E+10	0.08889
295	126.0	121.6	2.3543E+10	0.07000
395	108.0	104.2	2.0180E+10	0.06000
495	93.8	90.5	1.7527E+10	0.05211
1000	54.7	52.8	1.0221E+10	0.03039

* Reference 12

** [For power/canister distributed in volume defined by canister cross section and container length]

TABLE 1 (cont'd.)

SPENT FUEL UNIT THERMAL OUTPUT

PWR 5-yr-old, Normal Burnup Fuel (33000 MWD/MTIHM)

2:1 At-Reactor-Consolidation

Time since emplacement (yr)	3-D model heat generation* $(J/yr-m^3)$
0	2.6106E+10
1	2.2190E+10
2	1.9869E+10
3	1.8419E+10
4	1.7404E+10
5	1.6534E+10
11	1.3763E+10
13	1.3169E+10
15	1.2632E+10
20	1.1472E+10
25	1.0486E+10
35	8.8759E+09
45	7.6142E+09
55	6.5989E+09
65	5.7723E+09
75	5.1196E+09
85	4.5830E+09
95	4.1479E+09
195	2.3205E+09
295	1.8274E+09
395	1.5663E+09
495	1.3604E+09
1000	7.9332E+08

* [For power of one canister spread over volume of one borehole]

TABLE 2

MATERIAL THERMAL PROPERTIES

Material: TUFF[*]

MATERIAL TYPE: Isotropic
DENSITY: 2340. (kg/m^3)

CONDUCTIVITY (J/yr-m-K)	HEAT CAPACITY (J/kg-K)	TEMPERATURE (K)
6.528E+07	9.615E+02	273
6.528E+07	9.615E+02	372
6.023E+07	8.034E+02	373
6.023E+07	8.034E+02	773

Material: BENTONITE ANNULUS BACKFILL[**]

MATERIAL TYPE: Isotropic
DENSITY: 2000. (kg/m^3)

CONDUCTIVITY (J/yr-m-K)	HEAT CAPACITY (J/kg-K)	TEMPERATURE (K)
2.838E+07	8.368E+02	273
2.838E+07	8.368E+02	372
2.113E+07	8.368E+02	373
2.113E+07	8.368E+02	773

[*] Reference 13 (Newer data found in Reference 28)
[**] Reference 14 for conductivity and a density and heat capacity characteristic of clay

TABLE 2 (cont'd.)

MATERIAL THERMAL PROPERTIES

Material: 304 STAINLESS STEEL[*]

MATERIAL TYPE: Isotropic

DENSITY: 7940. (kg/m^3)

CONDUCTIVITY (J/yr-m-K)	HEAT CAPACITY (J/kg-K)	TEMPERATURE (K)
4.355E+08	4.89E+02	250
4.671E+08	5.06E+02	300
5.223E+08	5.30E+02	400
5.718E+08	5.49E+02	500
6.195E+08	5.65E+02	600
6.659E+08	5.80E+02	700

Material: 7030 CUPRONICKEL[**]

MATERIAL TYPE: Isotropic

DENSITY: 8900. (kg/m^3)

CONDUCTIVITY (J/yr-m-K)	HEAT CAPACITY (J/kg-K)	TEMPERATURE (K)
9.240E+08	3.766E+02	273 - 811

[*] References 15, 16, and 17
[**] Reference 16

TABLE 2 (cont'd.)

MATERIAL THERMAL PROPERTIES

Material: INCOLOY 825*

MATERIAL TYPE: Isotropic

DENSITY: 8230. (kg/m^3)

CONDUCTIVITY (J/yr-m-K)	HEAT CAPACITY (J/kg-K)	TEMPERATURE (K)
3.187E+08		255.4
	4.14E+02	273
3.503E+08		300
3.566E+08		311
3.882E+08		366.5
4.450E+08		477.6
	4.55E+02	573
4.986E+08		588.6
5.459E+08		699.7
	4.93E+02	773
5.964E+08		810.9
	5.30E+02	923
	6.46E+02	973

* Reference 17

TABLE 2 (cont'd.)

MATERIAL THERMAL PROPERTIES

Material: BWR & PWR DOUBLE PACKED CANISTERS[*]

MATERIAL TYPE: Isotropic

DENSITY: 2000. (kg/m^3)

CONDUCTIVITY (J/yr-m-K)	HEAT CAPACITY (J/kg-K)[**]	TEMPERATURE (K)
1.170E+06	2.640E+03	273
1.960E+06		323
3.000E+06		373
4.390E+06		423
6.150E+06		473
8.300E+06		523
10.92E+06		573
14.04E+06		623
17.67E+06		673

[*] Reference 1 ("effective" conductivity prediction incl. radiation and conduction modes with data curve fit to a $k=CT^3$ form about 423 K)

[**] For comparison-density times heat capacity=5.28E+06 J/m^3-K for canistered clad fuel vs 1.38E+06 J/m^3-K for just uranium oxide.

TABLE 2 (cont'd.)

MATERIAL THERMAL PROPERTIES

Material: BWR & PWR DOUBLE PACKED CANISTERS [Case 8]*

MATERIAL TYPE: Isotropic

DENSITY: 2000. (kg/m^3)

CONDUCTIVITY (J/yr-m-K)	HEAT CAPACITY (J/kg-K)	TEMPERATURE (K)
1.580E+06	2.640E+03	273
2.646E+06		323
4.050E+06		373
5.927E+06		423
8.303E+06		473
11.21E+06		523
14.74E+06		573
18.95E+06		623
23.85E+06		673

* Prediction derived from measured temperature profiles from Ref. 18 (thermal conductivity = 1.35 times the previous Table)

TABLE 2 (cont'd.)

MATERIAL THERMAL PROPERTIES

Material: AIR (at 1 atm pressure)[*]

MATERIAL TYPE: Isotropic

DENSITY: (included with heat capacity table)[**]

CONDUCTIVITY (J/yr-m-K)	HEAT CAPACITY (J/m^3-K)[**]	TEMPERATURE (K)
7.023E+05	1420.3	250
8.275E+05	1184.1	300
9.470E+05	1007.0	350
10.61E+05	895.0	400
11.69E+05	799.5	450
12.73E+05	725.6	500
13.75E+05	667.5	550
14.69E+05	620.3	600
15.62E+05	577.5	650
16.49E+05	540.8	700
17.37E+05	511.2	750

[*] Reference 19

TABLE 3

"CONVECTIVE" BOUNDARY CONDITIONS IN OPEN ANNULUS[*]

(Includes effects of conduction and convection)

Time since emplacement (yr)	Borehole wall temperature[**] (K)	Borehole wall temperature[***] (K)	Borehole wall temperature[****] (K)
0.	373.	373.	300.
.05	379.2	388.3	448.7
.20	409.5	423.2	494.5
1.00	443.	462.2	522.6
2.00	456.	474.3	520.8
3.00	463.	479.8	518.7
5.00	468.	484.6	515.8
9.00	471.	488.5	511.8
15.00	474.	490.	509.1
19.50	476.	489.4	507.1
24.00	474.	487.6	504.8
50.00	462.	465.1	487.4
75.00	448.	450.4	467.3
100.00	439.	440.5	453.8
150.00	426.	427.4	438.2
225.00	415.	416.3	427.3
300.00	409.	410.4	420.9
400.00	405.	405.7	414.7
1000.00	390.4	389.4	396.3

[*]   Temperatures also used for annulus radiative heat transfer calcs.
[**]   3-D analysis - coarse zoning, regular time step, 10-yr-old fuel
[***] 3-D analysis - refined zoning, halved time step, 10-yr-old fuel
[****] 3-D analysis - coarse zoning, regular time step, 5-yr-old fuel

TABLE 3

"CONVECTIVE" BOUNDARY CONDITIONS IN OPEN ANNULUS

(Includes effects of conduction and convection)

Annulus temperature (K)	Heat transfer coefficient* (J/yr-m^2-K)
380.	8.289E+07
400.	8.170E+07
450.	7.966E+07
500.	7.861E+07
550.	7.772E+07
600.	7.710E+07
650.	6.301E+07
700.	4.787E+07
750.	3.803E+07
800.	3.736E+07
850.	4.020E+07

* Developed using equation 7-51, Table 7.3, and Table A-6 (water vapor) from Reference 24.

TABLE 4

THERMAL ANALYSIS CASES / 3-D FINITE ELEMENT MODEL

Case No.	Id.	Tuff depth	Years-out-of-reactor	Thermal load	Other model parameters
1a/3-D*	coarse mesh	350 m	10	4740 W	25 ^{o}C upper surface -coarse mesh/step
1b/3-D	fine mesh	350 m	10	4740 W	25 ^{o}C upper surface -fine mesh/step
6/3-D	5-year fuel	350 m	5	7392 W	25 ^{o}C upper surface -fine mesh/step
11/3-D	adiab.surf.	350 m	10	4740 W	adiab. upper surface
12/3-D	700 m depth	700 m	10	4740 W	25 ^{o}C upper surface
13a/3-D	SCP layout	350 m	10	4100 W	25 ^{o}C upper surface -fine mesh/step

THERMAL ANALYSIS CASES / 2-D FINITE ELEMENT MODEL

Case No.	Id.	Structural material	Backfill material	Thermal load	Other model parameters
1	304SS	304 Stainless	None	4740 W	Historical model
2	7030	7030 Cupronickel	None	4740 W	Historical model
3*	IN825	Incoloy 825	None	4740 W	Historical model
4	loose backfill	Incoloy 825	loosely packed bentonite	4740 W	Cond. only to BHW
5	contact R.	Incoloy 825	None	4740 W	Real contact resist.
6	5-year fuel	Incoloy 825	None	7392 W	Historical model
7	emissivity	Incoloy 825	None	4740 W	Real surf. emissivity
8	fuel cond.	Incoloy 825	None	4740 W	Real fuel conductivity
9	gas cond.	Incoloy 825	None	4740 W	Conduction thru fill
10	best model	Incoloy 825	None	4740 W	Best model analysis
13a	SCP layout	Incoloy 825	None	4100 W	SCP borehole spacing
14	Firm Backfill	Incoloy 825	firmly packed bentonite	4740 W	Cond. only to BHW

* The reference cases for the 3-D and 2-D analyses, respectively

TABLE 5

TEMPERATURE RESULTS SYNOPSIS/3-D ANALYSES

Case No. / Id.	Min. borehole wall temperature (1000 y) ($^{\circ}$C)	Maximum temperature 1 m into tuff from BHW[**] ($^{\circ}$C)
1a / 3-D coarse mesh[*]	127	164
1b / 3-D fine mesh	127	167
6 / 3-D 5-year fuel	122	185
11 / 3-D adiab.surf.	128	164
12 / 3-D 700 m depth	127	164
13a / 3-D SCP layout	134	199

[*] The reference case for the 3-D analyses

[**] Most peak near-borehole temperatures occur 15 to 20 yr after emplacement.

TABLE 5 (cont'd.)

TEMPERATURE RESULTS SYNOPSIS/2-D ANALYSES

Case No./ Id.	Peak PWR[**] cladding temperature (^{o}C)	Peak BWR[**] cladding temperature (^{o}C)
1 / 304SS	329	313
2 / 7030	325	304
3 / IN825[*]	336	323
4 / loose backfill	391	383
5 / contact R.	336	323
6 / 5-year fuel	411	399
7 / emissivity	346	339
8 / fuel conductivity	322	315
9 / gas conduction	335	322
10 / best model	336	334
13a/ SCP spacing	335	334
14 / firm backfill	341	329

[*] The reference case for the 2-D analyses

[**] Most peak cladding temperatures occur 3 to 5 yr after emplacement.

TABLE 6

THERMAL LOADS FROM POSSIBLE CONTAINER CONTENTS

No.BWR canister	No.PWR canister	Years-out-of-reactor	Burnup	Consolidation	Thermal load
4	3	10	Normal	2:1	4740 W
4	3	5	Normal	2:1	7392 W
4	3	5	Normal	1:1	3696 W
0	3	5	Normal	2:1	5210 W
7	0	5	Normal	2:1	3815 W
4	3	10	Extended	1:1	4579 W
0	3	5	Extended	1:1	5268 W
6	0	5	Extended	2:1	4837 W

APPENDIX A

Bibliography of Additional LLNL Internal Documents
on Thermal Analysis of Container Design and Emplacement
(Copies available from G.L. Johnson, LLNL)

1. W. Stein, *Three-Dimensional Thermal Analysis of a Conceptual Waste Package Design for the Disposal of Pressurized Water Reactor Spent Fuel*, Unpublished Report, Lawrence Livermore National Laboratory, TF85-61, March 1985.

2. W. Stein, "Thermal Analysis of Common Canister Spent Fuel Waste Package Design," Internal Report-Thermo-fluids Group, Nuclear Test Engineering Division, Lawrence Livermore National Laboratory, TF85-61, 20 September 1985.

3. Memo from W. Stein to E. Russell, "Thermal Conductivity of Spent Fuel Arrays," Thermo-fluids Group, Nuclear Test Engineering Division, Lawrence Livermore National Laboratory, 13 June 1985.

4. Memo from W. Stein to E. Russell, "Maximum Spent Fuel Container Wall Temperature," Thermo-fluids Group, Nuclear Test Engineering Division, Lawrence Livermore National Laboratory, 30 April 1986.

5. Memo from W. Stein to E. Russell, "Disposal Container Temperature History For Use in Corrosion Analysis," Thermo-fluids Group, Nuclear Test Engineering Division, Lawrence Livermore National Laboratory, 14 May 1986.

6. Memo from W. Stein to T. Nelson, "Thermal Analysis of Waster Isolation Container (Hybrid Requirements)," Thermo-fluids Group, Nuclear Test Engineering Division, Lawrence Livermore National Laboratory, 4 September 1987.

7. D. Montan, *Thermal Calculations Pertaining to Experiments in the Yucca Mountain Exploratory Shaft*, Lawrence Livermore National Laboratory, UCID-20780, 1986.

8. D. Montan, *Thermal Calculations Pertaining to a Proposed Yucca Mountain Nuclear Waste Repository*, Lawrence Livermore National Laboratory, UCID in preparation, to be published 1988.